NEW APPROACHES TO APPLIED SPECTROSCOPY

Master's thesis

by

Mikkel Brydegaard Sørensen

Thesis advisor: Sune Svanberg

Lund Reports on Atomic Physics, LRAP-382

Atomic Physics Division, Lund University

Lund, Sweden

June 2007

Abstract

In this paper several new concepts of applied optical spectroscopy are proposed. One method suggest simultaneous instant acquisition of a fluorescence excitation emission matrix, absorption spectrum and scattering properties over wavelengths from UV to IR. A multispectral imaging concept introduced as Wien-shift imaging is proposed. Thoughts concerning simple LED based fluorosensors are presented. A systematic approach to spectral data processing is demonstrated.

Acknowledgements

Great thanks to my advisor Sune Svanberg for many fruitful and inspiring brainstorms in his sofa, thanks also for the advices concerning patenting new concepts during the thesis. Thanks to Stefan Andersson-Engels for assisting with doubts about light propagation in scattering media, thanks also for the optical components I borrowed from his labs during the practical work. Thanks to Sara Ek for the work we did together and for providing data from her instrument. Thanks to my handyman and chess mate Arash Gharibi. Thanks to the whole Division of Atomic physics, for the patience and the space for setups spread out over the laboratories in half the building.

Contents

1 Introduction

1.1 Motivation

1.1.1 Applied spectroscopy on volumetric samples

Optical spectroscopy in general provides the ability to detect and quantify substances macroscopically without the necessity to resolve them and actually count the molecules. We use spectroscopic methods every day in our life without even having to think about it. In food science we know that a banana is supposed to be yellow if we expect if to taste good, in medicine the doctors know that the throat should be red and not whitish and in traffic we do not expect to be run over if we drive for green light. It is understood that life would be considerable more difficult in a black and white world. The question is now: can life become easier by going the opposite direction, i.e. specify colors in a more detailed way?

We often refer to light from a certain object as “color” of that object. The so called “color” is described by the spectral contribution to each of our three spectral channels in the eye, red green and blue. Even if we are able to base a lot of decisions on what colors we see, we quickly realize that we are able to base a lot more decisions with a spectrometer, an instrument with several thousands spectral channels. Not only can we expand the spectral region to include ultra violet (UV) with wavelengths shorter than visible light and infrared (IR) with wavelength larger than visible light, we can also see spectral details that we were not able to resolve with the eye, even if the light was visible.

Spectral analysis again comes short either when we are not able to detect or quantify the substance of particular interest or when the quantification is so much disturbed by other present varying substances that the result is practically useless. One might then attempt to make the quantification chemically or biomedical, but that implies much more time and costs than a spectroscopic snapshot does.

Taking optics further we can move on to fluorescence spectroscopy. We now only detect light from a smaller subgroup of the substances present which are trigged by the excitation wavelength, and we can hope that quantification of the substance becomes clearer than before, a daily life example is when cashiers check the validity of big bills by illuminating them with UV light and observing expected responses. One might not hear a triangle playing if one ask a big symphony orchestra to play, but if the director asks just the triangle to sound it is more likely.

Fluorescence spectroscopy works fine from a single surface such as from a money bill, but again the method comes short in a number of scenarios. All these scenarios include situations where light is disturbed in a volume on the way to the fluorescent substances (fluorophore) or on the way back from fluorophore. Unfortunately this scenario is the case for many objects of great interest to us; it includes spectroscopy on volumes such as tissue, drugs, foods and unclear turbid liquids.

This thesis proposes a partial solution which could improve the success rate of applied spectroscopy of volumes.

1.1.2 Inexpensive applied spectroscopy

A number of fields can benefit from well known working spectroscopic methods today. However, a number of facts limit the implementation. Spectrometers are often expensive, fragile or non portable. Secondly, specialists are required to interpret the spectral data. Fields such as lower education, and agriculture and crop production in third-world countries have limited resources, and purchase of expensive spectrometers might further be unwise due to harsh environments, e.g. children play, electrostatic discharges, high humidity. Further the personnel might be untrained or unable to extract relevant information from the spectral data. Another field with interest in inexpensive spectroscopy is medical screening. If spectroscopy was inexpensive, compact and comprehendible devices could be placed in several hospitals and a large database of spectra could be gathered. Eventually, spectra can be correlated with the diagnoses of each person and the risk of suffering a specific disease might be estimated from a spectral function. Optical spectroscopy is particularly interesting in medicine due to the fast and noninvasive nature.

This thesis proposes two methods for inexpensive and compact spectroscopy. This thesis also includes upgrades to a previously developed instrument, for the same given purpose. This thesis proposes a general spectral data handling which is based on training and machine learning rather than the expert knowledge of a physicist.

2 Physics of the sample

2.1 Attenuation

Attenuation of light describes how light rays through a unit area are reduced in power. Intensity is light power passing through a unit area. Attenuation occurs due to geometrical divergence of rays in three dimensions, often referred to as the $1/r^2$ attenuation. A two-dimensional illustration gives us a 1/r relation between distance from point source to intensity measurement.

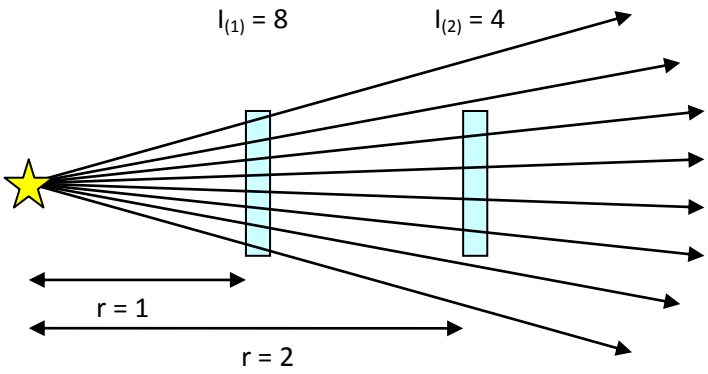

Fig 2.1.1 Light from a point source attenuates with 1/r in a two-dimensional ilstration and as $1/r^2$ our three-dimensional world.

Apart from this basic geometrical effect, attenuation might also occur following a single light ray, this happens when light interacts with matter. For low light intensities we can describe the loss as a linear fraction of the incoming light. Attenuation in a volume of thickness r follows Beer-Lambert's law:

$$dI/dr = - \mu_{att} * I$$

with the solution

$$I_{(r)} = I_{(0)} e^{-\mu att * r}$$

I_0	*incident intensity*
I	*intensity after attenuation*
r	*distance traveled through the medium*
μ_{att}	*combined attenuation effects*

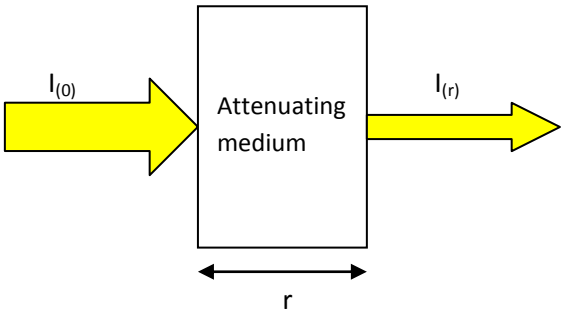

Fig 2.1.2 When light interacts with matter the intensity undergoes exponentially decay along the propagation length.

To realize a measurement of the attenuation coefficient in reality is not at all trivial. This is partly because $\mu_{att(\lambda)}$ is a complicated function of wavelength. Performing such ameasurement for a given wavelength implies emitting monochromatic light, and detecting the outgoing light only at that certain wavelength and only the rays going directly from the impact point to the observation point. To ensure direct propagation either time gating or collimators could be used. Furthermore, a considerable loss of intensity will be caused not by the volume but by the interfaces and mismatch in refractive indices, which gives rise to multiple reflections. Measurements on several thicknesses must be performed to cancel out the specular reflectance.

We could rewrite the attenuation loss:

$$I_{(r)} = I_{(0)}(e^{-\mu att * r} - 2*Ref)$$

Ref *primary reflection in interfaces.*

μ_{att} is a sum of several phenomena which occur when light interacts with matter. Understanding that $\mu_{att(\lambda)}$ is a function described by the atomic and molecular composition of the volume and even microstructures such as cells in tissue volumes, we also understand that we might be able to identify or quantify certain chemical compositions or microscopic structures, without the necessity to actually resolve them or see them. In other words, $\mu_{att(\lambda)}$ carries information about the volume. By analyzing $\mu_{att(\lambda)}$ we might or might not be able to obtain information which correlates with relevant properties. For tissue volumes such information could be: What is the probability for cancer? Is this tissue likely to come from a person with diabetes? Etc.

First analysis of $\mu_{att(\lambda)}$ shows that $\mu_{att(\lambda)}$ can be rewritten as a sum:

$$\mu_{att(\lambda)} = \mu_{sca(\lambda)} + \mu_{abs(\lambda)}$$

$\mu_{sca(\lambda)}$ *scattering coefficient*

$\mu_{abs(\lambda)}$ *absorption coefficient*

Here $\mu_{sca(\lambda)}$ is attenuation caused by scattering effects; a process which changes the direction of light. $\mu_{abs(\lambda)}$ is attenuation caused by absorption of light; light disappearing for the given wavelength.

2.2 Absorption

Absorption $\mu_{abs(\lambda)}$ is governed by different physical phenomena depending on the wavelengths. Also an absorption phenomenon depends heavily of the state of the matter, e.g. solid, liquids, gases or plasmas. In the optical region phenomena are electronic excitation and molecular vibration.

By electronic excitation electrons are lifted up into a higher electron band. The energy of the light goes into the increase of potential energy. Since the bands are discrete due to the dualism of the electron, only photons with the energy matching existing band gap transition will be able to excite the electrons. Energy for visible light is mostly related to the outer most electrons in the atoms. In liquids and solids outer electron bands are heavily influenced by interaction with surrounding molecules. The result is distorted band gaps. Since band gaps are not well defined in solids and liquids, the absorption spectra for such become smeared out. Spectral features for solids and liquids rarely become narrower than 10-20 nm. This fact lowers the requirements on the instruments for measuring on solids and liquids.

Sharp spectral features of less than a fraction of a nanometer might be generated by free gas molecules in liquids or solids. The absorbing mechanism in the visible spectrum is electronic transitions in the atoms in the gas molecule. The instrument presented in this project will not be able to resolve free gases. Thus, we will not pay much attention to gas absorption.

2.3 Fluorescence

Fig 2.3.1 A variety of fluorescence dyes made from quantum dots exposed to the same excitation light. (Source: Dr. D. Talapin, University of Hamburg)

Surely conservation of energy is also valid on the atomic level. It can be understood that atoms cannot absorb and accumulate light energy for ever. They thus have to be able to release the energy. In every time unit any excited state will have a certain probability of undergoing decay, lowering the potential energy of the electron by getting closer to the nucleus. The probability is related to the quantum mechanics of the system. When an excited atom or molecule undergoes a transition it releases energy, we refer to the released radiation as fluorescent light. The energy can also be released as heat. An excited state has the possibility to undergo many different transition decay chains to reach its ground state. For a given substance the yield for producing fluorescent light can be large or small. For example, a substance might emit 5% of the absorbed energy as green light, 10% as infrared and remaining 85% as heat. Skin autofluorescence refers to the fluorescence of skin itself without adding any fluorescent marker drugs. Light emission yields for skin auto fluorescence are low, thus requiring an intense excitation light. The large difference in intensity creates difficulties to capture the signal within the dynamic range of a detector instrument. For this reason the exciting light must be filtered away before detection of the fluorescent light. However, absorbing light filters also need to release their energy and fractions of the absorbed light will also undergo fluorescence, thus mixing with the signal of interest. One interesting fluorophore in skin is Advanced Glycation End (AGE) product which is thought to be a major factor in the aging process.

Fluorescent spectra or profiles can be described in intensity, as a function of both excited wavelength and emitted wavelength:

$I_f = F(\lambda_{ex}, \lambda_{em})$

I_f	*fluorescent light intensity*
F	*surface function dependent on the present substances*
λ_{ex}	*excitation wavelength*
λ_{em}	*emission wavelength*

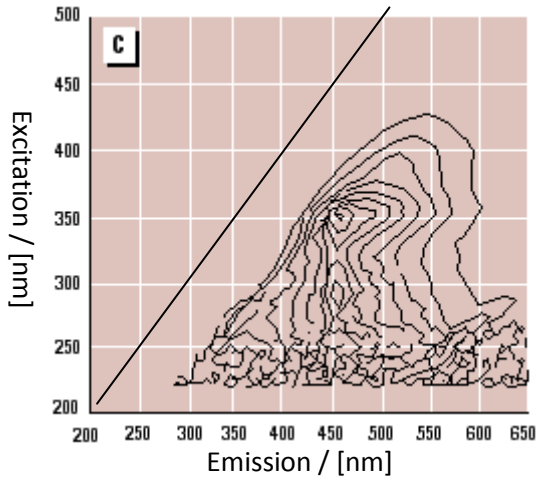

Fig 2.3.2 Contour plot of a fluorescence surface (Source: ehponline.org)

Since no larger energy quanta can be emitted than the excitation quanta, F has to be zero when $\lambda_{ex} > \lambda_{em}$. (Special cases with high intensities involved also exists, where this is not a necessity)

Measuring I_f for a given substance provides vast information on the chemical composition. However, it is not trivial to measure I_f alone. Since I_f is produced in matter, the exciting light will be altered while traveling in that same matter. Absorption features from substances others than the one yielding the fluorescent light might absorb light when traveling from the source to the fluorophore. On the return path from the fluorophore to the detection, the spectral profile may once again be influenced by absorption features in the surrounding matter. Not only absorption can influence shapes of spectral profiles reaching and leaving a fluorophore; since attenuation is closely related to the traveled distance of the light, and scattering events influence the distance the light travels. Thus scattering can also influence fluorescence spectra. This becomes a greater issue when observing longer wavelengths. Thus, scattering is interfering more on the return path from a fluorophore. The fact that spectral profiles get distorted on the way to and from fluorophores limits the success of application of pure fluorescence measurements in scattering media.

Attempts to measure $\mu_{abs(\lambda)}$ simultaneously with a white light source, will partially fail and sometimes even produce negative absorption coefficients. This occurs due to the fact that fluorescent light excited by lower wavelengths will contribute to the spectral bins where the absorption is being measured. Since wavelengths are shifted upwards by fluorescence we might call it a nonlinear phenomenon because the frequency of light is changed.

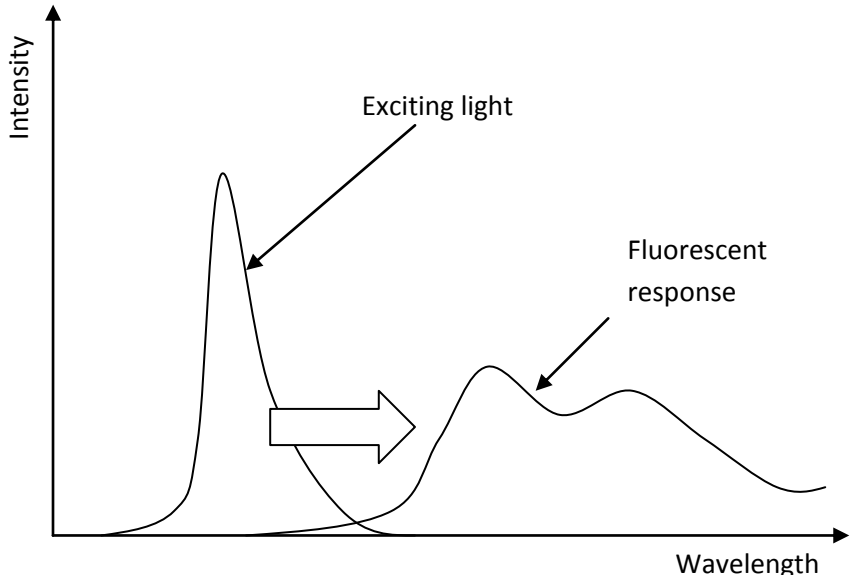

Fig 2.3.3 Light is converted upwards in wavelength by fluorescence.

Fluorescence in tissue is emitted omni-directionally (apart from laser emission due to stimulated emission), and we might say that emitted fluorescence light partly looses information of polarization, phase and direction of the original exciting light.

In time-resolved fluorescence the decay times rather than the energy of emitted light is analyzed. This technique requires short exciting light pulses and fast time-resolved detection. Optical lifetimes in medical diagnostics are typically in the range from 5 ns to 100 ns. Also fluorescence might not be the only phenomenon delaying the light, scattering substance also have this ability. However, the delay from scattering phenomena in tissue is rather of the order of 2 ns for red light backscattered on a tissue surface.

Absorbed energy might also go into ionization or breaking molecules. This is in general unwanted in medical diagnostics, the ionization creates the free radical OH^- which has the possibility to break or alter DNA code strings. If the altering is of relevance the most frequent consequence is cancerous cells. Therefore a light wavelength with ionizing ability is often referred to as carcinogenic, and it thus determines the lower limit for wavelengths used for in vivo measurements. Other applications, where radical induction is less crucial might though benefit from lower wavelengths.

2.4 Scattering

Scattering refers to the fact that light changes direction multiple times when interacting with interfaces of microstructures. Considering light propagation in tissue, scattering becomes a considerable issue because of lipids, cell membranes, blood vessels etc, which all have slightly different refractive indices and which all will deflect light in random directions.

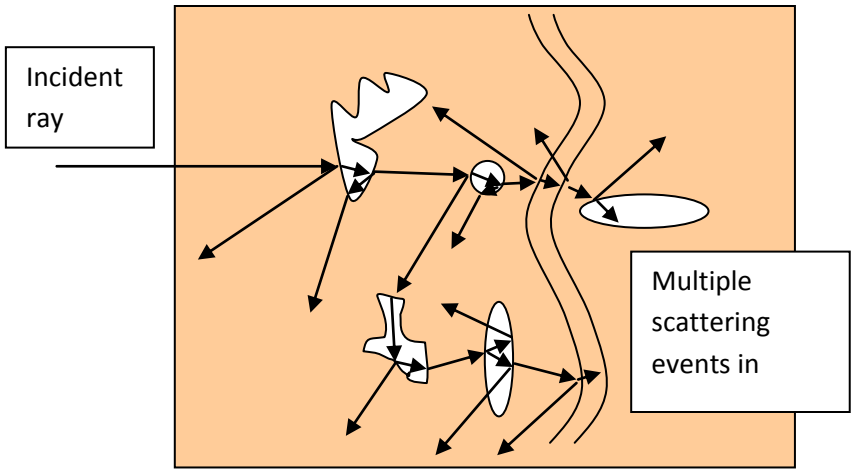

Fig 2.4.1. Multiple scattering dominates for light propagation in tissue

As for absorption we can describe scattering macroscopically with the probability for a scattering per unit distance; $\mu_{sca(\lambda)}$. The coefficient does not fully describe light propagation in scattering media since scattered light from a homogeneous volume might be more of less dependent on the direction of the incident light. A g-factor from zero to one can be used to describe this uniformity. A g-value close to zero indicates that light is scattered in a random angle independent of the incident angle. A g-value close to one indicates that light is mostly scattered forwards. The reduced scattering coefficient $\mu_{sca(\lambda)}' = \mu_{sca(\lambda)}(1-g)$ compensates for the g factor.

In the optical region mainly two scattering processes dominate - Mie scattering and Rayleigh scattering. Both phenomena refer to elastic scattering events. Elastic scattering means that photons conserve their energy but change direction during a scattering event. In other words, the wavelength of light does not change when light is scattered in a medium. Different wavelengths will be attenuated unequally much because of the absorption spectra of the molecules present and since different wavelengths are scattered differently. This means that different wavelengths travel different distances inside the absorbing volume, not to mention that different wavelengths travel differently deep into the volume and in a inhomogeneous volume such as skin on top of a muscle, deep penetrating wavelengths will have been influenced by other absorption profiles than low penetrating wavelengths. Thus red and blue light will have different absorption imprints since it visited different regions.

In fluorescence, light has to reach the fluorophore and return; thus it will be influenced in both ways by $\mu_{abs(\lambda)}$ and $\mu_{sca(\lambda)}$' when propagating in the medium. The effective wavelength dependence of scattering relies on the dominant scattering phenomenon. Whether Mie scattering or Rayleigh scattering dominates is determined by the wavelength and the particle diameter of the scatters; d. When λ<<d Mie scattering dominates, when λ>>d Rayleigh scattering dominates.

Rayleigh scattering occurs when scatters can be seen as dipoles, where the entire scatterer is influenced by an electrical field, since the wavelength is large in comparison to the scatterer size. Rayleigh scattered radiation is described by the relative simple equation

$$I = I_0 \frac{1+\cos^2\theta}{2R^2}\left(\frac{2\pi}{\lambda}\right)^4\left(\frac{n_1-1}{n_2+2}\right)^2\left(\frac{d}{2}\right)^6 .$$

The scattering coefficient is given by

$$\mu_{sca} = \frac{2\pi^5 d^6}{3\lambda^4}\left(\frac{n^2-1}{n^2+2}\right)^2$$

θ	*direction of scattered light*
R	*distance to scattering volume*
n_1, n_2	*refraction index of scatterer and ambient medium, respectively.*
d	*scatterer diameter*

However, Mie scattering is the dominant process for light transport in tissue. The wavelength dependence of Mie scattering is a complicated function evolving from solutions from spherical boundary condition equations. Interference phenomena generate periodical features in the coefficient arising from scatterers with one single diameter. Obviously, tissue contains scatterers of all possible diameters, and thus the spectral scattering coefficient contains information on the content of microstructures of various sizes in the tissue. Mitochondria are the strongest scatterers but also cell membranes and lipids contribute.

As to relation to scatterer size, we can conclude that the shape of the reduced scattering-coefficient-spectra will contain information about scatterer size. The g-factor is directly related to the scatter size, but unfortunately we cannot determine the g-factor very well from observations of surface scattering. This problem arises because we cannot project an infinitively small point on the surface. When projecting a real sized spot the scattered light that escapes the surface becomes the convolution of many point solutions, since light transport is a linear place independent phenomenon. The g-factor could be determined by having a non perpendicular light incidence and observing the displacement of the maximal light escaping the surface with respect to the incident point.

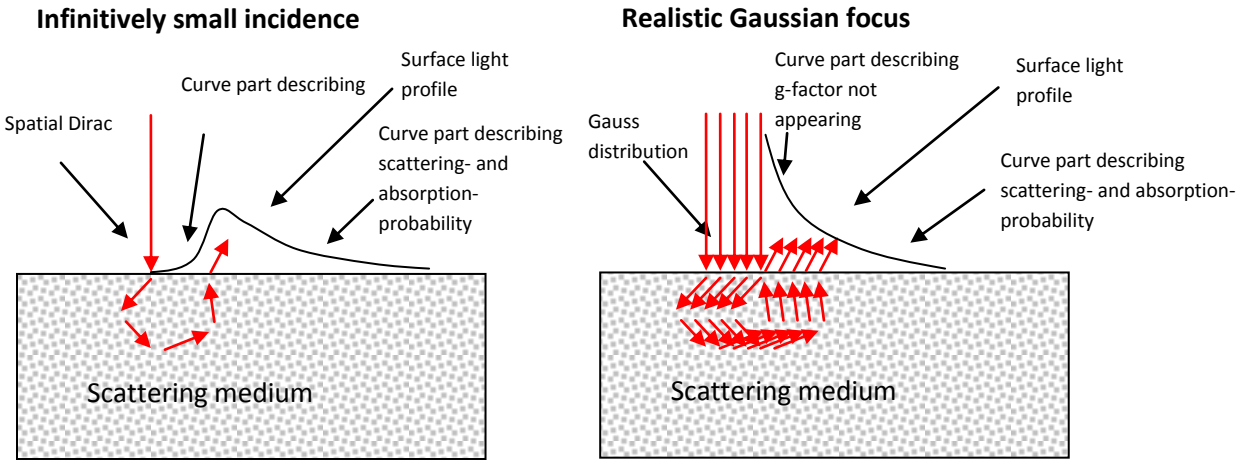

Fig 2.4.2. The reason why the g-factor is difficult to determine by surface observations.

Short light pulses in scattering media will broaden in time. Incident light on a glass of milk is scattered from the lipids and the average photon might travel a distance around five meters before it escapes the glass in a random place at the surface in a random direction. Dividing the distance with light speed in milk, we find that photons that have traveled a short distance are emitted before the ones who traveled far inside the milk volume. Typical broadening values are around 2 ns in tissue. As such both scattering and fluorescence give rise to temporal light delay in scattering media. (Yavari, 2006) (Andersson-Engels, 2007)

2.5 Reflection

Reflection refers to the fact that every object sends back light when illuminated. However we need to divide reflection into two phenomena; specular reflection talking place in the interface, and scattered reflection talking place in the volume of the object.

Specular reflection is what a mirror does. Light is reflected in the interface to the object according to the famous law: the angle of incidence equals the angle of reflection, where the angles are measured in relation to the normal of the surface. Interfaces possess two characteristic reflectance functions which depend on wavelength and angle of incidence. $R_{P(\alpha,\lambda)}$ and $R_{S(\alpha,\lambda)}$ (Fresnel formulae). One function is valid for light polarized parallel to the angle of incidence and one is valid for the light perpendicularly polarized to the angle of incidence. Specularly reflected light conserves the polarization of the incident light if any.

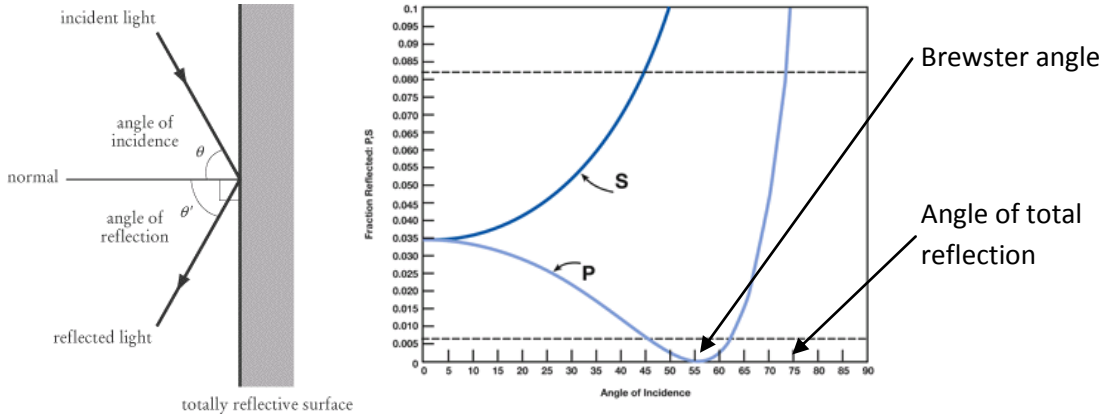

Fig 2.5.1 Left: Specular reflection (Source: http://www.sparknotes.com/testprep/books/sat2). Right: Angular dependence of reflection properties for differently polarized light (Source: http://www.spiricon.com/techinfo)

Reflectance and transmittance of polarized light is given by the Fresnel equations:

$$R_S = \left(\frac{\sin(\theta_t - \theta_i)}{\sin(\theta_t + \theta_i)} \right)^2 = \left(\frac{n_1 \cos(\theta_i) - n_2 \cos(\theta_t)}{n_1 \cos(\theta_i) + n_2 \cos(\theta_t)} \right)^2$$

$$R_P = \left(\frac{\tan(\theta_t - \theta_i)}{\tan(\theta_t + \theta_i)} \right)^2 = \left(\frac{n_1 \cos(\theta_t) - n_2 \cos(\theta_i)}{n_1 \cos(\theta_t) + n_2 \cos(\theta_i)} \right)^2$$

θ_i *incident angle*

θ_t *transmitted angle*

The reflectance applies regardless which direction the light passes the surface. However, the angle for total internal reflection is not the same. We quickly realize that specularly reflected light can hold no information about the volume or the color of the volume, because the light was never inside the volume. One also realizes that it is not possible to see the color of a mirror by looking at it. In spectroscopy, which concerns itself with colors, efforts are made to avoid specular reflections. One strategy is to irradiate polarized light and only detect light which lost its polarization. Here one polarization filter is used in front of the illumination and another one perpendicularly in front of the detector. Another strategy is to detect light from any other angle than the angle of incidence.

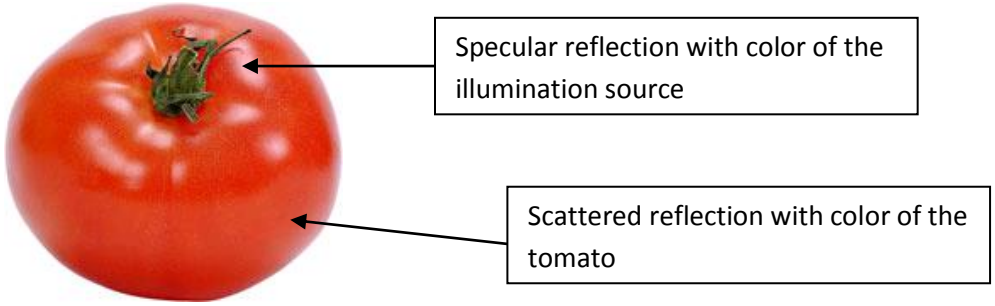

Fig 2.5.2. Specular reflection can hold no information of the volume since the light never entered the volume.

Scattered or diffuse reflection is observed from a glass of milk. Most objects including tissues reflects both specularly and diffusely. Diffusly reflected light is caused by multiple scattering events inside the volume of the object. A fraction of the light will be scattered back to the interface and escape the object; the spectral profile of such light will have been influenced by absorption- and fluorescence spectra of the material in the object. The distance traveled and locations visited by the light, will furthermore be determined by the scattering coefficients $\mu_{sca(\lambda)}$. When reaching the object interface photons will undergo specular reflection once more, but now from the inside of the object and finally, remitted photon will escape the object. The angle of escape is only limited by internal reflection. The polarization is randomized. The incidence and the positions of escape will be a probability function over the surface called a Green's function which relates intensity observed at a given point to the distance of the point of incidence. The Greens function is a solution to the light transport equation approximated by the diffusion model as a inhomogeneous differential equation.

To summarize this chapter we can conclude that absorption, fluorescence and scattering are all functions of wavelength and are characteristic by the composition of a given volume. Neither of the three phenomena can be measured fully correctly in a volume because of the diffuse reflection.

3. Physics of the instruments

3.1 Light sources

3.1.1 Planck radiator

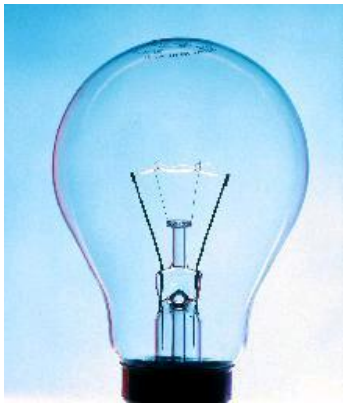

Fig 3.1.1.1 Filament lamp (Source: gallery.hd.org)

The basic concept of filament illumination is to heat up a substance and take advantage of the black body radiation. The black body radiation is generated by vibrations of atoms. The spectral distribution is given by Planck's law of black body radiation:

$$I(\lambda,T) = \frac{2hc^2}{\lambda^5 (e^{\frac{hc}{\lambda kT}} - 1)}$$

T	*temperature*
h	*Planck's constant*
c	*speed of light*
k	*Boltzmann's constant*

Integration gives us the total emitted radiation by the Stefan-Boltzmann law:

$I = \varepsilon \sigma (T^4 - T^4_{amb})$

T_{amb} *ambient temperature*

σ *Stefan's constant with the value* $5.670\,400 * 10^{-8}\ W * m^{-2} * K^{-4}$

ε *emissivity*

By solving for the point where the derivative equals zero, we get the peak radiation position given by Wien's displacement law

$\lambda_{max} T = b$

λ_{max} *peak radiation wavelength*

b *Wien's displacement constant*

The last equation suggests that we can tune the position of the peak emission by changing T. Now T can be found by measuring the electrical resistance in the filament R since it is linearly proportional to T for metals. R can be determined from U and I over the filament. T is controllable through varying the dissipated power P=U*I; thus the peak wavelength of the light source is controllable through varying the applied voltage. However, the total emission is much more strongly dependent of T.

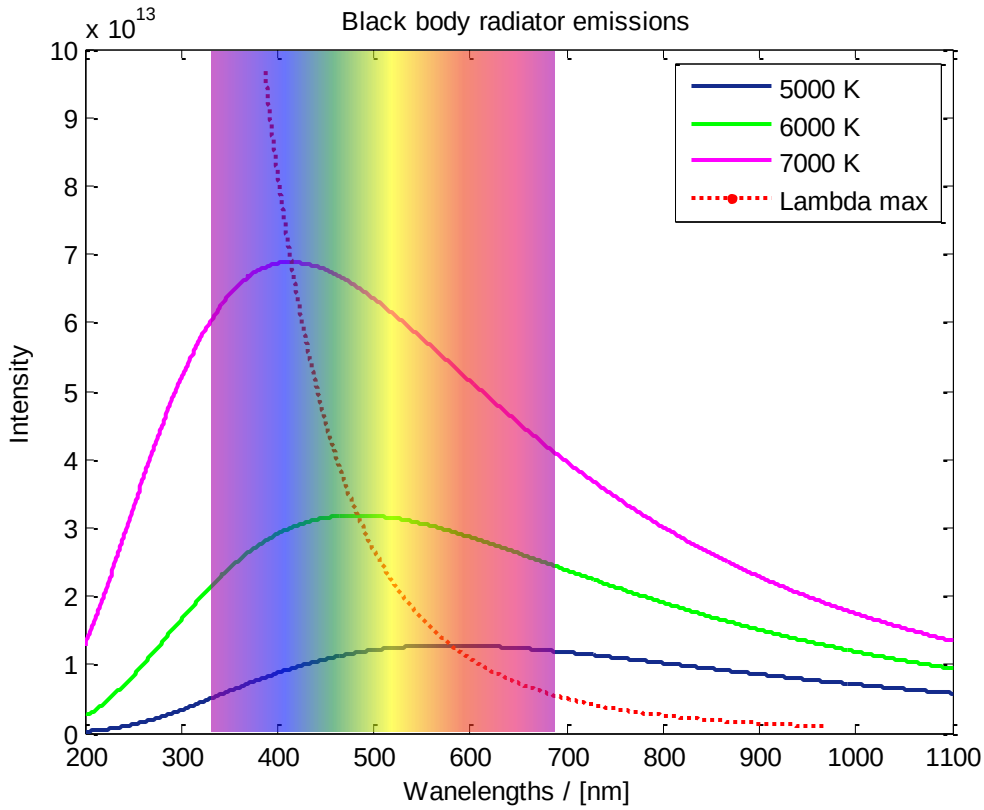

Fig 3.1.1.2 Different temperatures give rise to different spectral contents and peak radiation shifts toward UV when the temperature rises.

3.1.2 Xenon flash

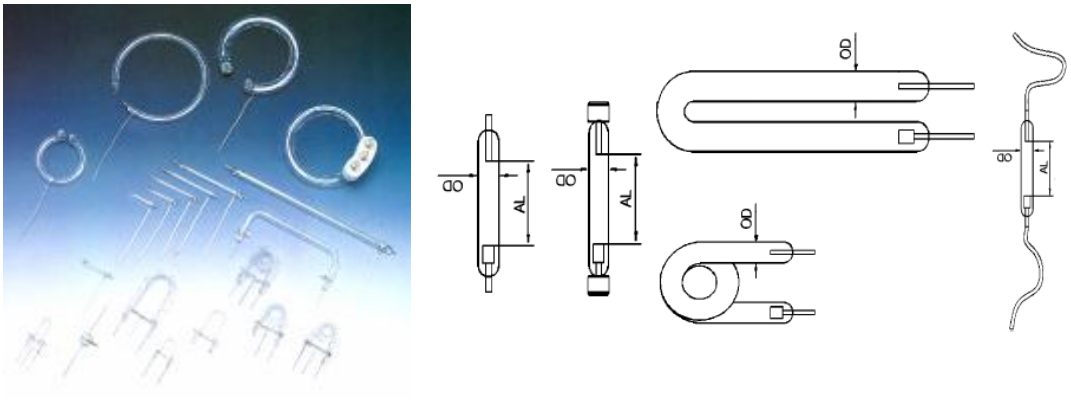

Fig 3.1.2.1 Various shapes of xenon flash tubes. (Source:* EUBON PRODUCTS CO LTD*)

Xenon flash tubes are discharge tubes made from glass or quartz and filled with gas mixtures containing xenon and usually mercury vapor. They are commercially available in various shapes for various applications. They are operated by charging up a capacitor to several hundreds or thousands of volts and connecting it over the tube. When the gas is broken down by an even higher voltage spike applied to a shorter path electrode within the tube, the gas becomes a conductor and shortcuts the capacitor. The extreme current will run through the tube for approximately 200 µs. While electrons pass through the plasma they collide with the atoms of the gas mixture and they excite them, leading to emission of radiation when recombining. The total emitted energy for the pulse corresponds to the capacity and the voltage of the charge capacitor as follows:

$E_{em} \sim E_{el} = ½C*U^2$

C *capacity of condensator [F]*

U *accumulated voltage potential [V]*

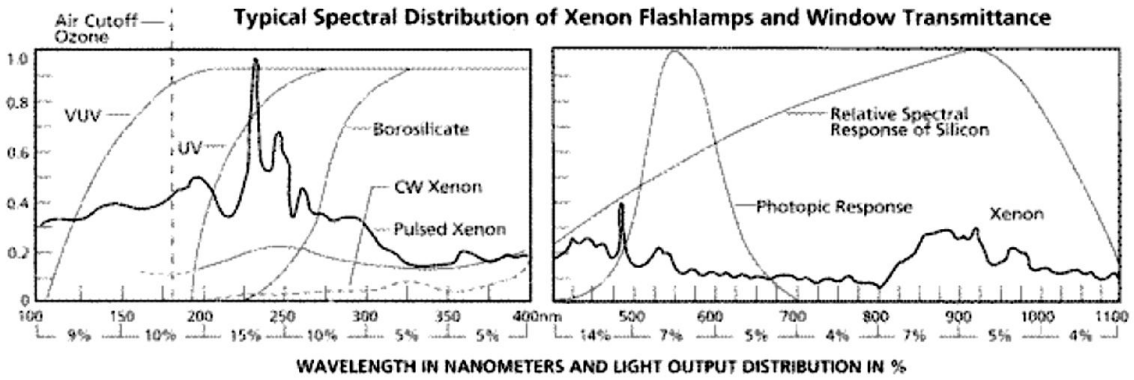

Fig 3.1.2.2 Distribution of energy in the electromagnetic spectrum for pulsed and continuous xenon lamp light. (Source: Perkin Elmer, white papers)

The spectral profile is a combination of a continuous plasma radiation from acceleration of charges and specific spike series from the gas mixture which correspond to the energy levels of the gas atoms. The continuous radiation can be compared to a black body radiation with color temperatures going as far as 15.000K.

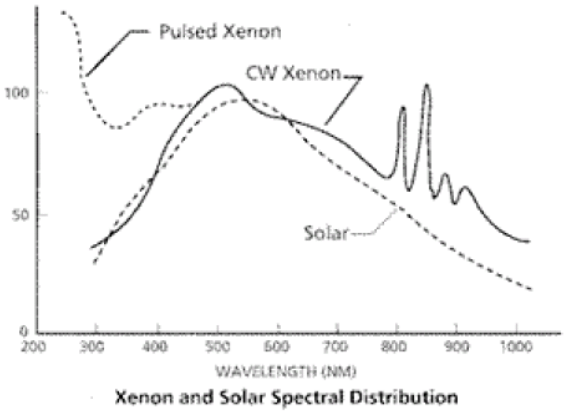

Fig 3.1.2.3 A pulsed xenon flash emits UV suitable for fluorescence (Perkin Elmer, white papers)

The energy of generated photon from a xenon flash is generally limited by the enclosing glass or quartz case. Quartz allows short UV radiation to escape the discharge tube. The next limit will be molecular oxygen absorbing the light and generating toxic ozone. Further to the UV, more species will absorb, requiring vacuum systems.

When it comes to the dynamics of a discharge, the stability will be related to the triggering circuit. The total emission will vary both in time and size. Even with a perfect circuit the gas will introduce uncertainty during break down. This problem might be overcome by letting the discharge tube glow continuously and applying the discharge potential just in time; this more advanced operation mode is used in laser triggering systems. In this project a commercial xenon flash for 10$ was analyzed in time. The pulses were highly unstable, due to the circuitry. The discharge process can typically be described by a function:

$$I(t) = e^{-t/\tau_1} * (1 - e^{-t/\tau_2}).$$

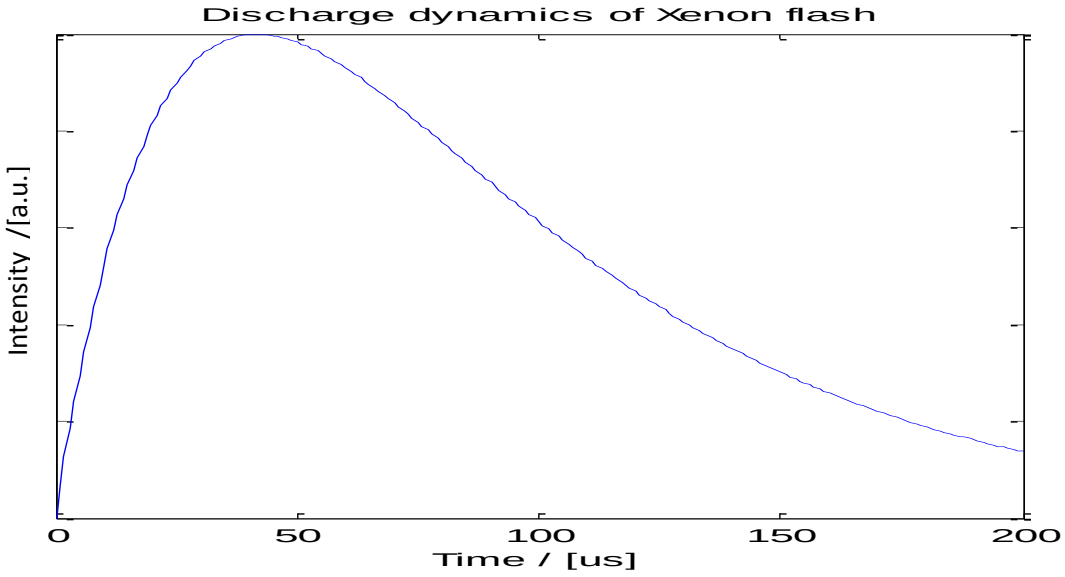

Fig 3.1.2.4 Time dependent intensity during flash discharge

The shape suggests a second-order system, governed by the discharge capacitor and the inductance of the connecting wires. (The heat capacity of the gas should be so fast in comparison and could therefore be neglected as a dynamic state in the model).

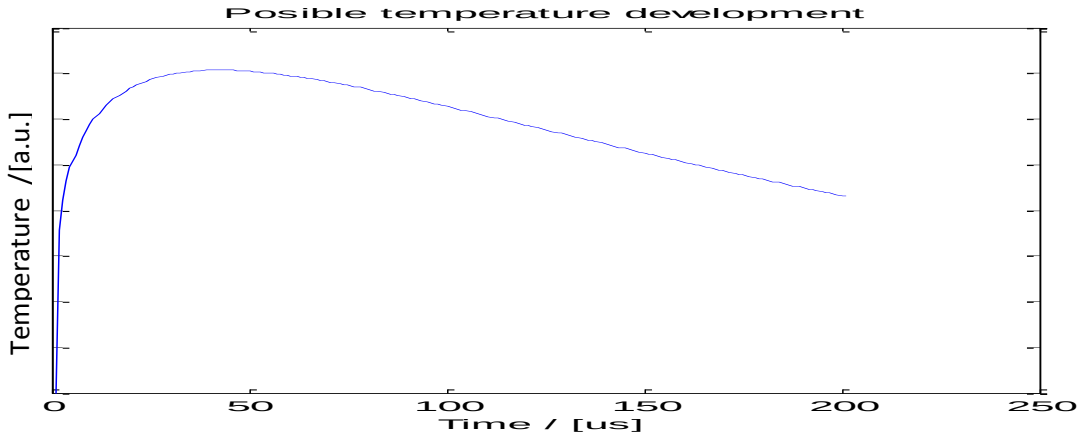

Fig 3.1.2.5 Temperature shift during discharge.

With the Stefan-Boltzmann law in the mind, one might take the forth root to deduce the plasma temperature. Obviously the emission profile will be different for different times; however, a very fast gated spectrometer would be needed to demonstrate this. For spectroscopic issues this fact may cause difficulty to obtain consistent measurements, if the discharge process is not stable. Also it might be a nice source of Wien-Shift spectroscopy since the temperature range is much higher than those for filaments since the dynamics are much higher than those for filaments. Problems will be related to having a fast enough acquisition system.

3.1.3 Short Arc

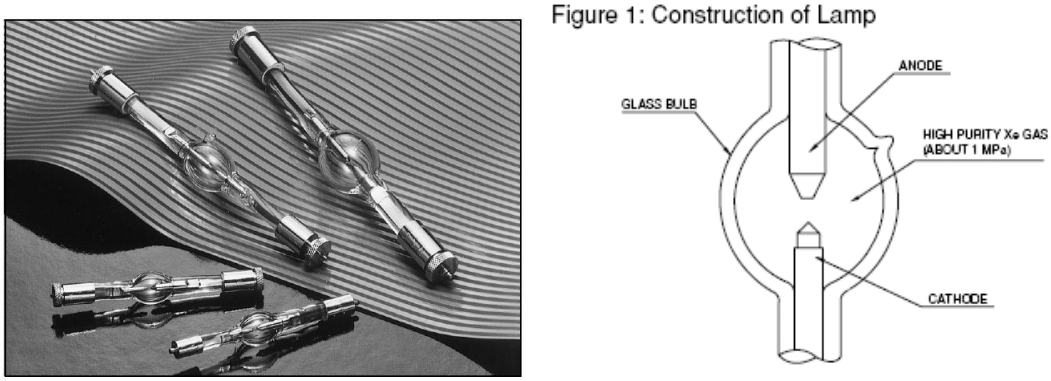

Fig 3.1.3.1 Left: High pressure short arc lamp. Right: Schematics (Source: hamamatsu.com)

Short arc lamps are in many ways similar to Xenon flashes. However, the discharge arc is very small, down to 0.25 mm in diameter. In order to have such a small volume producing considerable light, the pressure is raised up to 70 bars. This makes xenon one of the brightest white light sources available. Such devices are commercial available for movie theaters and as white light sources for spectroscopy. They are usually operated continuously which means that the temperature of the whole device rises to considerable temperatures. The enclosure must therefore be made of quartz to resist the temperature. Any dust or fingerprint on the quartz surface will immediately turn into coal, absorb the light and cause temperature gradients in the quartz, which eventually will led to a violent explosion of white glowing quartz pieces. Apart from the high pressure, the lamp requires extreme high voltages for break down and operation. The radiation generates toxic ozone and the produced UV radiation is highly carcinogenic. The device requires air or water cooling. The lamp can only be placed in approved systems which are generally big in size. Also these systems have a integration timer of the operation shutting down the lamp before its actual life time expires. Lamp mounting must be performed by government approved personnel with protection suits similar to those of military mine sweepers.

3.1.4 Light Emitting Diodes, LEDs.

The light emitting diodes are currently under fast development, and better emission powers and lower emission wavelength are continuously introduced to the market. The devices are relatively inexpensive; prices typically vary from 10 cents to 10$ depending on the wavelength. The low voltage and current enables simple, inexpensive and compact circuitry as well. LED are semiconductor devices and emission is produced when electrons make a transition in energy levels from the valence band to the conducting band in the so called *depletion layer* or junction of two differently doped materials. The recombination can either be emissive or non-emissive and electric-power to light-power conversion efficiency is optimized by adjusting the doping level, crystalline- and chip geometries. The devices have conversion efficiencies or external quantum efficiencies, depending on the wavelength. This efficiency refers to the ratio between consumed electric-power and light-power that escapes the device. (Schubert, 2003)

Generally, light intensity and emissive recombination is proportional to the hole-electron concentration which is again proportional to the current within the region of operation. LEDs generally have two limiting factors for maximal throughput - power dissipation which generally is a heat transfer issue, and maximal current for the chip. Usually, the power dissipation limit shows up long before the maximal current limit, which mean that the LED can be pulsed with a current of a factor ten times larger than the current recommended for continuous operation.

The center wavelength of emission depends on the fabrication material selection and the doping levels. Thus, the wavelength is basically fixed for a given device apart from small dependencies of current and temperature. The emitted center wavelength corresponds directly to the energy drop which can be measured directly on the characteristic voltage drop over the device. As a result, 930 nm IR LEDs typically have around 1.3 V drop, while a 250 nm UV LED have a 6.5 V drop. When current is passed through the LED an additional voltage drop is generated by the bulk resistance. This drop is, however, minimal.

$$\lambda_0 \sim \frac{1}{U_g}$$

λ_0 *Emission wavelength*

U_g *Characteristic voltage drop*

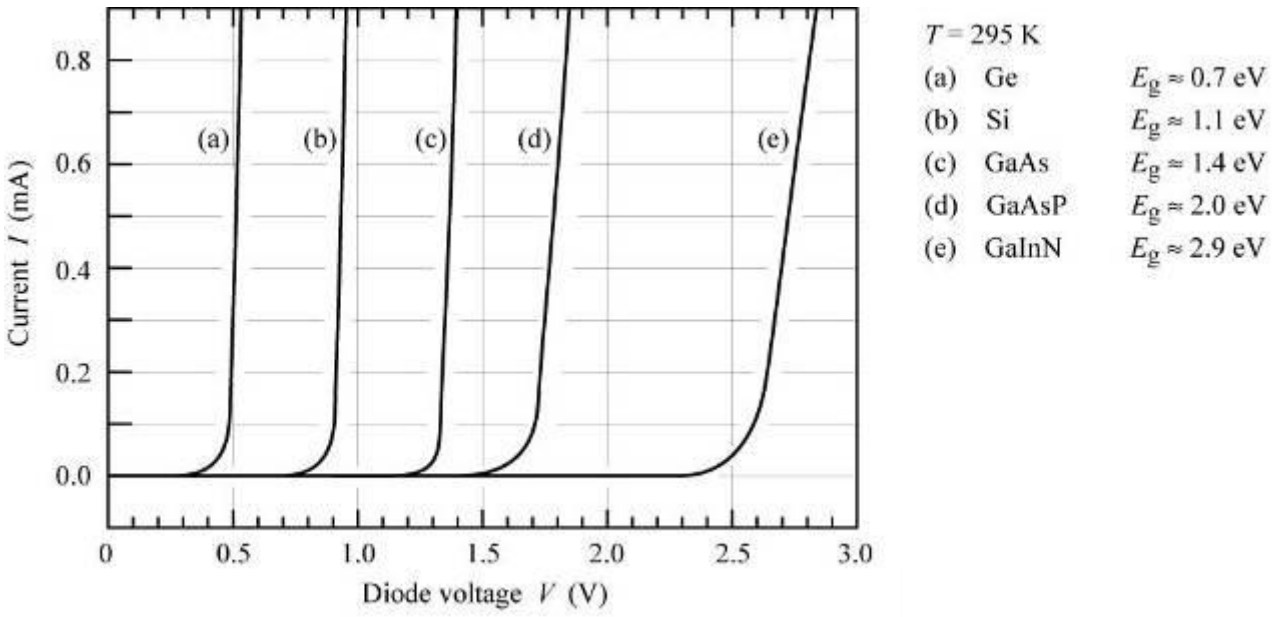

Fig 3.1.4.1 Characteristics voltage drops for LED made from different materials. (Source: lightemittingdiodes.org)

The spectral width depends on the temperature and center wavelength. It is typically described by its full-width-at-half-maximum (FWHM), see fig. 3.1.4.2.

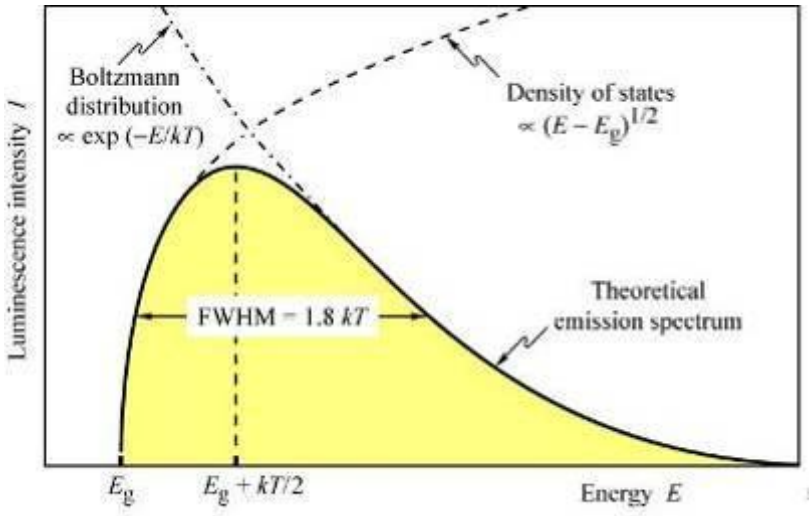

Fig 3.1.4.2 Theoretical emission calculated. (Source: lightemittingdiodes.org)

The spectral width, Δλ, is given by

$$\Delta\lambda = \frac{1.8kT\lambda_0^2}{hc}$$

In reality LED emissions are better approximated by a Gauss probability function, and the FWHM is typically 10-20 nm for UV LEDs.

When modulating LEDs the cutoff frequency is generally limited by two phenomena. One is the capacity created by the thin depletion layer, which is related to the thickness of the layer which again is related to the voltage applied over the device. In parallel to this capacity we will also delay the phase due to electron diffusion in the depletion layer; this is the time that is takes electrons to diffuse out from the depletion layer after operation. As a result the capacitance will influence the rise time and the fall time differently. IR LEDs designed for communication can be operated up to hundreds of MHz. UV LED-based lifetime fluorescence spectroscopy has been reported, also in the hundreds of MHz region. (Herman, 2001)

The casing is typically made of epoxy and also act as a focusing lens defining the emission divergence. For UV LEDs; special UV hardened epoxy must be used, in order to avoid molecular UV breaking of the casing. Even quartz ball lenses are used for the lowest wavelength. For power LEDs, the casings are optimized for heat transfer and are equipped with a metal pad for heat conduction.

3.2. Wavelength separating optics

3.2.1 Prisms

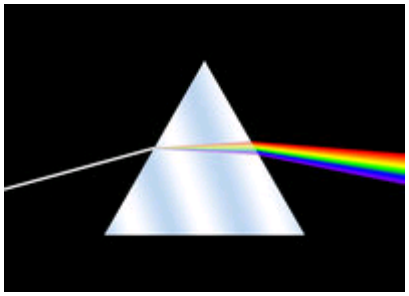

Fig 3.2.1.1 A prism changes light direction according to the wavelength content.

When following a light ray impinging on an interface with a change in refractive index, the process might be thought of as a marching band of soldiers walking into a swamp. In one row the soldiers first stepping into the swamp will be slowed down in comparison to the soldier at their side. The phase delay will cause the direction change of the whole parade. The phenomenon is referred to as refraction and evidently happens in any mismatch interface of two media with different refractive index, e.g. any transmittive optical component, lenses, prism, etc. In such events, the angle change is related to the light speed change, and light speed in many media is again dependent of the light frequency. Different frequencies will split up to different angles, according to Snell's law:

$n_1 \sin\theta_i = n_2 \sin\theta_t$

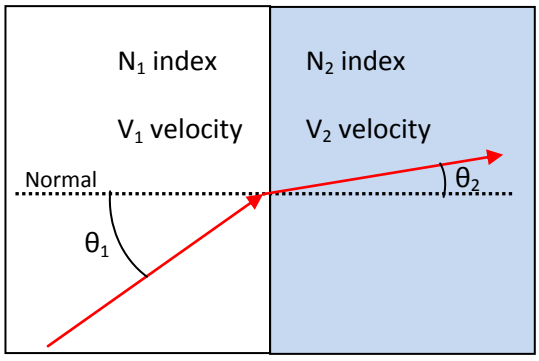

Fig 3.2.1.2 Illustration of Snell's law for refraction

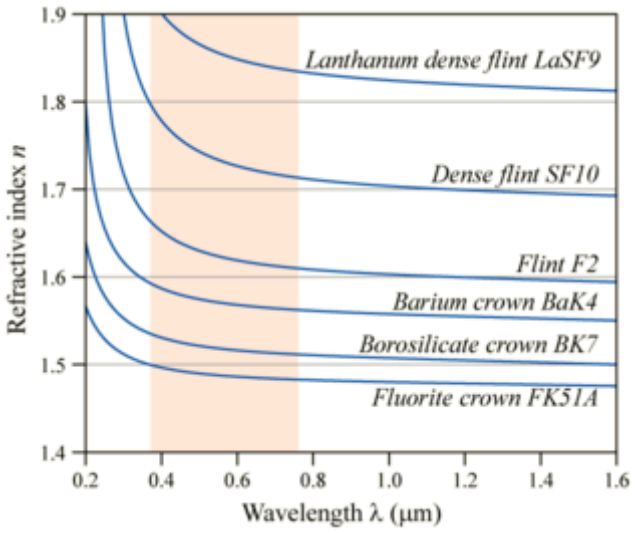

Fig 3.2.1.3 Real part of the refractive index. (Source: Prof. Bob Mellish)

When electromagnetic waves propagate in a medium, the phase velocity will be slowed down since the wave will introduce disturbances of the electric potentials of the atomic charges, the electrons. The influenced charge will in time radiate at the same frequency when they oscillate in the applied electromagnetic field. However, their oscillation will be slightly phase delayed, since the charge cannot respond in polarization immediately to the field change. The macroscopic result of such an atomic phase delay is that frequency is conserved but wavelength diminishes. In other words the light speed is decreased.

The refractive index, n is the ratio between the light speed in vacuum, c, and the light speed, v, in a given medium.

$$n = \frac{c}{v}$$

Under normal circumstances n > 1. Light in a medium is governed by the relative permittivity ε_r, and relative permeability , μ_r. Permeability represents the degree of magnetization of the medium of propagation. For optical frequencies $\mu_r \approx 1$ in most media. ε_r is a complex function of frequency $\varepsilon_{r(\omega)} = \varepsilon_{r(\omega)+} i\,\varepsilon_{r(\omega)}$. $\varepsilon_{r(\omega)}$ changes in relation to structures and phenomena of the corresponding frequency. Causality refers to the fact that it is impossible for a given system to react to a action before the action has impacted on the system. This mean that photon impacting on a given system, can only be delayed. As for other linear systems, the response for a linear mediums to a photon can be described by a complex transfer function or response function. Because of causality poles of the response function must be stable and therefore situated in the negative half plane of the imaginary axis. This means that there will be only energy losses and no energy gain in the medium. The Kramers-Kronig relations state that in analytical functions of the form $\chi(\omega) = \chi_1(\omega) + i\chi_2(\omega)$, real and imaginary part cannot be independent functions (Svanberg, Atomic and Molecular Spectroscopy, Basic Aspects and Practical Applications, 3rd Edition 2001). They must have the relation:

$$\chi_{1(\omega\omega} = \frac{1}{\pi} P \int_{-\infty}^{\infty} d\omega \frac{\chi_{2(\omega\omega'}}{\omega' - \omega}$$

Thus, having one part the other part can be reconstructed, and as can be seen below one part is coupled to the derivative of the other part.

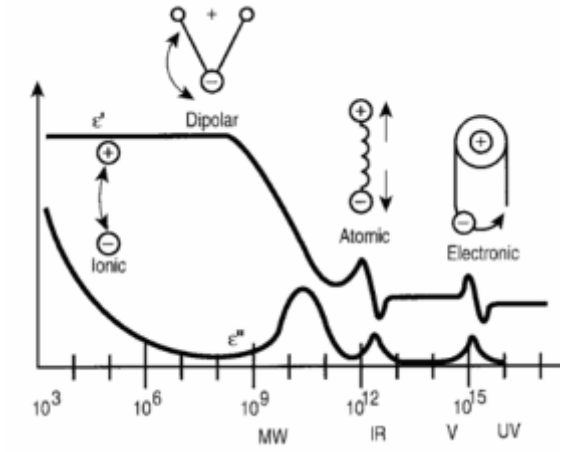

Fig 3.2.1.4 Absorption reflects in behavior of refraction (Source: Prof. Kenneth A. Mauritz)

Complex values of permittivity evidently yield complex values of the refractive index. The real part of n denotes phase velocity, while the imaginary part denotes the extinction coefficient, or as we know it, the absorption coefficient. As a result, light speed and light absorption in a medium cannot be independent functions.

A prism medium with good dispersing properties for a given wavelength means a medium with a large value of $dn/d\lambda$ @ λ_0, which again lead to high absorption and low throughput for λ_0. I.e., one cannot have a prism with good dispersing and transmitting properties for the same wavelength.

When trying to split up a white-light point source and image it according to the wavelength contents, one would require a focusing component, such as a lens or a spherical mirror. The dispersing prism must have the longest possible distance to both point source and image plane, this in order to gain maximal effect of the small divergence angles between wavelengths. This means that the prism should be located as close as possible to the focusing mirror or lens. Considering a cone-shaped ray set converging to a focus, which we want to disperse with a prism, we require the rays to impact of normal axis to the prism surface to obtain a dispersing effect from Snell's law. A cone intersection with a plane of the normal axis will produce a paraboloid, the result of which is that the focus will suffer from heavy astigmatism. Possibly this can be compensated for with a cylindrical focusing component, but again this will create more complexity. A typical setup to avoid this is to make the set of ray parallel when impacting on the dispersing interface; again this requires one additional focusing component.

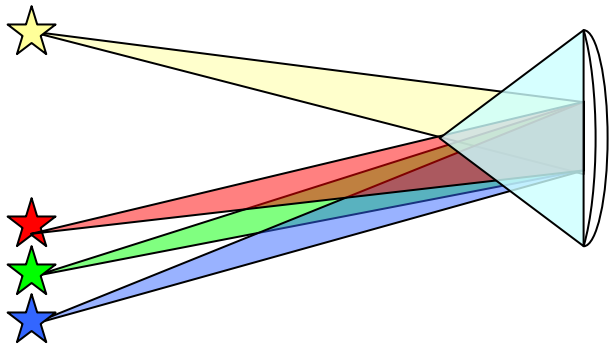

Fig 3.2.1.5. Prism separating wavelength with a single focusing component.

3.2.2 Gratings

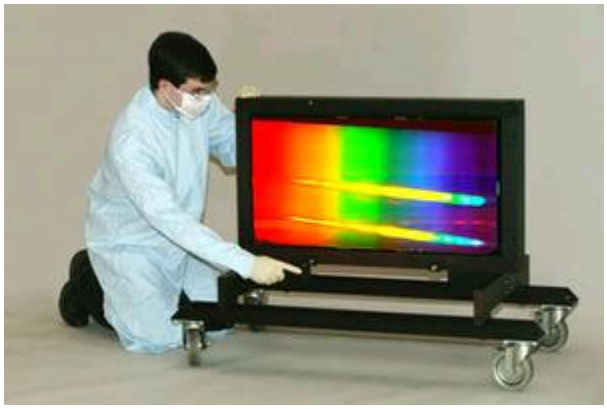

Fig 3.2.2.1. Large grating for space purpose (Source: Nasa.gov)

Gratings have a pattern of narrow lines superimposed either on a reflective mirror or on a transmittive window, typically with hundreds to thousand lines called grooves per millimeter. Each illuminated line reacts as a line light source, and each such line source interferes with the others, because of the wave photon dualism, photons are coherent with themselves and can even interfere with themselves. Having "many" interference sources as we do when illuminating several centimeters of a grating, we produce great contrast between angles where constructive interference dominates for a given wavelength and areas where destructive interference occur. In other words, a certain wavelength will be diffracted in certain directions given by the grating equation

$\sin\alpha + \sin\beta_m = m\lambda/d$

α	*incident angle, blaze angle*
β_m	*diffracted angle for order m*
d	*groove density*

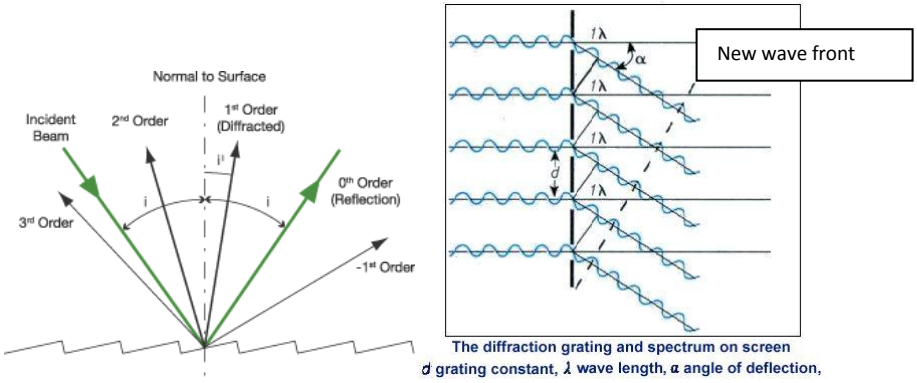

Fig 3.2.2.2 Left: Diffracted orders from a single wavelength. Right: Grating rules can be thought of as interfering line sources. (Source: thinkquest.org)

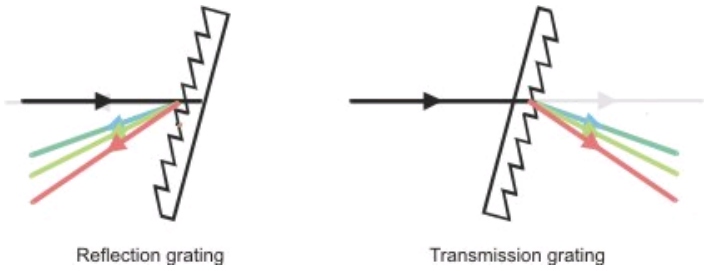

Fig 3.2.2.3 Gratings can be both reflective or transmissive.

As can be understood from the interference drawing, not only one, but several directions yield constructive interference for a given wavelength. The incident light power for a given wavelength is distributed among the diffraction orders in decreasing intensity. The zero'th order is usually the strongest one but represents a specular reflection without any color seperation. By optimizing the line pattern spatial waveform, the optical energy can be optimized to dominate for a given diffraction order and for a given incident angle and wavelength. Changing the spatial waveform of the pattern is referred to as *blazing*. Blazed grating are made with a specific blaze angle where the diffracted efficiency in a particular wavelengths region and a particular order is optimized. To this angle also correspond a blaze wavelength, for with the efficiency is optimized.

Since mostly just one order of a diffracting grating is utilized, the efficiency of a grating is set by the energy transfer from a specific wavelength to emittance of the same wavelength in the $+1^{st}$ or -1^{st} diffracted order. Apart from the pattern waveform also the reflectance of the coating determines the efficiency for a given wavelength. Since reflectance depends on the polarization of the incident light, gratings will have two efficiency curves depending on whether incident light is polarized parallel or perpendicular to the grove lines.

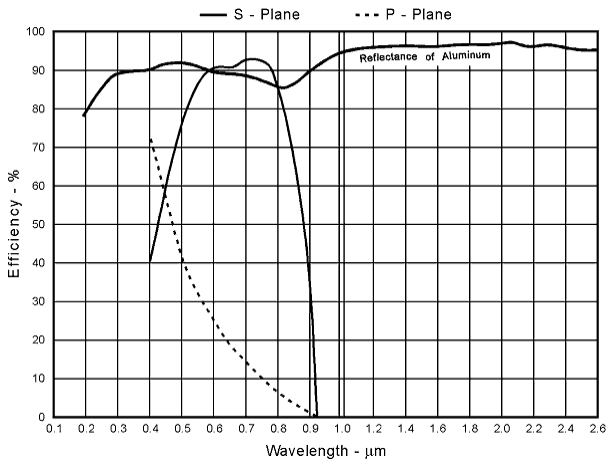

Fig 3.2.2.4 Efficiencies for different wavelengths and polarizations. (Source: Newport)

Overlapping orders constitute a considerable issue whenever one wishes to cover a spectral region containing one or more integer multiplication of the smallest wavelength of interest. Covering a region from 300 nm to 1100 nm, means that the +2nd order of 300 nm light will be diffracted in same angle as +1st 600 nm, and +3rd 300 nm light the same as +1st order 900 nm light. Higher-order diffractions can either be cancelled by digitally subtracting the repetitive spectra; however this will yield decreased dynamic performance. Or, higher-order diffraction can be filtered out by high-pass filters, in such cases filter fluorescence can be an issue.

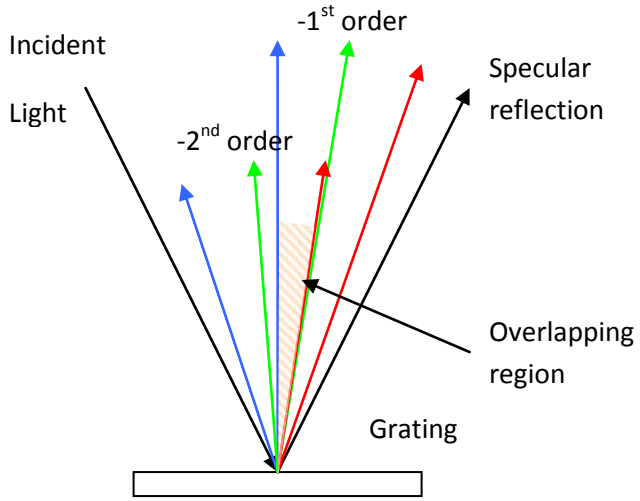

Fig 3.2.2.5 Overlapping spectral regions.

Production of gratings is generally expensive, since few consumer products are based on spectroscopy. A grating of a couple of square centimeters typically costs hundreds of dollars and much more if a custom grating is required. Gratings are typically ruled or holographic. Ruled gratings are superior in efficiency while holographic are superior in reduction of *stray light* (Light scattered in other direction than expected). Ruled gratings are produced with a ruling machine with a diamond tip guided by laser interferometry. Holographic gratings are produced by a laser produced optical interference pattern followed by etching.

The geometry of a grating is originally a plane, but advantages can be made by superimposing the pattern on a concave mirror; by doing so there is no need for additional focusing components, and a slit or point source can be imaged directly according to it's spectral contents. If considering monocromators which reject all but one wavelength, gratings may even be created inside fibers, so called fiber Bragg gratings. By applying strain to the fiber the wavelength can be slightly tuned. (Kumazaki, 2000)

3.2.3 Linear Variable Filters (LVF)

Fig 3.2.3.1 Collection of linearly interference filters. (Source: Ocean optics)

Linear Variable Filters (LVF) are interference filters. They are made from several wedge-shaped coatings and by destructive and constructive interference they can either block or pass certain wavelengths at certain position and in certain direction. Highpass, lowpass and bandpass filters are commercial available. The blocking efficiency increases as an exponentially decaying function of the number of coating interfaces. This means that only by infinitively many interfaces complete blocking can be achieved. The transmission is not ideal. However, the filter being reflective of nature, has an advantage over absorption filters; there will be no distorting filter fluorescence, which has proven to be a considerable issue in fluorescence measurements. In general all interference filters are angular dependent. When either considering bandpass, lowpass or highpass filters the specific cutoff wavelength can be shifted by changing the angle of incidence.

$\lambda_\theta=\lambda_0[1-(n_0/n^*)^2\sin^2\theta]^{½}$

λ_θ cutoff wavelength

λ_0 cutoff wavelength at normal incidence

n_0 refractive index of surrounding medium

n^* effective refractive index for filter

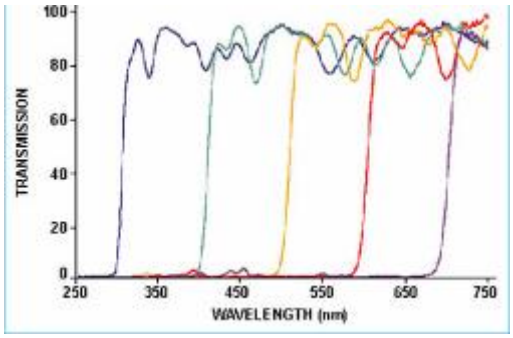

Fig 3.2.3.2 Sample transmissions at different positions of the filter. (Source: Ocean optics)

3.3.Focusing optics

3.3 Mirrors

In imaging and even in spectroscopy where we wish to image a slit or a point source on a spectral plane, a focusing component is required. Focusing components are in general lenses or spherical mirrors, and they act as a combination of an aperture and a converter between angle and position. Regardless of considering lenses or mirrors, distances from the component to the object and the image plane is given in relation to the focal distance as follows:

$$\frac{1}{S_1}+\frac{1}{S_2}=\frac{1}{f}$$

This is an approximation for small incident angles of light, θ, when sin(θ)≈θ due to Taylor's expansion. When rays origin from an object off axis further Taylor terms must be taken into account and a point source is no longer imaged to a point. The phenomenon is referred to as astigmatism.

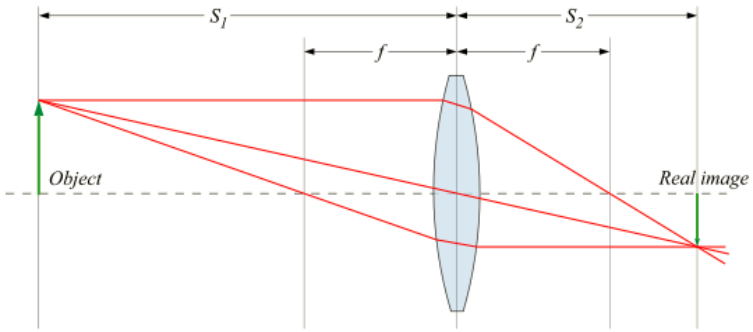

Fig 3.3.1 Classical lens formula

The focal lengths, f, depends on the geometry of the lens or mirror, and furthermore on the wavelength for lenses. Image magnification, M, is given by the relation $M=S_1/S_2$ while minimal focus, d, and diffraction limits are related to wavelength, focal length and aperture.

$$\mathrm{d}=1.22\lambda\frac{\mathrm{f}}{\mathrm{a}}$$

d *diffraction limit size*

f *focal length*

a *aparture*

In spectroscopy and not least in fluorescence spectroscopy, any transmittive component the light will not only introduce absorption losses which need to be calibrated for, but also instrument fluorescence will occur in the components. Since such fluorescent light will be emitted omnidirectionally and will be dependent on both the impinging wavelengths and power, and posses instrument-specific fluorescence profiles for each incoming wavelength, it is basically impossible to calibrate exactly for such phenomena. Furthermore the focal distance for a lens depends of the wavelength of light. For this reason one will find minimal use of transmissive components in spectrometer and similar polychromatic instruments for fluorescence.

Spherical mirrors are typically produced by applying aluminum coatings on a spherical glass substrate. For improved and extended reflectivity in the UV region special interference coatings can be applied. IR response is typically achieved by gold coatings.

3.4. Light detection

The components responsible for light detection transform intensity of light into to an electrical signal. For spectroscopic purposes it is preferable to acquire a whole series of light signals in different colors. For such purposes imaging devices are suitable. Imaging devices consist of arrays of light detectors; we refer to them as *pixels*. We will discuss two technologies which are particularly useful for this project; CCD and CMOS imagers.

The performance of light detectors in general is given by the sensitivity, S(λ). If the incident light on the is I(λ), the signal from the light detector is given by:

$$u_1 = \int_0^\infty S(\lambda) I(\lambda) d\lambda$$

u *electrical signal*

S *sensitivity*

The signal also depends on the two angles of light incidence. Thus we can write: $I(\lambda,\alpha_1,\alpha_2)$. However in imagers, all detectors are in a relatively small plane. Thus, we can assume light from a given point to impact on all detectors in the same angle.

Few systems are perfect and neither are light detectors. Not only light gives rise to signal readout. Noise is a general concern, and the dominant noise sources are referred to as dark current, thermal noise and shot noise, depending on the detector type. Noise can be reduced considerably by lowering the temperature, but cooling systems take up space both in the application and in the budget. Worst of all, cooling the detector yields condensing of water, which distorts both measurement and equipment. Adding noise *w* the detector now has the following read out:

$$u_1 = \int_0^\infty S(\lambda) I(\lambda) d\lambda + w$$

Furthermore in imagers the signal accumulates during an exposure. The signal after an exposure is proportional to the exposure time.

$$u_2 = u_1 * \Delta t$$

Accumulating imagers have a maximum limit of accumulated signal. This is generally referred to as *full well capacity*. If one desires to make an image of a still standing rain cloud, one could arrange an array of buckets on the ground and derive the shape and density of the cloud by measuring the level in each bucket after a certain rain *exposure time*. If all buckets are put in at once instance of time and collected in another instance of time, it is referred to as *global shutter.* If buckets are put one by one by a man, and later collected one by one in the same orders as they were put by another man we call it a *rolling shutter* (Meingast, 2005). In last case exposure time correspond to the time a single bucket was standing in the rain, not the time for producing the entire image. The two shutter techniques will give the same result as long as the cloud remains still during exposure. The bucket size would be the *full well capacity*. The ratio between bucket-filled area and the total area is referred to as the *fill factor*. If the cloud in some place is particularly dense the rain will fill up the bucket completely at certain places. We refer to this phenomenon as *saturation*. Saturation destroys the relation between the buckets, since we have no way of knowing if the cloud was just slightly denser at this spot or if it was many million of times denser for some reason. Of course we can change the exposure time and take several pictures - one of the million times bigger spike and one of the rests of the cloud, with the saturated bucket. However, this will not be possible on the CCD since charge from one pixel will spread to neighboring pixels. Think of it as water not only floating over the bucket side and wasting the water, but ever distorting the neighboring pixels by spilling water into those buckets as a result of the saturation. This phenomenon is referred to as *blooming*. Now, let us imagine that every bucket has centimeter marks to quantify the rain levels. Converting the levels into cm would be called *discrimination*, and the space between the marks would be the *dynamic resolution.* A level change lesser than ½ cm will be neglected. *Dynamic resolution* is mostly specified in # of bits or dB. New imagers might be *logarithmic;* this correspond to having cone-shaped buckets, where little rain gives big level change, while much rain gives less level change. To finish this small illustrative example, think of dark current and noise as random contribution to the bucket array as the birds flying over and dropping who knows what in the buckets.

Color imagers are detector arrays with color filters superimposed on the chip. In this way only certain bandwidths of light are able to activate certain pixels. One color pixel is later created from several monochromatic pixels with color filters by spatial interpolation. As understood, photon economy is poor since light is lost in the filters, and furthermore spatial resolution is lost since it requires several pixels to create one color pixel. The superimposed color filters emulate the human eye in respect to wavelength; as such there is not much use of color imagers in science and spectroscopy. The standard red, green, blue- color filter is referred to as Bayesian color filter.

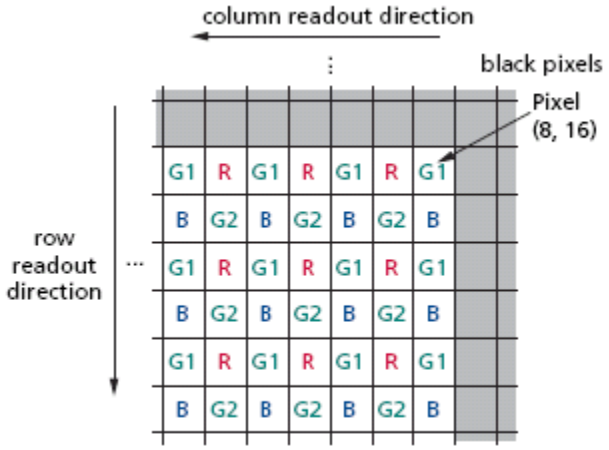

Fig 3.4.1 Red, Green, Blue Bayesian color filter. (Source: Micron)

3.4.1 CCD – Charge Coupled Devices

Charge coupled devices (CCD) take advantage of the photoelectric effect. When photons impact on a pixel, they remove electrons and charge accumulates. From the back side of the pixel the opposite charge is applied during exposure so that the accumulated photon charge remains on the pixel. Readout is done only at the borders of the CCD; therefore the charge from each pixel must be moved to the border of the sensor. This is done by sequentially moving the potentials on the backside of the CCD. The result is a displacement of all photon charges along one axis. The row of charges which left the sensing area is later moved to a amplifier and ADC one by one, by the same method that was used to move charges in on the sensor. If the exposure time is too long, charge at certain pixels will eventually overflow and leak to the neighboring pixels - the phenomenon of blooming. It not only distorts the linear relation for than certain pixel but even distorts neighboring values. This is a considerable issue when requiring high dynamic resolution in images with extreme contrast, as for example spectroscopy with large peaks of excitation.

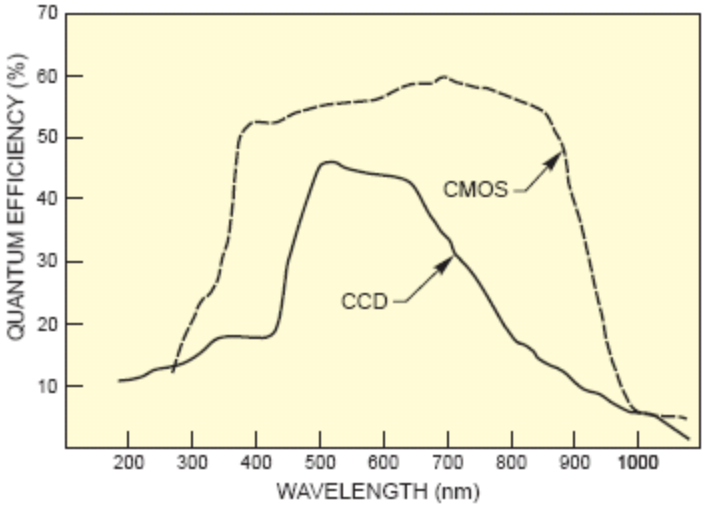

Fig. 1 Quantum efficiency of CCD and CMOS Detectors.

Fig 3.4.1.1 Comparison of quantum efficiencies for different technologies. (Source: Oriel)

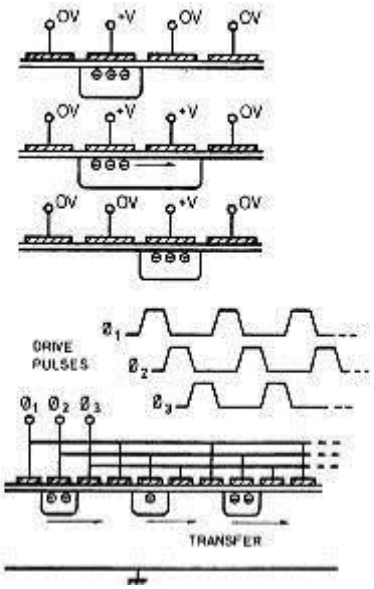

Fig 3.4.1.2 Schematics of movement of charge in time (Source: www.astro.virginia.edu)

CCDs are considerable expensive, not at least CCDs for astronomical and scientific use. Sensor chips easily cost 20,000 $ especially for improved sensibility sensors. Also CCDs are analog and require considerable additional circuitry for amplification, filtering, discrimination and interface. Several efforts can be made to increase or extent the spectral response of CCDs. Scientific CCD are often “back thinned” and light impacts on the chip from behind instead. This option allows new chip geometries where light has to travel less inside the silicon before it generates the photon charge. Because of bulk absorption in silicon, especially in the blue region, back-thinned CCDs increases quantum efficiency significally. However, it decreases the red response. Coatings for improving transmission and trapping photons inside the sensitive region can also be applied. Generally, high wavelength response extension is limited by the photon lack of energy to get the electron over the band gap, while blue or UV response extension is limited by the penetration depth for the light in the sensor chip. The last mentioned limitation can be overcome by down-conversion; this technique refers to a phosphor coating transforming UV efficiently into longer wavelengths where better spectral response prevails.

3.4.2 CMOS Imager - Complementary metal–oxide–semiconductor Imager

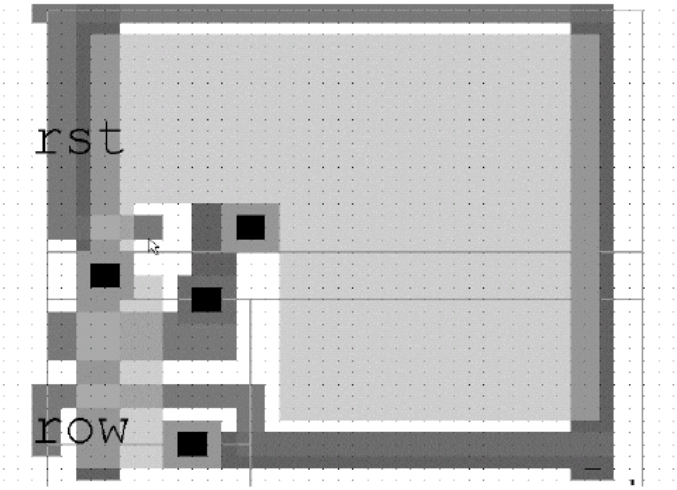

Fig 3.4.2.1 Typical L-shaped CMOS pixel revealing pixel circuitry in lower left corner. (Source: Yadid-Pecht, Senior Member, IEEE)

Complementary metal–oxide–semiconductor Imagers (CMOS imagers) represent a young technology, which goes back to the beginning of the millennium. Markets show rapid development of CMOS imagers, and they are expected to outcompete CCDs in the coming decades. Also they have enabled various new application such as cheap webcams and imagers in cell phones. In comparison to the CCD, where the charge is accumulated on the pixel it self, in the CMOS imager, the pixel consists of a photodiode. The photons can be absorbed in the depletion layer of the photodiode and generate a reverse current which accumulates on a nearby capacitor until read out. For this reason, every single pixel will even contain a small circuit for amplification, accumulation, reset and read out. Since such circuits also takes space on the chip the photosensitive ratio or *fill factor* is generally lower than for CCDs. Also the pixels are typically L shaped, which can generate certain artifacts in the images under special conditions. (Yaddid-Pecht, 2005)

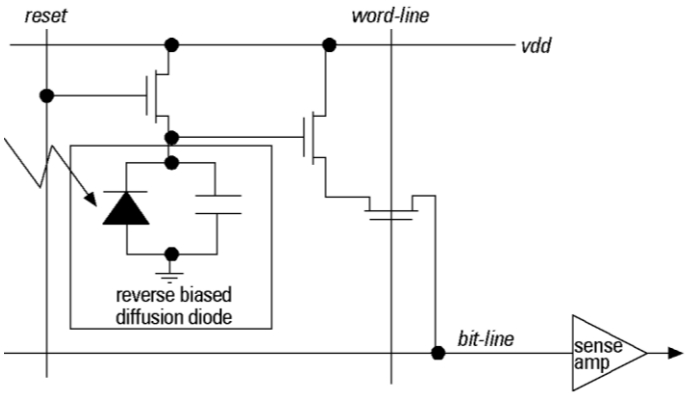

Fig 3.4.2.2 Example of a CMOS pixel circuit. (Source: www.emeraldinsight.com)

Inexpensive CMOS imagers typically come with rolling shutters. This mean that rows of pixels are not exposed to the image in the same time space. First a reset row will roll down over the sensor and after a readout-row will roll over the sensor. The time between a reset and readout passes a certain row, is the exposure time. Thus in a movie capture sequence with rolling shutter the image frames are not orthogonal to the time axis. Image artifacts occur when scenery is moving or the illumination changing. For this purpose most webcams have the option for indoor/outdoor illumination and 50/60 Hz power frequency. More expensive CMOS imager version have global shutters as CCDs, however. Uniformity is slightly worse for CMOS than for CCDs; this is due to wafer quality. Electronic noise is worse for CMOS, due to the on-chip circuitry.

CMOS advantages over CCD are several. CMOS is a standard chip fabrication procedure, which makes CMOS imagers cheap in comparison to CCDs, especially considering the whole system, since electronics can be incorporated on the chip. Megapixel sensors can be bought for a couple of dollars. Furthermore additional circuitry can be placed on the same chip; this includes analog signal processing, ADC, frame memory, image processors, compression algorithms, computer interface and communication protocols. This means that basically nothing more than a cable is required to connect a CMOS imager to a computer, and the sensor output will be delivered digitalized. Processing can take place at pixel levels, for instance a logarithmic function can be applied to avoid saturation, and much higher dynamical resolution can be achieved by CMOS imagers by converting pixels to floating-point-like values individually (Webinformation, 2007). Since CMOS imagers accumulate, the photon charge on a isolated capacitor, there will be no blooming and overflowing of charge from one pixel to another. Responsivity is surprisingly better for CMOS even thought the fill factor is smaller; this is due to pixel-based amplification. Power consumption is less for CMOS which makes them attractive to mobile applications. CMOS also provide much faster readout, and frame rates can be in several hundreds of Hertz.

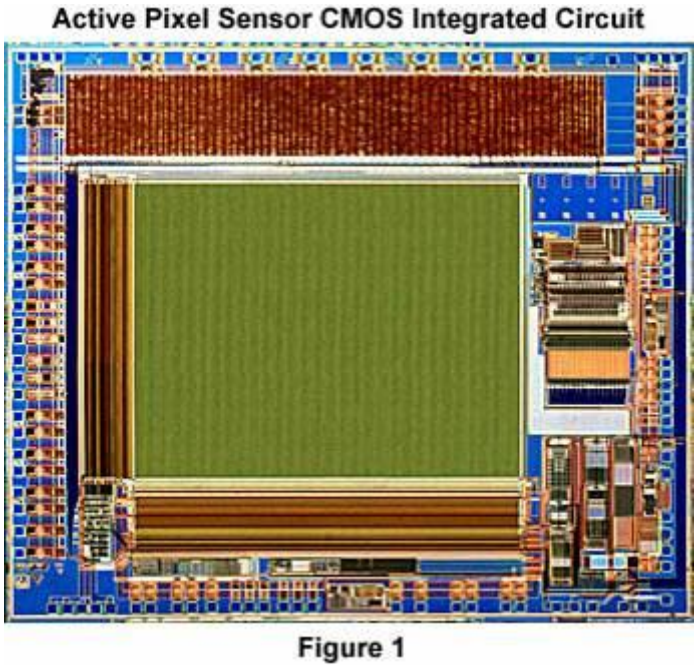

Fig 3.4.2.3. CMOS image sensor layout. The additional amplification, signal processing, memory; interface is placed on the same chip. (Source: www.microscopy.fsu.edu)

4 Measurement setups

4.1 Simultaneous measurement of fluorescence, scattering and absorption.

4.1.1 Inspiration and evolution of concepts

Since we concluded that the volume characteristic factor for fluorescence, absorption and scattering cannot be measured independently, we quickly realize that when we wish to build a model to quantify or identify a certain chemical composition by just one of the three factors, we will come up with a model which is not necessarily unique. If we build a model for estimating the AGE content in a individual only using fluorescence, then we cannot expect the model to answer correctly for both a Swedish person and an African person, because absorption in the skin differs considerably and the model has no knowledge of differences in the absorption spectra. In another case a fat individual with the same AGE content as a slim individual might produce different fluorescent spectra due to increased scattering by lipids. It is clear, that in order for the model to provide exact results for a verity of individuals it must be fed with all relevant information. This is similar to when a doctor needs all relevant information to produce a reliable diagnosis.

It makes sense to ask ourselves, is there a simple way to measure fluorescence, absorption and scattering for a range of wavelength? Fluorescence is often presented as an excitation / emission matrix (EEM). In this case a surface is built from several fluorescence spectra with different excitation wavelengths. Is there a way to physically construct such a matrix and project it onto an imaging device? In that case, what signal can we expect at the imager?

We would need to project a small rainbow line onto the skin. Points along the line would be illuminated by different wavelengths. We will refer to this axis as the excitation axis. It will be projected through a narrow slit. We could produce such a line on the skin by imaging a white point source, e.g. a fiber tip through a grating or prism. By imaging the line through a grating perpendicular to the first grating, we will project emitted light from each point according to its wavelengths content. We will refer to this axis as the emission axis. The two axes expand a plane image that we will project on an imager.

A pure reflecting object will only emit the same wavelength as it was illuminated by in every point along the excitation axis. The result on the imager will be zero apart from the diagonal values. The values along the diagonal will represent the reflection spectrum of the subject. The spectral resolution or width of the diagonal is determined by the size of the point source and a slit towards the sample.

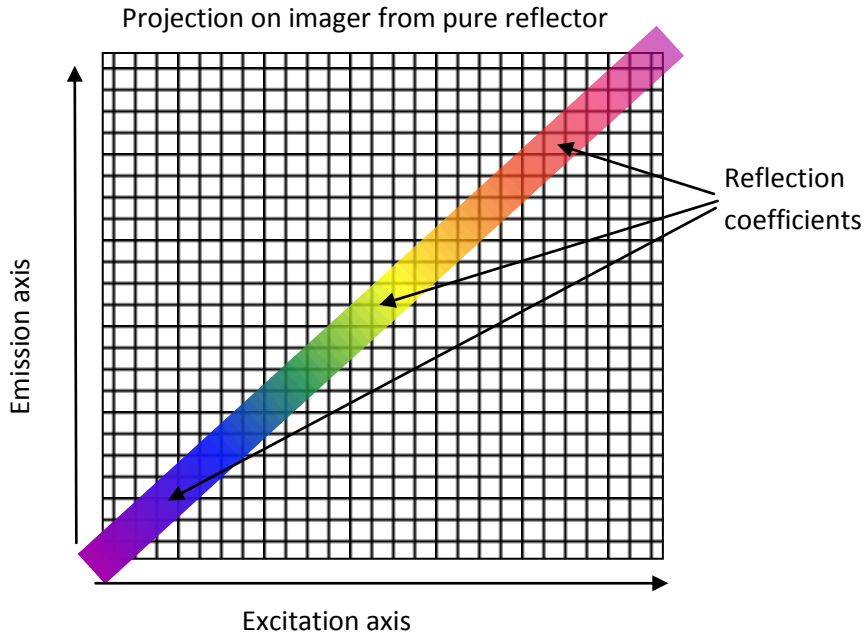

Fig 4.1.1 Reflection is measured on the diagonal

In a elastic scattering object illumination at one wavelength, at a given point in the line, light will scatter and escape the surface at neighboring points. Neighboring points include points along the excitation slit; this means that a given wavelength at a point makes a spectral contribution in the neighboring point through scattering events. The spreading will occur along the excitation axis only, since the slit only sees along the excitation axis. Spreading will depend on wavelength, but it will be symmetric from the point of incidence. Red and IR light will spread more than blue and UV light. The scattering can be evaluated from the intensity obtained at different distances to the diagonal on lower triangle of the matrix. We will refer to the light intensities at pixels in the lower triangle as the scattering coefficients. In order to have symmetric scattering the light most impact perpendicularly in the plane containing the excitation slit. Non perpendicular incident would provide the g-factor for the scattering, but since the scattering would no longer be symmetric, information from fluorescence would be lost.

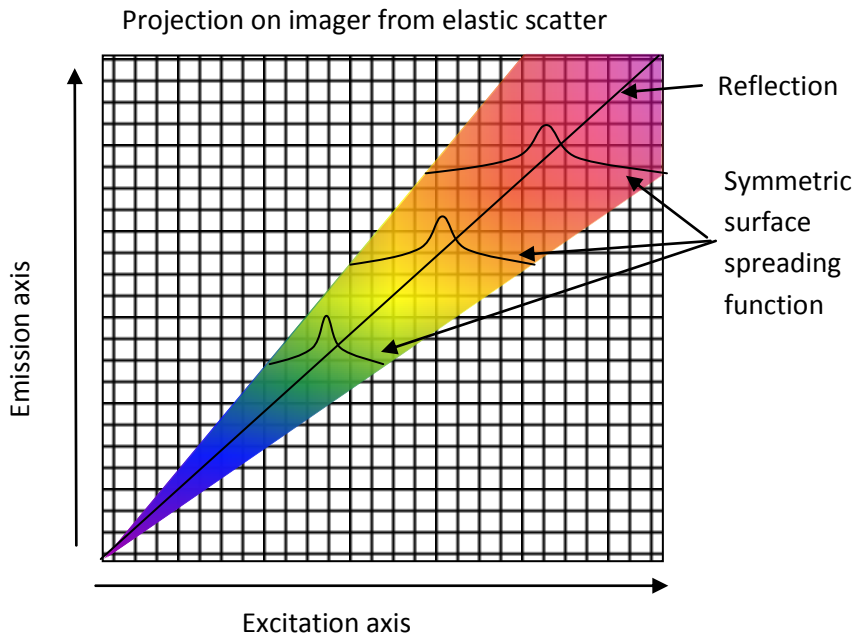

Fig 4.1.2 Scattering and absorption determines how light spreads out along the excitation slit

A fluorescent object will emit a fluorescent spectrum for each excitation point. Since fluorescence only has the ability to shift wavelengths upwards, only the upper triangle will be influenced by fluorescence. We will refer to the light intensities in pixels at the upper triangle as the fluorescence coefficients. It may very well be argued that the excitation light can also spread by scattering and result that one fluorescence spectrum is excited at various wavelength, but fortunately fluorescence is a consequence of absorption, and absorption limits light from being spread, in other words; IR light spreads much, but does not excite, UV light excites much but does not spread.

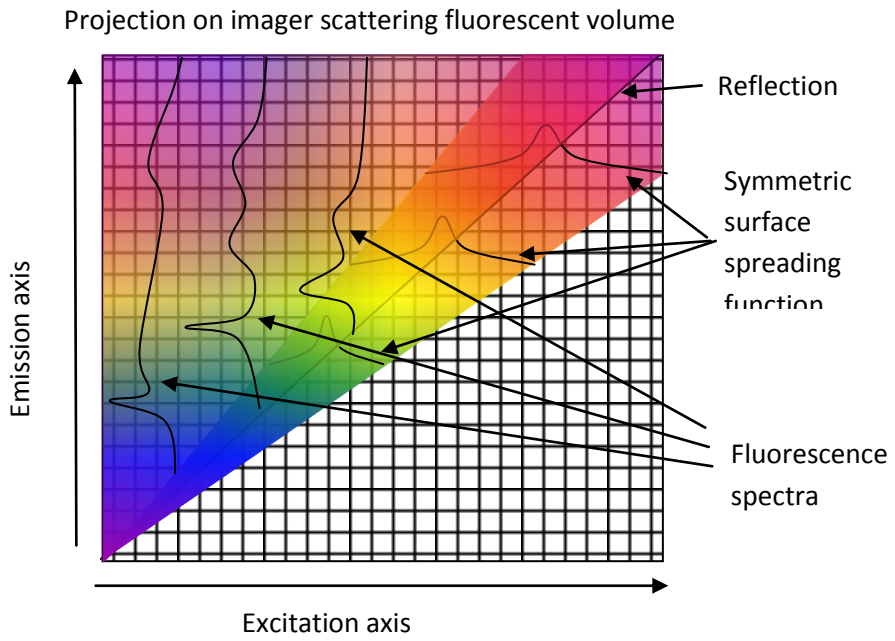

Fig 4.1.3. Fluorescent light only contributes to the upper diagonal.

Efforts may be made to extract physically understandable and comparable coefficients; however, this will not make any difference when using the data to teach a computer model to quantify biochemical components or identify tumors or lesions. As long as physical information is present in a given data set, it is irrelevant to the computer how the data are presented. We might use a prism and get nonlinear wavelength resolution, we might use grating and have repeated data in form of higher order reflections. This will push limits of spatial and dynamical resolution of the imager, but it will not increase or change complexity of data processing.

One might expect more information from fluorescence than from scattering, also it is seen that theleft corner of the lower triangle is expected to be unexploited since the UV light does not scatter. If we introduce a prism and a grating instead of two gratings, we achieve higher resolution in the UV region and the covering of the imager might be more efficient.

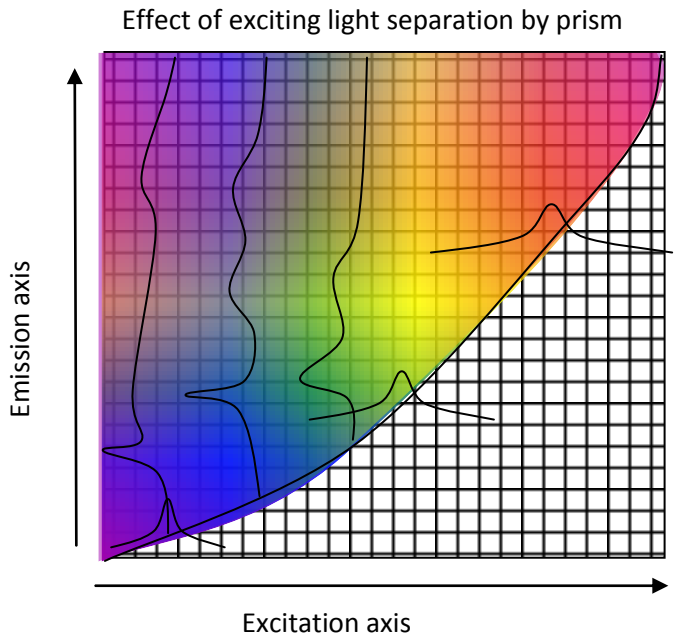

Fig 4.1.4 A combination of prism and grating will bend the diagonal and exploit otherwise unused area of the imager.

Clearly, the three different phenomena have different strengths, and all three phenomena have to fit within the dynamic range of the imager. Fluorescence coefficients are expected to be weak in comparison to the reflection coefficients. Fortunately, the read out of the coefficients are spatially separated. This means that we can introduce a natural density filter on top of the imager which is most dense around the diagonal and more transparent in outer corners. For a given application with a given relation between the strength one could make a prior measurement, and obtain the average spectrum also known as principal component one (PC1). If PC1 in converted to a density filter, it can be superimposed on the imager. This would cancel out PC1 which consumes most of the dynamic range. This would greatly increase the dynamic resolution for the given application. When using CMOS imagers where no blooming effect is present, we may simply take several images with different exposure times.

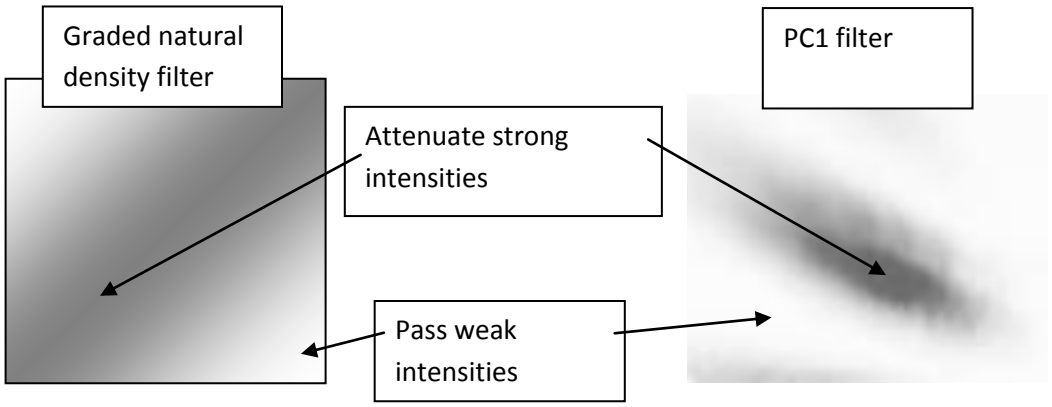

Fig 4.1.5 Graded natural density filter placed directly on the imager, to compensate for different strengths of phenomena.

Since differently illuminated points along the excitation slit are not exactly the same point, the object has to be homogenous for the method to work. One way of increasing homogeneity along the slit is to make the slit very short. However, a very short slit will mean that the spreading due to scattering will blur out all the information. Thus an optimum must exist in between too short and too long, and the optimum will depend on the surface spreading in tissue. Inhomogeneities in skin measurement might be cancelled out by scanning the slit over a larger area and take the signal acquired as average.

Others applications where homogeneity is insured along the slit is analysis of liquids. Milk, blood or urine might flow in a small quartz tube along the excitation slit. Another possible subject which has been in focus for optical measurements before are drug pills. Pills are usually dominatingly scattering and also homogeneous.

Since the method involves no moveable parts and all acquisitions are made instantaneously and simultaneously, this method could be used fully for measuring changes over time, and even fast chemical reactions or micro structural changes could be studied.

Because of the nature of scattered light the observation will depend on the borders of the volume. If the volume is big in relation to the extent of the scattered light, the border conditions of the volume will be negligible. One border which always remains near to the measurement will be the slit blocking scattered light from spreading along the emission axis. The reflectance of the slit surface will thus influence on the measurement.

When estimating a reasonable slit length white light was focused on the author's arm, in a spot that appeared to be homogeneous. A frame of 2 cm was drawn on the skin. A picture was taken of the light spot with a Sony F828 digital still camera. The picture was analyzed in Matlab and red, green and blue pixels were sorted according to their distance to the incident point. The surface spreading function seemed linear on a logarithmic scale and regression was applied to each color channel. The distance of half intensity was calculated:

- Blue: 0.35mm
- Green: 0.58mm
- Red: 0.92mm

Position of color channels are not known on an absolute scale but could be estimated relatively depicting a fiber tip through a grating.

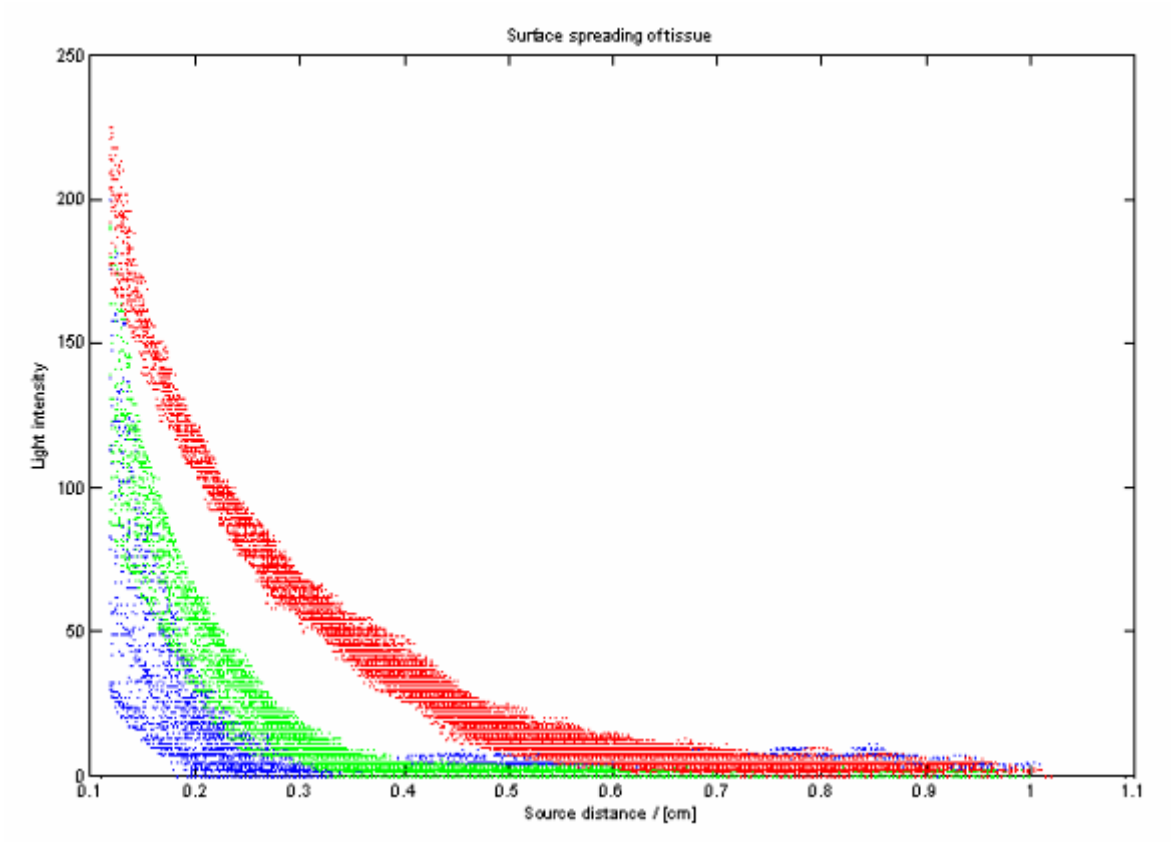

Fig 4.1.6 Red, green and blue pixel intensity as function of distance to incidence point.

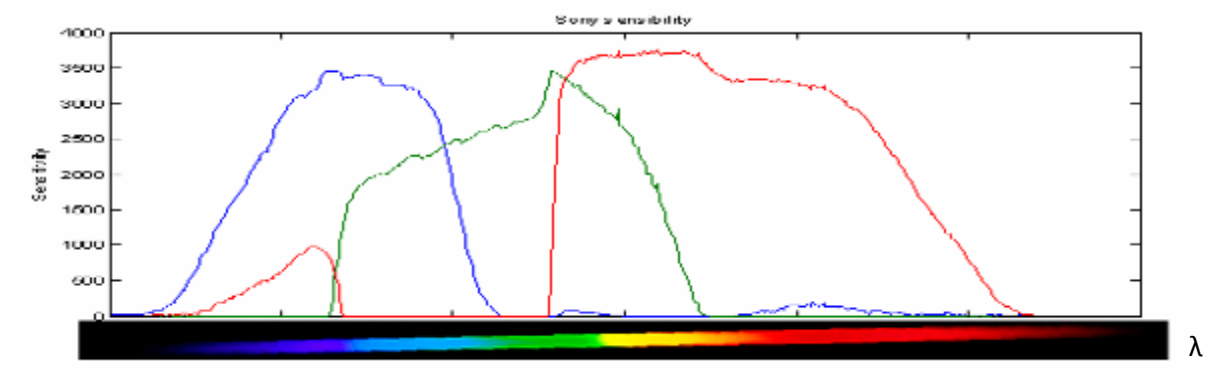

Fig 4.1.7 Estimated sensibility of Sony F828 digital still camera

It seemed reasonable to have a slit length of 4-6 mm, where scattering would not blur out all fluorescence information but scattering information would still be useful.

For detection a CMOS based USB camera was purchased from Mightex. The image sensor is from Micron Systems, MT9M001C12STM (Monochrome). The sensing area is 6.66 x 5.33 mm.

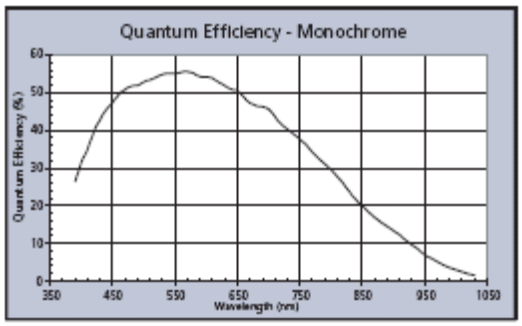

Fig 4.1.8 Spectral response for the MT9M001C12STM (Monochrome) sensor

The sensor has a rolling shutter, a wide range of exposure times, output and input for flash synchronization and also 4 LED drivers.

For the white light source both a point source and a line source were considered. The line source would be a xenon discharge tube and the point source would be a short arc lamp or a fiber tip.

Focusing a line source to a point involves a cylindrical lens and a diffracting grating. An example of geometry for excitation light is given in Fig 4.1.9.

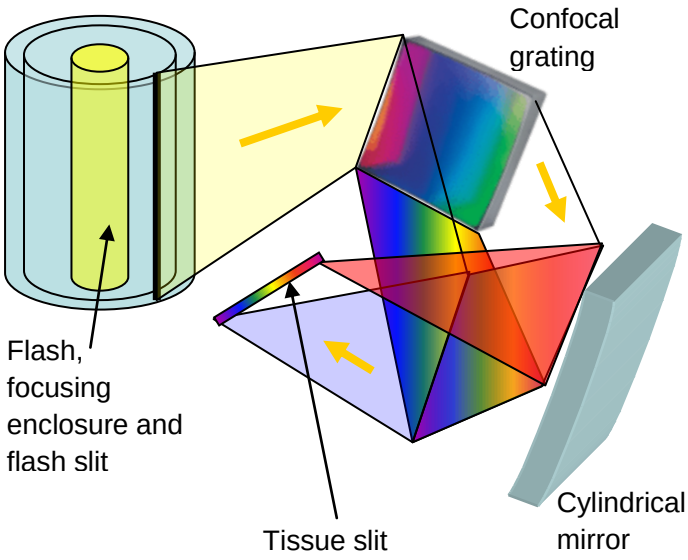

Fig 4.1.9 Generating the excitation line from a line source with a cylindrical mirror.

Generally the line width of a line source or the diameter of a point source will determine the spectral resolution along the excitation axis. The line width of the opening towards the tissue will determine the spectral resolution along the emission axis. Further, more, the scattering properties of the sample will influence the resolution along the excitation axis.

Another approach would be to image the line source through a color filter. If a linearly variable interference filter is used a continuous excitation spectrum is achieved. The set up could work with a discrete excitation axis if the filter was replaced by a row of differently colored LEDs. LEDs would solve a great deal of problems with power electronics required for white light sources.

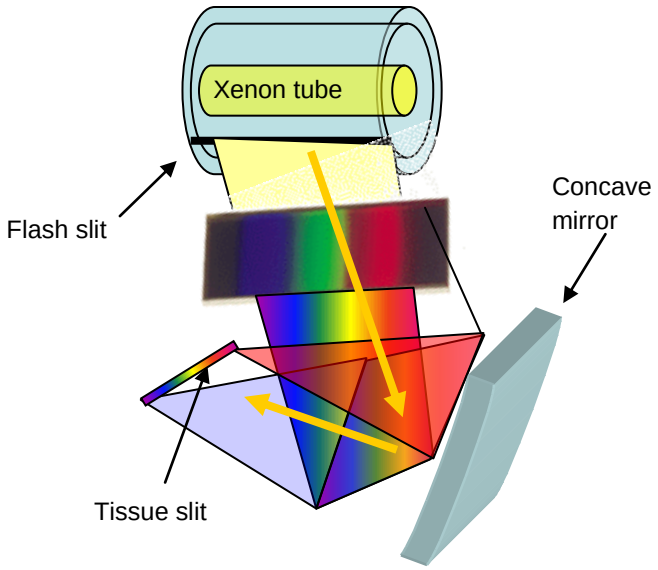

Fig 4.1.10 Line source with LVF imaged directly on the excitation slit.

One could try to take advantage of the rolling shutter of the CMOS and the Wien shift of a flash tube during the discharge. The plasma temperature would raise in less than 50 µs to temperatures as high as 15000 K. Unfortunately, the broad emission spectra would most likely override any fluorescence.

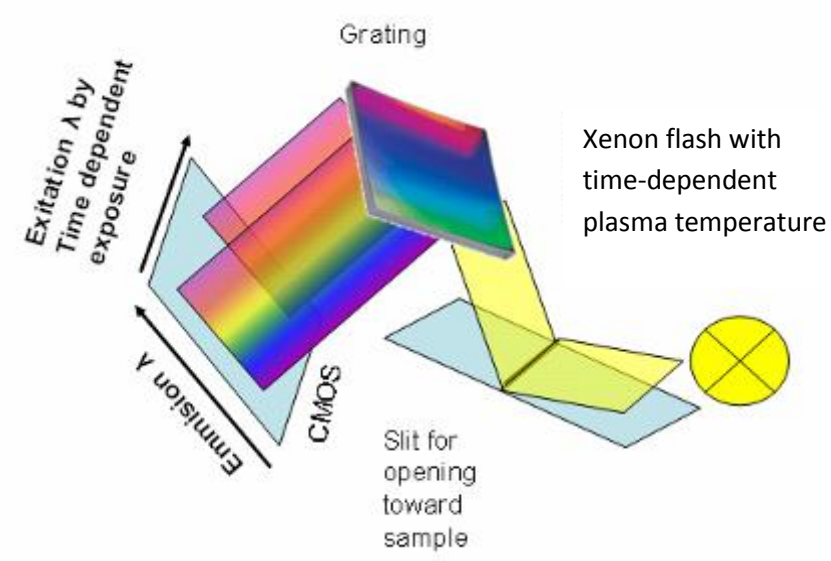

Fig 4.1.11 Time axis on rolling shutter will be illuminated by different plasma temperatures.

A point source could be imaged through a diffraction grating or prism to make the excitation axis. Confocal gratings could be used to reduce the number of components and the complexity of the system; however, the only available confocal gratings are designed to image a point source in linear detectors of the length 2.5cm, which would be too large an area for the detector purchased.

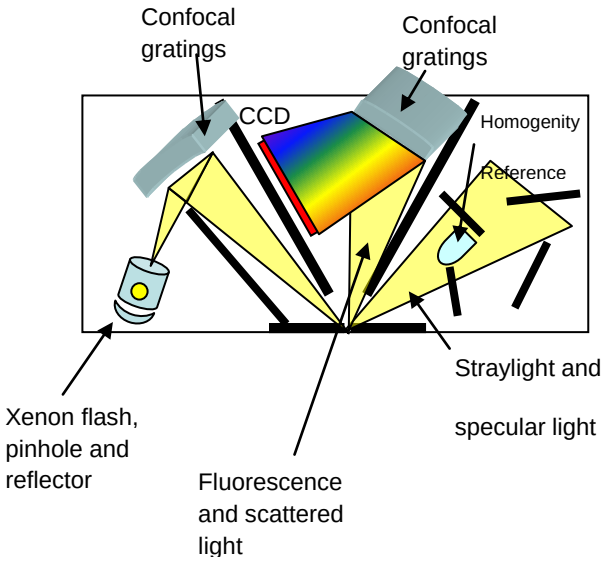

Fig 4.1.12 Confocal gratings greatly reduce the number of components.

An additional white light source could be placed to illuminate the tissue slit equally. This would serve as an indicator of the homogeneity along the excitation axis.

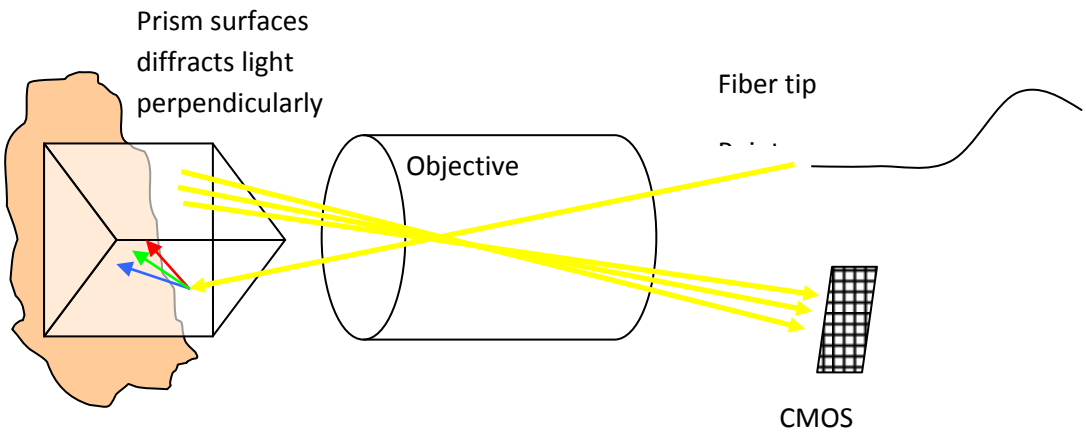

Fig 4.1.13 Exploiting perpendicular interfaces of the same prism.

Another approach would be to use a single prism and a zoom objective. The prism could be equilateral or right angled, even a hemisphere lens could be used. The sample would be held directly onto the surface or the prism or lens.

4.1.2. Setups used for acquired data.

The final setup used for the measurements is based on a white point source and two diffraction gratings and two concave mirrors. The light source is a fiber-coupled pulsed xenon flash, PX2 from Ocean Optics. The fiber is 600 µm in diameter and is solarization resistant. The gratings are 25x25 mm and from Newport, the blazing is at 300 nm. The first grating has 150 grooves/mm and the second has 300 grooves/mm. The two identical mirrors are also from Newport. They are coated for improved UV performance, the diameter is 5 cm and focal length is as well 5 cm.

The setup consists of two optical planes, one in which the excitation light is separated perpendicular to Fig 4.1.13 and another where the emission light is separated perpendicular to Fig. 4.1.14.

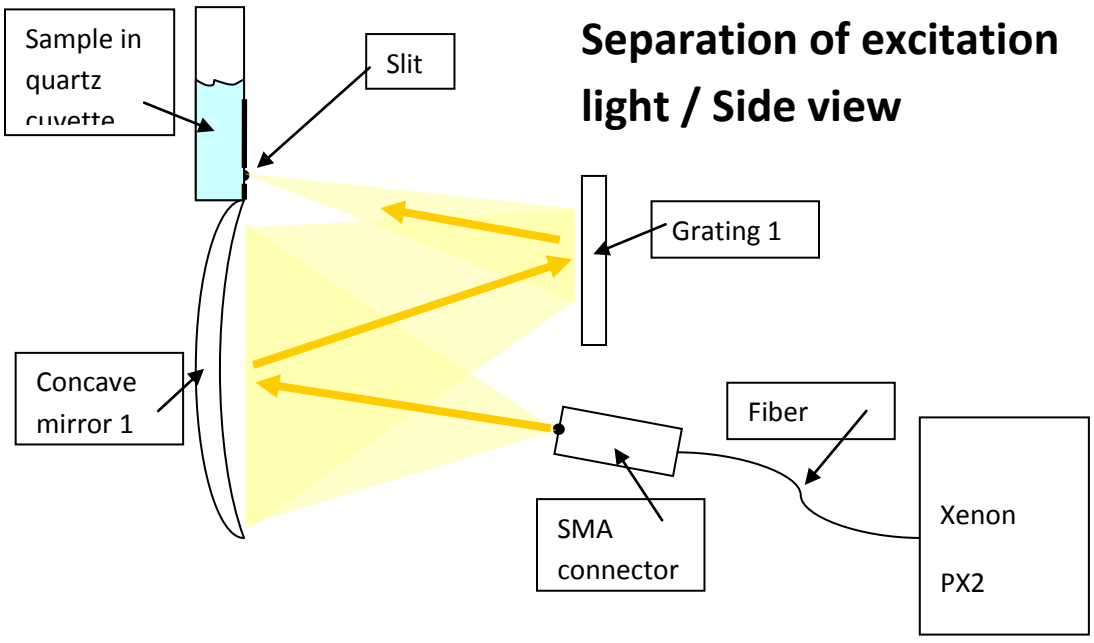

Fig 4.1.2.1 First optical plane separate the excitation light perpendicular to the plane.

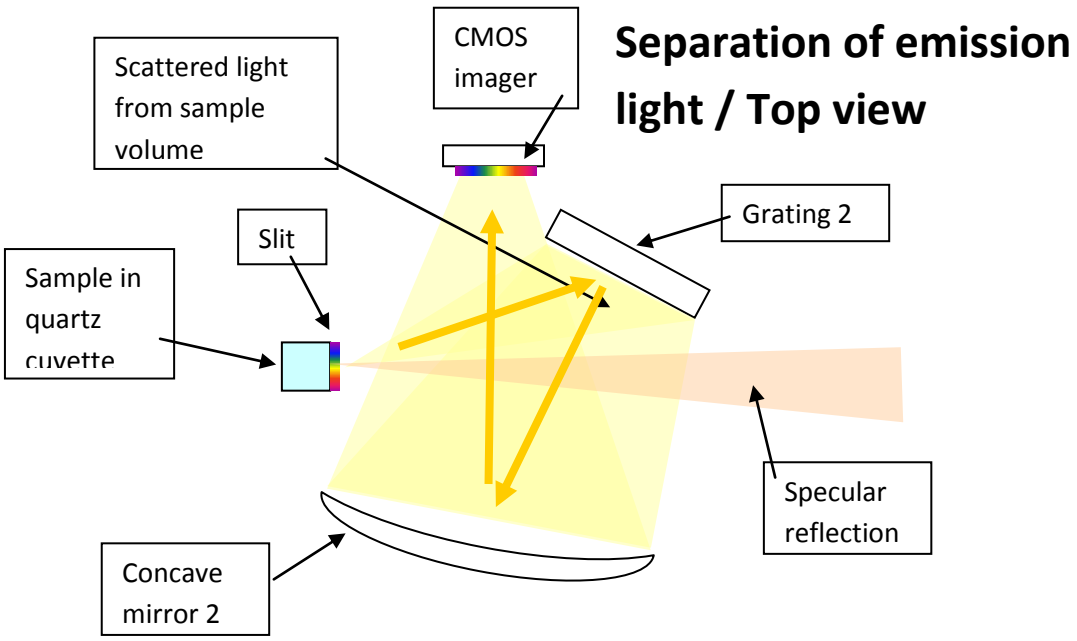

Fig 4.1.2.2 Second optical plane split up the emitted light perpendicular to the plane.

Initially the setup was thought to be built as a portable instrument. However, because of the complicated geometry, the instrument was first build on an optical table. Concave gratings would have decreased the number of components to the half, but the spectral range would not have fit in the purchased imager. The fact that object has to be off axis when depicted by a mirror introduces considerable astigmatism, this would as well be avoided by concave gratings which are corrected for astigmatism.

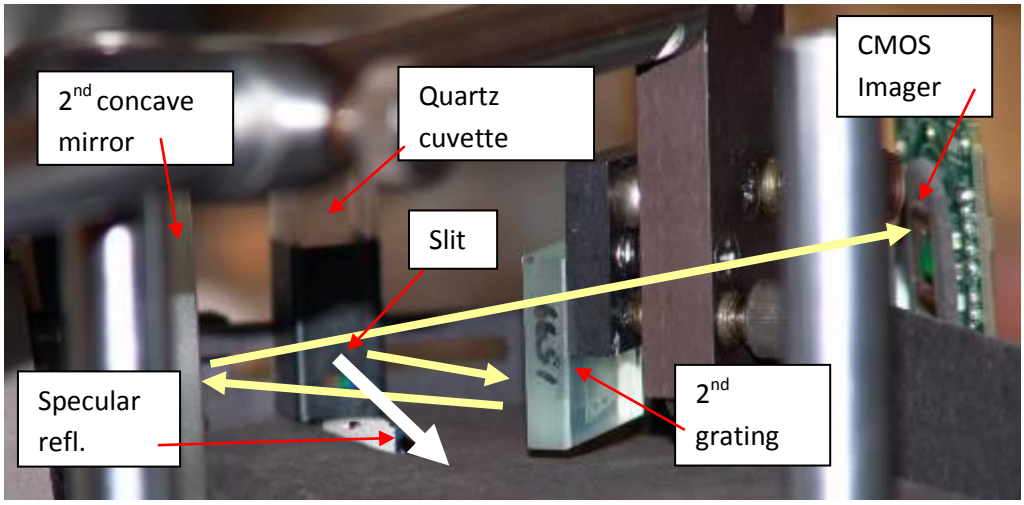

Fig 4.1.2.3 Picture of the setup

For the second series of measurements first, the plane was rebuilt in the way that rays incident parallel on the first grating. In the second optical plane the concave mirror was substituted with a zoom objective, this eased the alignment of the system.

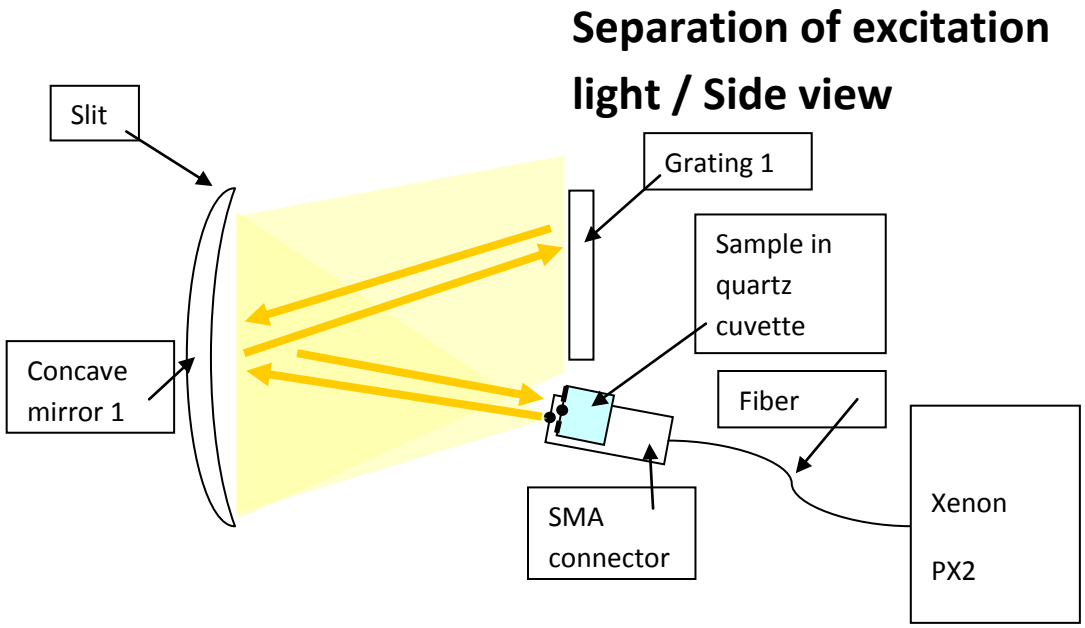

Fig 4.1.2.4 Parallel incidence on the grating improves excitation axis resolution

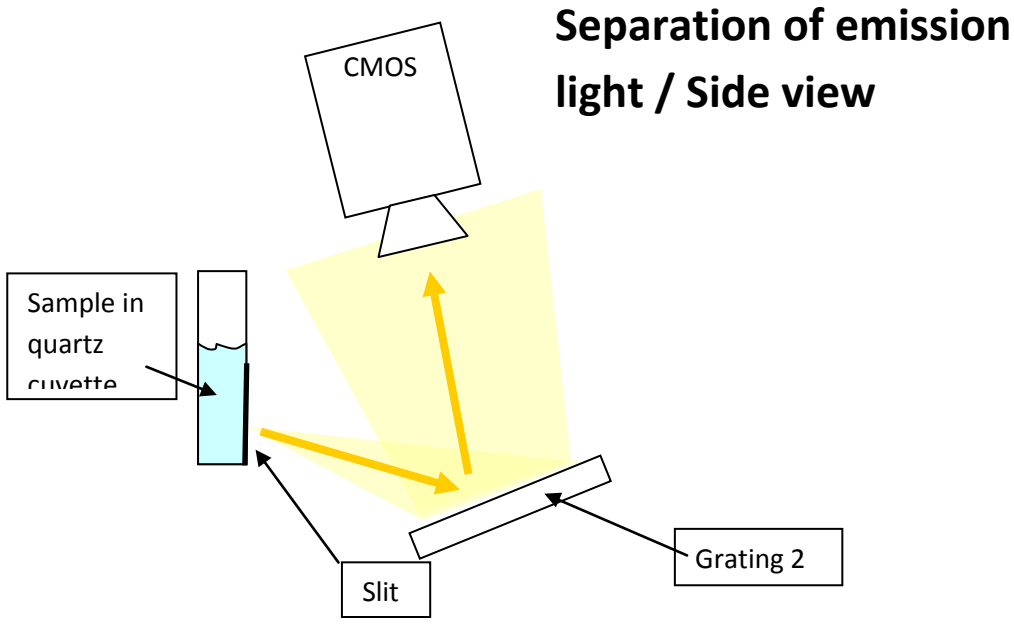

Fig 4.1.2.5 Transmissive optics was introduced for the second imaging.

4.1.3. Future setups, after experience gained.

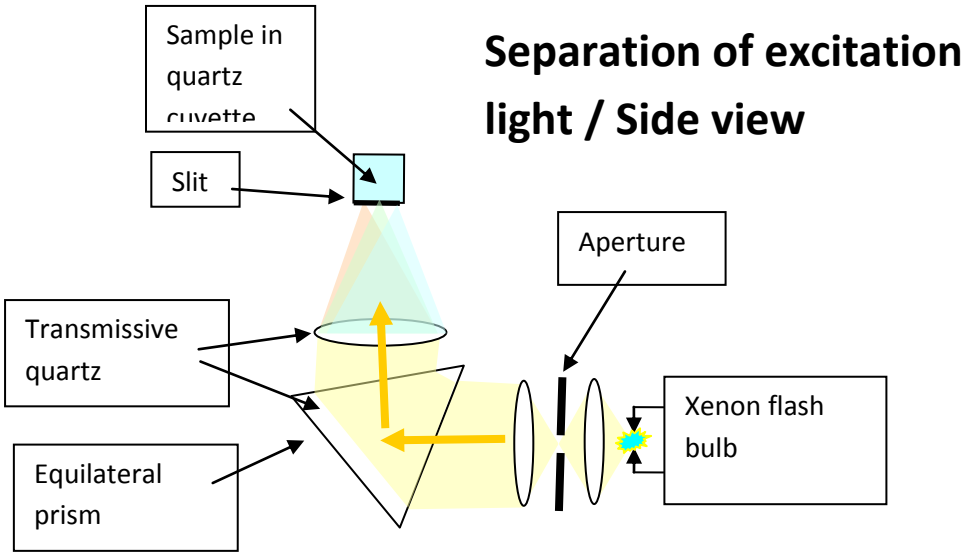

Fig 4.1.3.1 Prism provides better resolution for lover wavelengths which are expected to contain more information.

For separating the excitation light a prism could be used to get higher resolution in the UV region, where fluorescence is likelier to be introduced. Depicting with mirrors involved several complicities. A UV transitive microscope objective in combination with a plane grating might be preferable.

Slightly similar setups have recently been considered by other groups. (Hart., 2002) And (Jobin Yvon, 2002) (Gouzman, 2004)

4.2 Compact inexpensive fluorescence measurements

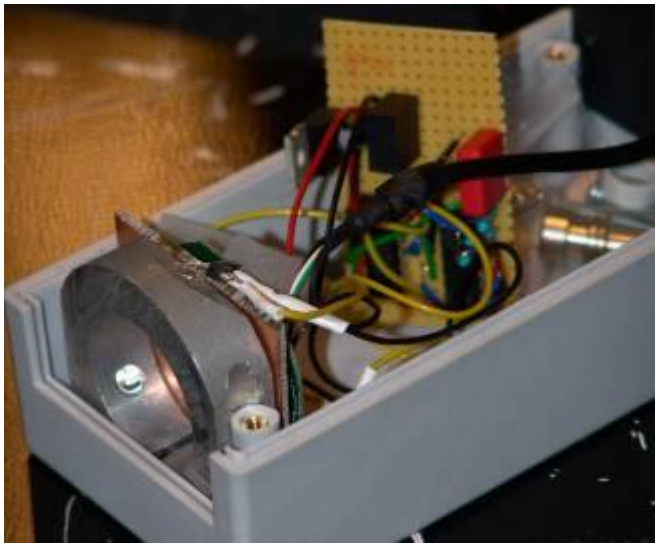

Fig 4.2.1 Fluorosensor made from a webcam fitting a big match-box.

The first thing to do if a focus is on producing a cheap spectroscopic equipment is to identify the least expensive components available. When considering surrounding electronic as well it is obvious that UV LEDs offers the most inexpensive source suited for fluorescence, furthermore UV LED are currently undergoing fast development, which makes them promising future sources as well. There is a row of inexpensive light detectors. However, we expect to perform certain statistics and want to apply several mathematical operations to the detected signals, which would suggest a computer interface which is of considerable cost. Turning the eyes to the consumer market we find that CMOS Web Cams are available everywhere for a negligible cost. Web cams are not only inexpensive, computer-interfaced and compact. Their also have spatial resolution which can be taken advantage of in several ways.

For a specific application and detection of one certain fluorescent protein, one realizes that perhaps only a small part of the UV spectrum will be considered. Filters can be distributed over the imaging surface. By placing UV absorption filters on the imager certain regions of the frames acquired will have certain spectral sensibility.

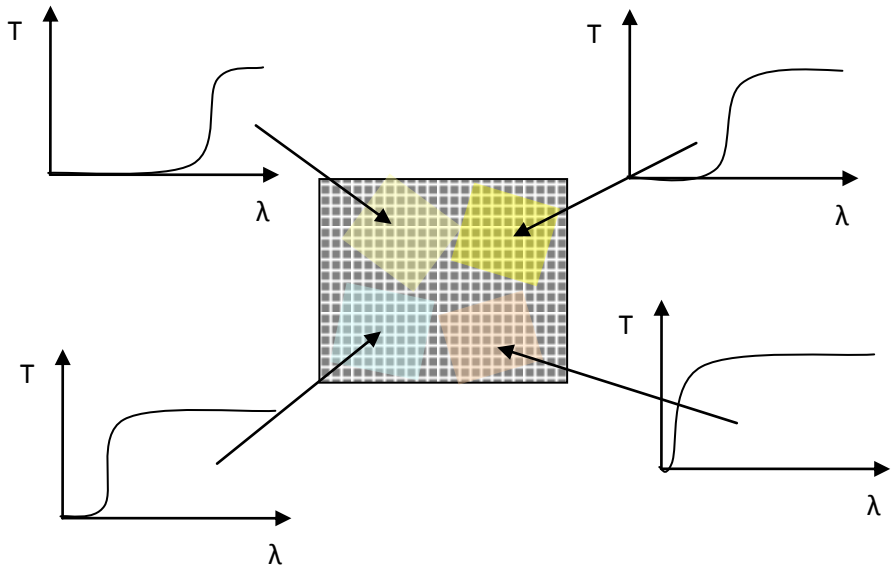

Fig 4.2.2 Inexpensive absorption filters placed on a imaging device provide a multi wavelength sensible sensor.

If an interference filter is placed on the imager the angular dependence could be exploited from a fiber tip source.

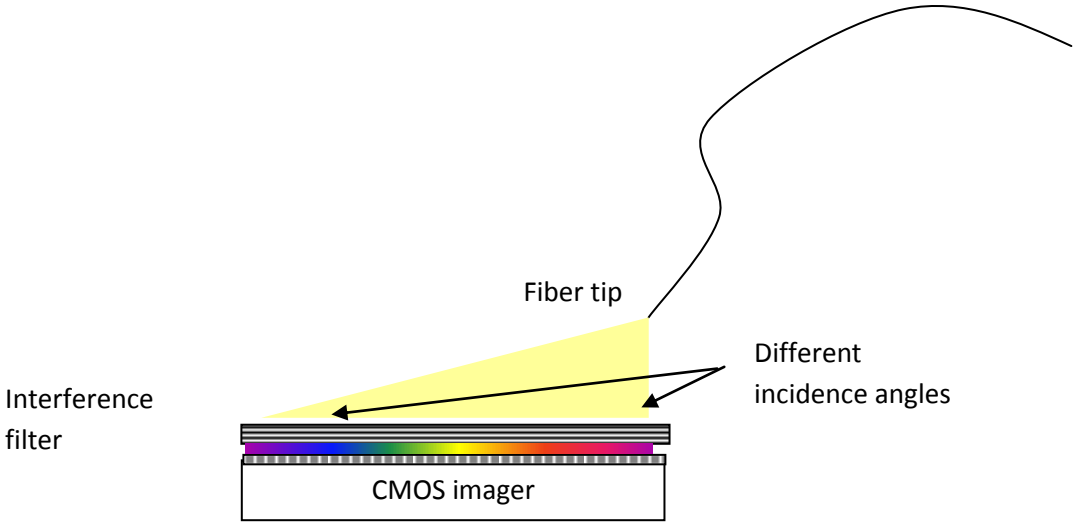

Fig 4.2.3 The angular dependence of the interference filter passes different wavelengths on different positions of the imager.

Linearly variable interference filters could be coated directly on the imager to produce a miniature spectrometer. Unfortunately such operation is considerable expensive and no LVF are commercially available at sizes of the imagers in webcams.

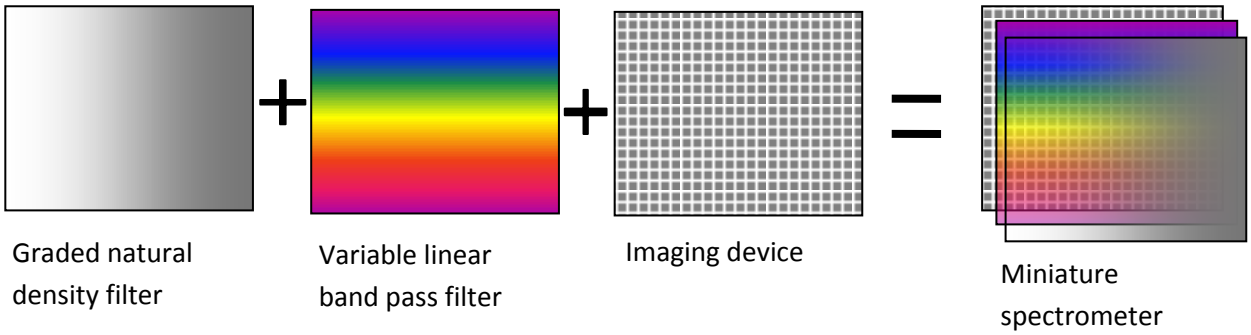

Fig 4.2.4 The LVF turns the imager into a linear spectrometer.

The Bayer color filter already present on the imagers could also be exploited. Droplets of fluorescent substances could be placed on the imager. Their excitation wavelength would act as sensibility regions for the imager.

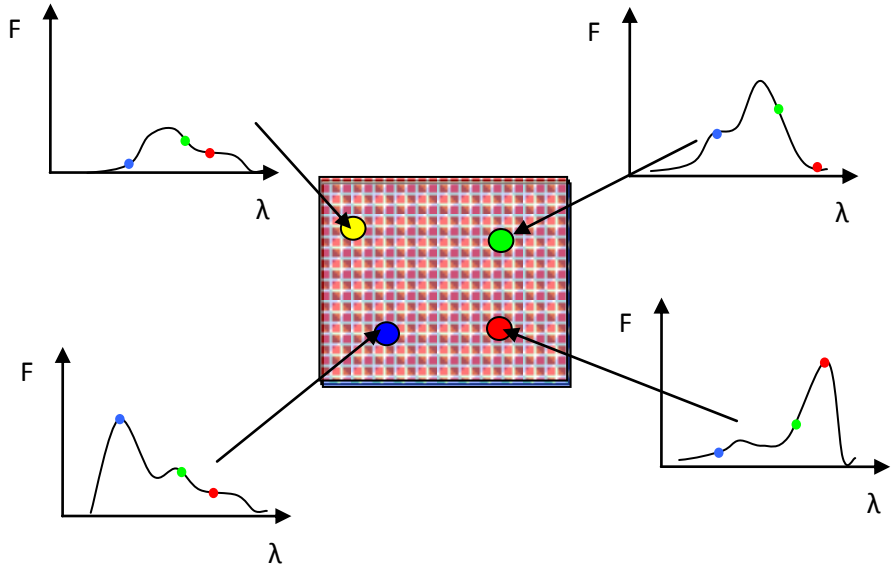

Fig 4.2.5 Fluorophores droplets on the imager up converts UV light.

Powering LEDs requires a voltage reciprocal to the emission wavelength. When entering the UV regime the voltage drop surpasses the 5V provided by the computer through the USB. To avoid external power supplies or batteries upconversion can be done. The DC-DC converter works by the switching principle and multiplies the input voltage by a factor of three. Since the USB voltage can change in the order of hundred millivolts depending on other devices accessing the power supply of the computer, the variances will be multiplied by a factor three as well. For that purpose a voltage regulator is coupled after the switching unit. The regulator requires a small drop of 1.2 V from input to output in order to work properly. For that reason a 12 V regulator is chosen. The switching frequency is typically 90 kHz and further oscillations might be introduced by the regulator. They are both damped out by a polyester capacitor of 100 nF at the output.

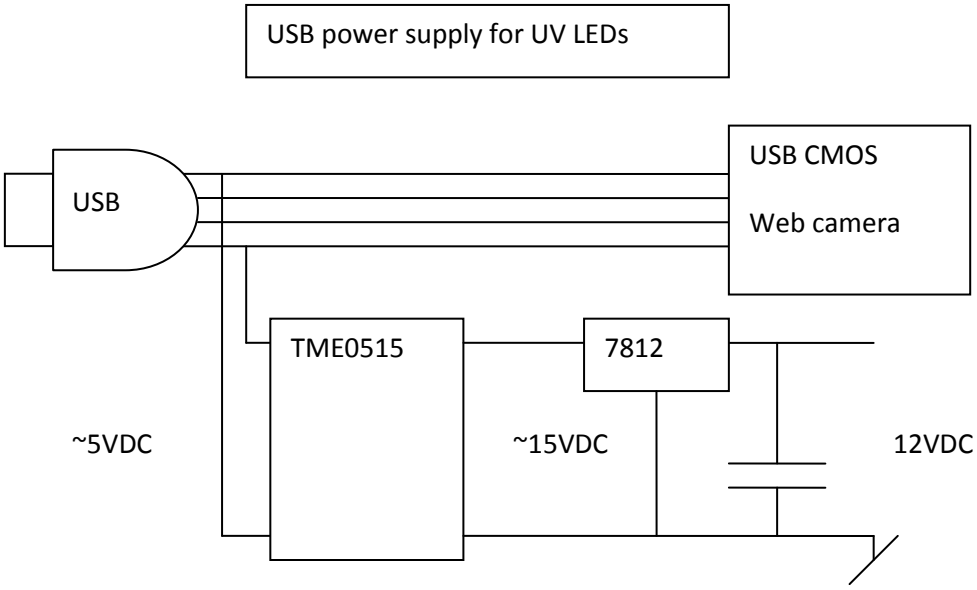

Fig 4.2.2 Generation of 12 V from the USB.

Considering the characteristic I-U curve for an LED and the fact that the emission is determined by the current it is realized that LEDs must always be controlled by current and not by voltage. Further, the characteristic voltage drop E_g changes slightly with the device temperature. Because of the negative temperature coefficient for the bulk semiconductor one would quickly damage the LED permanently if controlling by voltage because of the positive temperature feedback. A constant current generator is introduced for each LED. Current is determined by R2 = (12V-0.6V) / I_{LED}. The current might also be controlled individually by providing each LED with a resistor to ground. By doing so we can compensate for different recombination efficiency among the LEDs or even detector efficiency. Equal excitation illumination is preferable in order to fit all signals within the dynamic resolution of the detector.

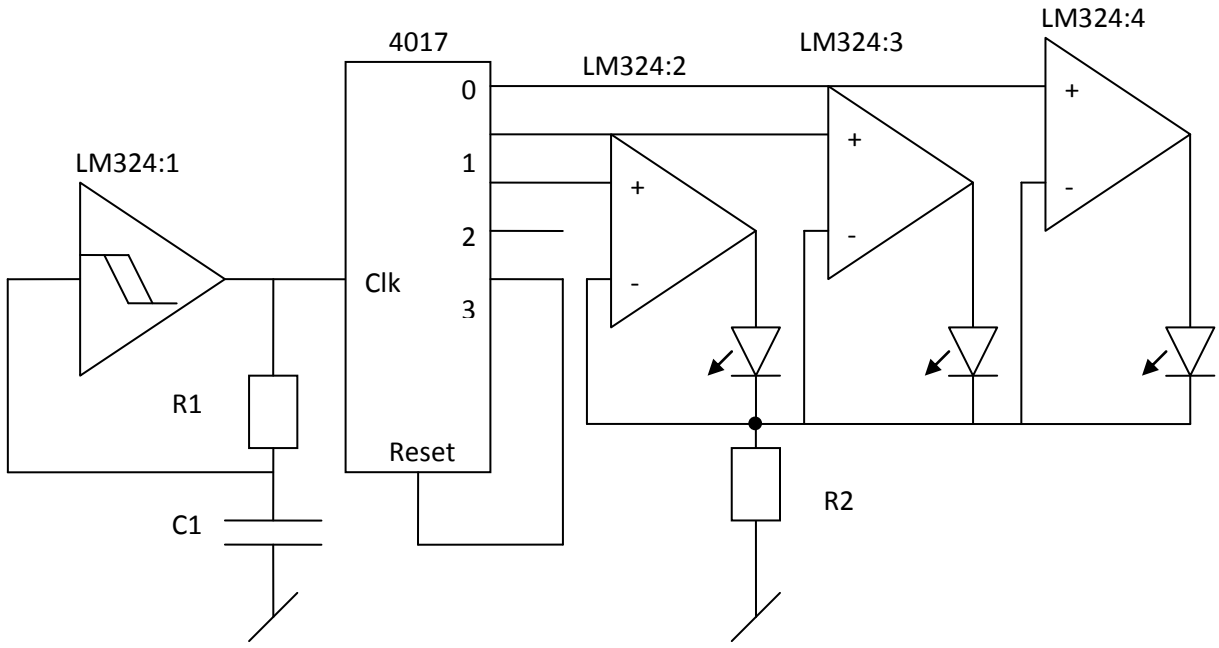

Fig 4.2.3 Sequential modulation and LED drivers

The LEDs are modulated sequentially in time by the counter CMOS 4017. If needed additional temporal slots can be added. One temporal slot is left empty, this solves two problems; the background can be measured in the empty tie slot, and also that certain slot can always be identified by being the lowest. Therefore there is no need to synchronization with the detector; this saves us from a number of complications and additional costs. The modulating frequency is determined by τ = R1*C1. One approach would be to let each timeslot cover two frames of the detector, alternatively high-frequency modulation could be used in combination with rolling shutter imagers. This would generate line-filled images in each frame, where each line represents a time slot. The darkest line would represent the background and the start of a new sequence.

4.3 Wien shift imaging

Fig 4.3.1. The constructed instrument for Wienshift imaging

Wien shift imaging is introduced as a spectroscopic method, were the spectral content is varied by the temperature of the illumination source rather than trying to separate the spectral content in the detection. The spectral content is retrieved by sliding Planck's black body radiation distribution over the sensibility curve of the given detector. Filaments represent excellent black body radiators but even radiation from plasma in flash lamps experience temperature shifts during the discharge. Often the temperature could be determined electronically from measurements of power dissipation; thus there is no need for expensive spectrometers.

Obviously the total emitted energy will change a lot more with the temperature than the peak wavelength will. Thus, we will need to modulate the intensity and this could be done by changing exposure time, aperture and electronic gain in the imaging device. Alternatively, we could try to modulate the emitted intensity with a graded neutral filter, a liquid crystal (LCD) or a micro electromechanic system (MEMS)

The basic idea would consist of a variable power supply sweeping the temperature of a filament. The filament voltage and current will be measured to calculate the temperature. The light will illuminate the sample and be detected by a camera.

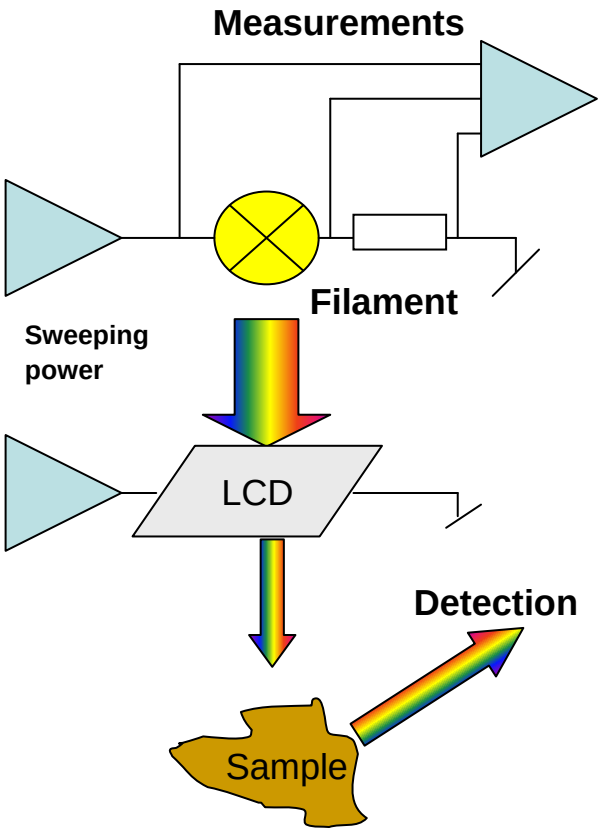

Fig 4.3.2 Basic concept of Wien-shift-imaging, intensity modulation could be made with a LCD or a MEMS.

Using filaments two problems arise. The heat capacity of the metal in the filament limits the speed of the sweep, but perhaps more importantly the filament only tolerates rather low temperature, or else it melts or evaporates. Using flash lamps greatly expands the temperature range. Plasma temperatures increase to 15,000 K equaling peak emission of 193 nm (Capobianco, 2006). The change happens within hundreds of micro-seconds. This would mean that very fast imaging is needed. Few cameras can film this fast; however rolling shutters do reach these timings. This means that when taking a picture with a flash and a rolling shutter camera, different rows in the image would have been illuminated by different plasma temperatures. By taking several pictures and delaying the flash with respect to the camera trigger, a multispectral image could be reconstructed.

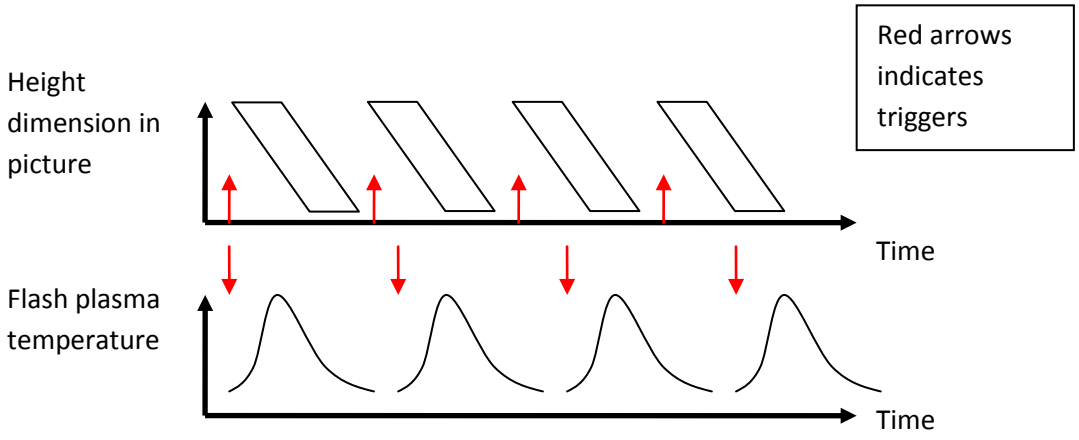

Fig 4.3.3 Different rows in the pictures are imaging the object when illuminated by different plasma temperature.

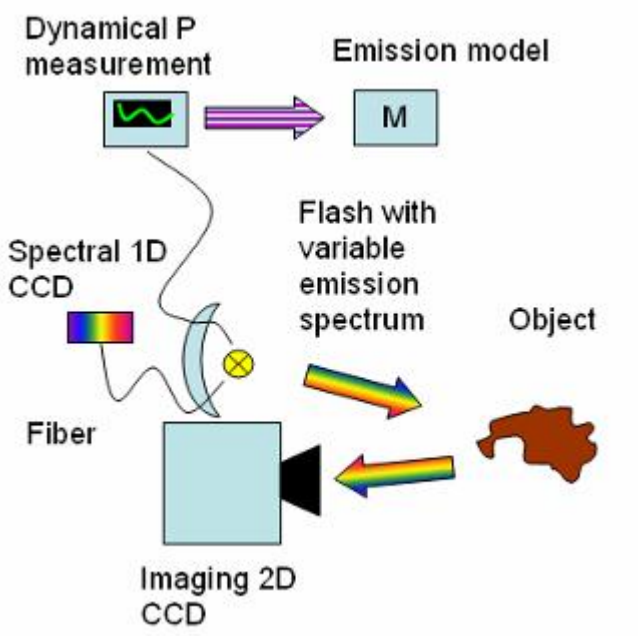

Fig 4.3.4. A flash plasma undergoes Wien shift during the discharge

Considering that flash lamps have several narrow peaks in the spectrum, which are expected to vary greatly in intensity depending on the temperature, one might also attempt to build a simple point spectrometer with a xenon flash. The first problem arises with the stability of the lamp. One possible solution is to measure the electrical input power dynamically, this is expected to correspond to the radiated power. By taking the ratio one would cancel out instabilities and the $P \sim kT^4$ dependence.

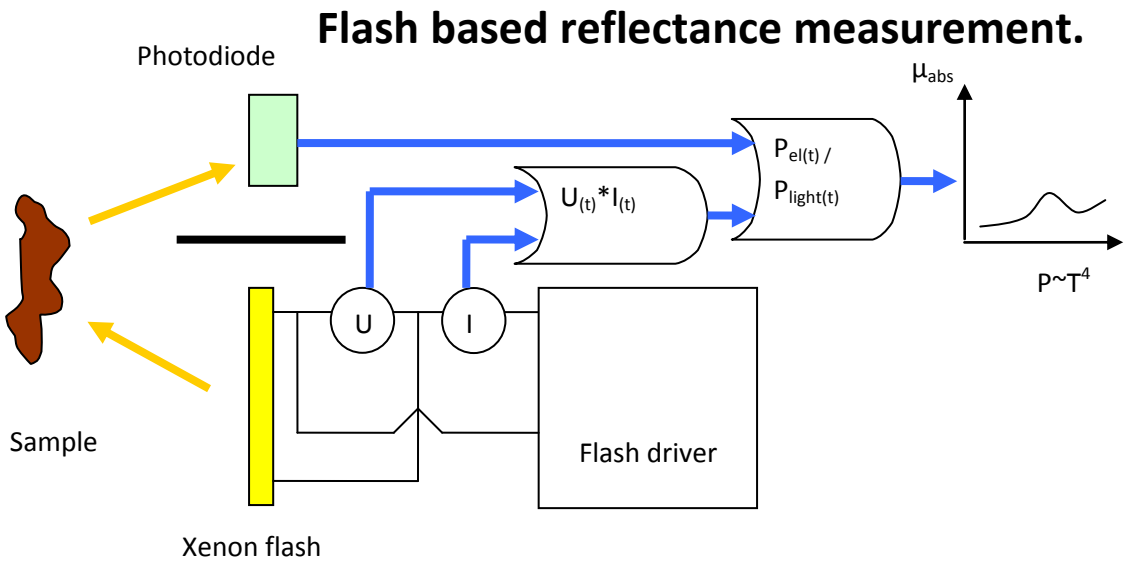

Fig. 4.3.5 Setup for measuring absorption of light from different plasma temperature emissions

Wien-shift imaging is unsuited for fluorescence imaging since the broad emission profiles would overwrite the fluorescence signal.

4.4 Improvements in an existing portable multi-wavelength fluorosensor based on UV Light Emitting Diodes

This instrument is originally constructed by Sara Ek as her master diploma thesis (Ek, 2006). However, a number of changes were made to the instrument in an evolutionary process of improvement. The eight batteries were replaced by a power supply equal to that in *Fig 4.2.2*. The batteries took up considerably space inside the instrument. The voltage is expected to drop during the life time and they are heavy. When transporting connectivity in any of the sixteen connections with the socket was often lost, and time was spent in locating the failure. When changing the batteries new calibration of the instrument had to be performed because the optical coupling inside was highly sensitive. Preferably the instrument should remain closed, which is possible with the power supply.

A spectral peak was generated by a leakage caused by the reflection from the absorption filter, which reflected again on the SMA connector and was transmitted through empty filter slot in the wheel of the instrument. The error was corrected by blocking the slot.

In order to increase the transmission pig tailing of the LEDs has been performed. LEDs was washed from drilling oil. Glycerol was added to the fiber tips inside the LEDs to decrease reflection losses. The fibers has been performed using thicker fibers to increase coupling efficiency in the bifurcations, and a device for the pig tailing was constructed in order to be able to reuse the fibers even if the LEDs are replaced. The fibers had to be cut, polished and glued before replacement.

Colored glass absorption filters are known to be fluorescent. The fluorescence gave rise to substantial background. Since the added fluorescent light depends on the reflectivity of the sample, which is unknown it becomes problematic to remove the instrument fluorescence by data processing. For resent projects, this effect was generally not an issue. Possibly the problem arose as a result of the chosen geometry.

Absorption filters, UV lens, filter wheel have been removed. Apart from the fluorescent light from the filters the mechanical structure was rather unstable and required frequent calibration and refocusing. The filters are now replaced by a single commercial LVF interference filter which overcomes the problem of instrument fluorescence being reflective in nature. The filter slides in a commercial holder with fiber connection and fixed UV lenses inside the SMA connectors.

5 Data handling and results

5.1 Spectral identification and Wien shift imaging.

Here follows a proposed laboratory exercise in Wienshift Imaging. Spectral data handling, polar color spaces, principal component analysis and contrast functions are discussed. Similar methods will be applied in later chapters.

Spectral identification and Wien shift imaging.

Mikkel Brydegaard Sørensen

Division of Atomic Physics, Lund University

1 Introduction and motivation

X-ray imaging exploits the fact that different atoms absorb radiation unequally much, and the fact that different regions in the body have different atomic compositions. X-ray absorption coefficients vary with the energy or wavelength of the radiation. Just as for visible light we might say that different atoms have different colors, based on their absorption spectrum. One approach to single out specific atoms and thereby a specific component in the body is to look at various colors of X-rays. After that we can map out just bone, or just blood etc. and determine content of each pixel or voxel individually. We call this spectral identification, and in contrast to spatial identification, shapes and forms of the object of interest are irrelevant.

When generating X-rays, traditionally an X-ray tube is used. It is an evacuated tube, where electrons are released by a hot cathode and later accelerated into a anode by an electrical field. The current determines the intensity of the produced radiation, while the tube voltage determines the spectral distribution.

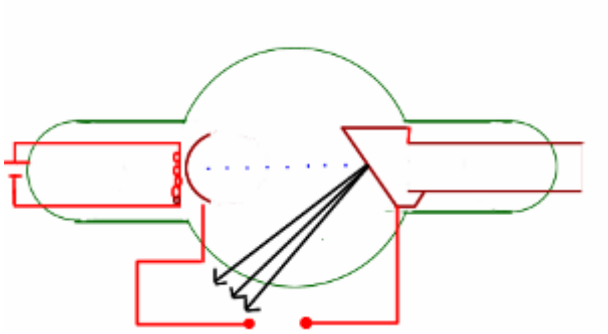

Fig: 1 Schematics of an X-ray tube (Source: www.teachnet.ie)

The emitted spectrum consists of two components; 1) Bremsstrahlung generated when electrons are decelerated inside the anode. 2) Specific K-lines generated when electrons expelled inner shell electrons of the atoms in the anode. The K-lines are determined by the composition of the anode material and only varies in intensity. The Bremsstrahlung is a continuous distribution with the most energetic photons equaling the tube voltage. By talking several X-ray photos of the same object with differently colored X-ray illumination we can distinguish several atomic elements and several organs with different composition. We might think as pixels or voxels from different organs as separated clouds of points in the X-ray color space. In the example below it becomes clear that blood and tissue cannot be distinguished using only a 40 kV tube voltage. (Svanberg, Multispectral Imaging, 2006)

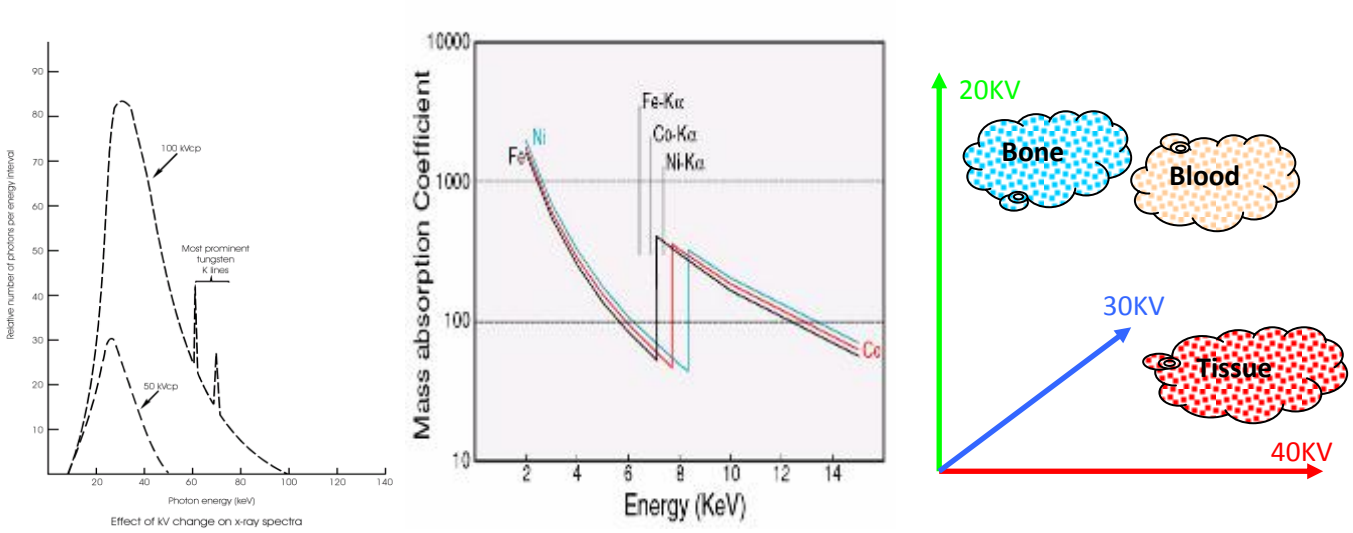

Fig: 2 Left: X-ray emission with different tube voltages (Source: ehs.unc.edu). Middle: typical absorption spectra in X-ray region (Source: www4.nau.edu). Right: X-ray color space

X-rays constitute ionizing radiation; they create free radicals in the body and are carcinogenic. As such X-rays are not suited for simple teaching experiments. Instead we will concentrate on the interpretation of the data and emulate the X-ray tube with a filament, which has a similar property: When we vary the voltage over the filament we control the temperature through the power dissipation. The filament will emit according to Planck's radiation distribution for black bodies:

$$I(\lambda,T)=\frac{2hc^2}{\lambda^5(e^{\frac{hc}{\lambda kT}}-1)}$$

The intensity is given by integrating I over all wavelengths:

$I=\varepsilon\sigma(T-T_{amb})^4$

and the peak wavelength is given by making the derivative of Planck's equation and solving for $dI/d\lambda = 0$. The result is:

$\lambda_{max}T$ = Constant

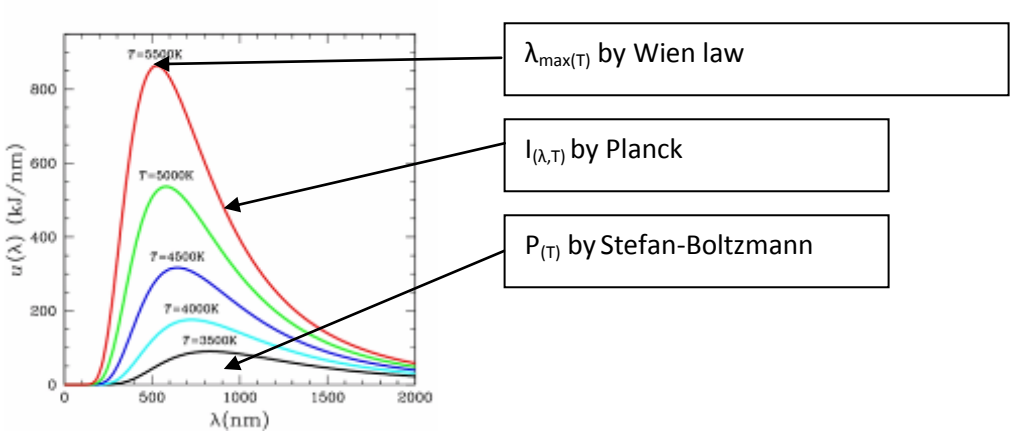

Fig: 3 Black body radiation for different temperatures and related equations. (Source: www.maxmax.com)

2 Setup

The equipment used for the measurements is schematically illustrated in Fig. 4

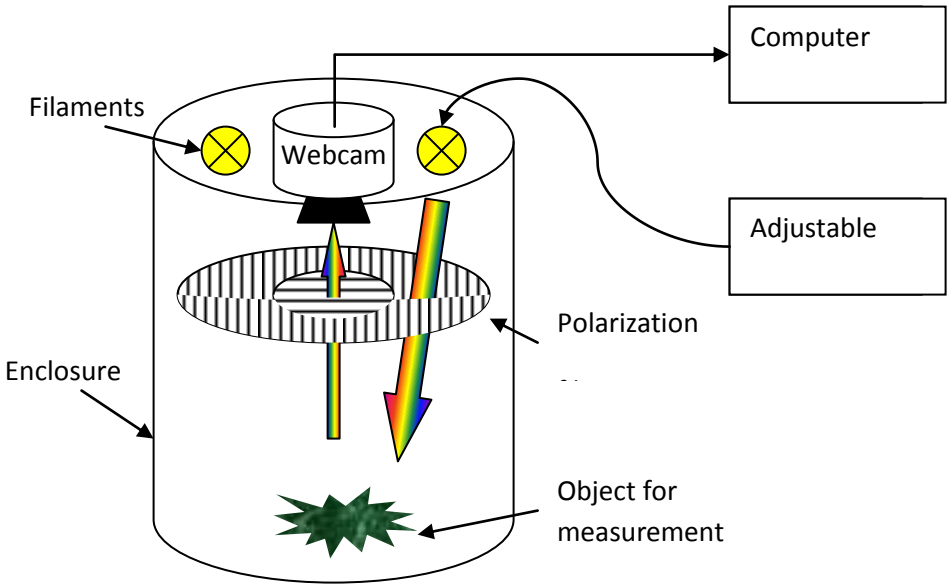

Fig: 4 Setup for Wien shift Imaging

With the given setup we will take several pictures of the same object varying the temperature of the illumination, thus taking frames with different Wien shifts. If the picture only contains one material we can express all frames as linear combinations of each other. If the picture contains various substances with different spectra we will not be able to express different frames as linear combination of each other, though we will be able to express the frames as linear combination of N frames if the frames contain N different spectra. We will need to ask the computer: How many frames or basis functions are needed to express the object for a given illumination temperature?

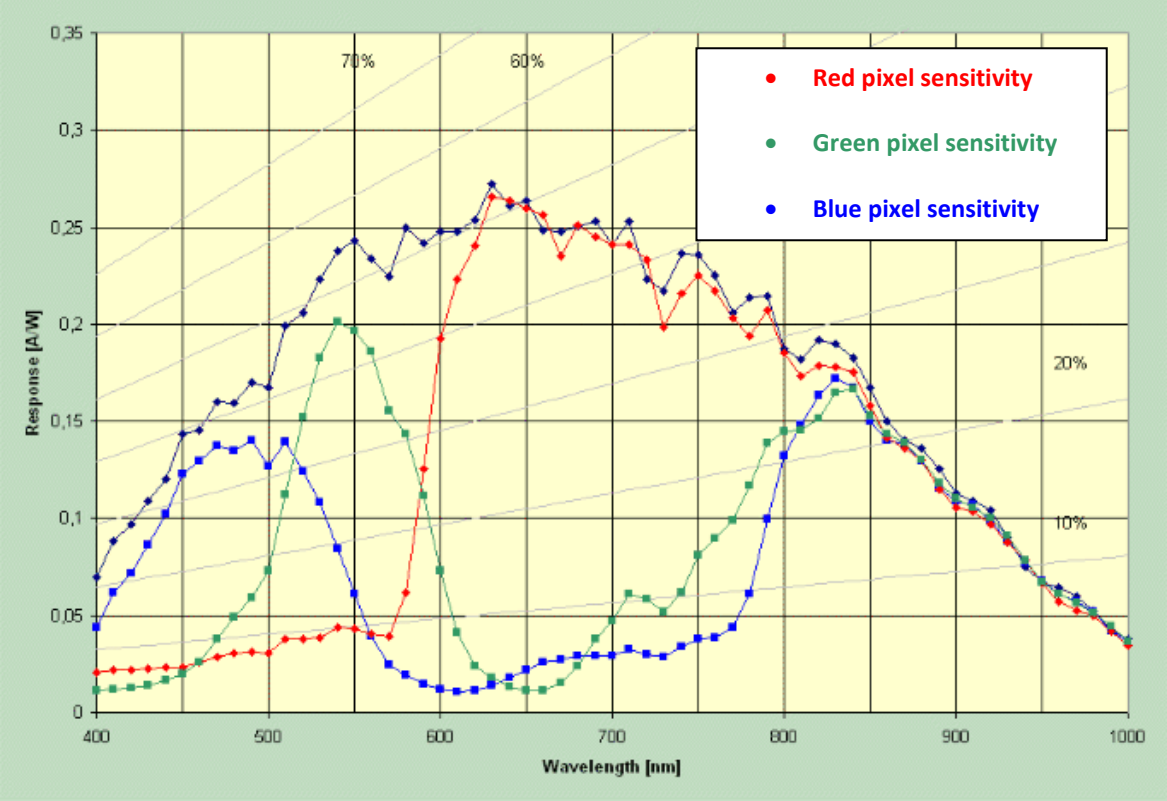

Figure: 5 Sensitivity spectrum from CMOS imager. Usually an IR cut off filter is superimposed in cameras, to suppress IR sensitivity.

Note 1: Polarizing filters are introduced to avoid specular reflections and insure that light has penetrated the object, i.e. has been influenced by the absorption of the object.

Note 2: Auto exposure is slightly slow for a Webcam. If sweeping from low to high voltage images might be saturated; for this reason we sweep from high to low instead.

Note 3: Inexpensive Web cameras use rolling shutters; this means that frames are not orthogonal to the time axis. In other words, all pixels in a frame are not exposed simultaneously. Sudden changes will thus introduce image distortions. For this reason we need to sweep slowly, say from 16 V to 1 V on a time period of one minute.

3 Color data handling: Logics and linear regression.

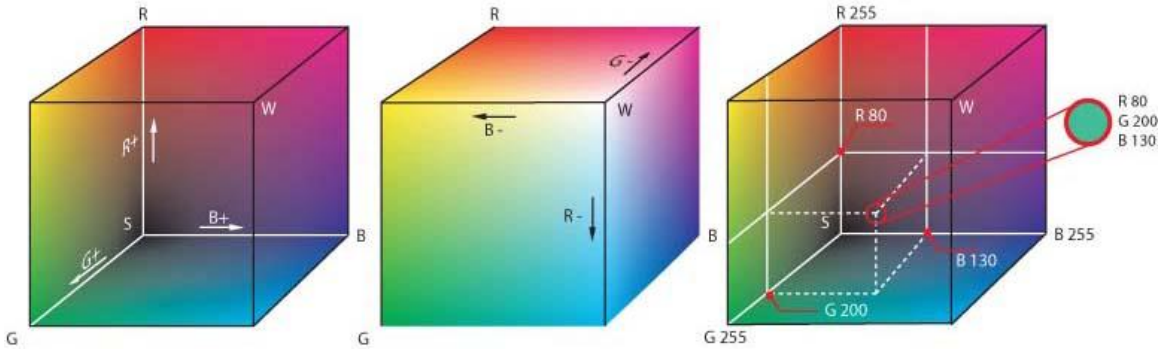

Digital picture can often be described as a three dimensional matrix, where first two dimension are spatial dimensions of the image plane and the third dimension is spectral content. The spectral content is usually described by a red, green blue color space (RGB) matching the human spectral receptors. Imagine an RGB color picture of a banana lying on a white sheet of paper. We need all three color channels to produce white paper; we need red and green channel to represent a yellow banana. However, we might choose to describe the picture in terms of paper color and banana color rather than red, green and blue. In this case we only need two color channels to produce the image; the reason why this is possible is that the picture only contains two different objects. We choose to describe each pixel as a linear combination of white and yellow.

In terms of identifying objects from its color, linear processing might not be enough. Consider a picture containing a banana, a tomato and a cucumber. The red color axis indicates tomato, green indicates cucumber. However when a banana is presented it will answer positive to both tomato and cucumber. We might introduce fuzzy logics[1] converting the linguistic expression "tomatoes are red and not green" into: *isTomato = R*(1-G)=R-RG*. The complexity quickly rises when increasing the number of objects, and we will need a more analytical way to identify objects. Consider for instance radishes, they are red, but not as red as tomatoes; however, it does not mean that a radish is a little tomato.

It is clear that we might choose any imaginable function to identify a certain object by its color. However, there are good functions and there are bad functions. The quality of a contrast function (Ref: Multispectral imaging, Sune Svanberg), F, is given by the ability to distinguish an object A from B, where B is everything presentable which is not A.

$$Q_{(F)} = \frac{\left| m_{F(A)} - m_{F(B)} \right|}{\sqrt{\sigma^2_{F(A)} + \sigma^2_{F(B)}}},$$

When trying to derive an unknown function, one good approach is to Taylor expand the function and determine the polynomial coefficients. Increasing the polynomial order we might express just any imaginable continuous function, including the best possible contrast function.

It is easy to understand that the polynomial order of a contrast function which distinguishes radishes from tomatoes has to be of at least order two. “Radishes should be red but not too red” *isRadish = R*(1-R) = R-R²*. In the previous tomato, cucumber and banana example we saw that functions might need to combine different color channels. Thus, we not only need polynomial expansion of R in R^0, R^1, R^2… we also need RG, RB, RGB, R^2G, RG^2… We recall that this is similar to the inter-combination of frequencies on different axis when performing multidimensional Fourier or Cosine transforms.

$$
\begin{array}{c} pix_{1\ldots N} \\ G^0 \\ G^1 \\ \ldots \\ G^m \end{array}
\begin{array}{c} \begin{array}{cccc} R^0 & R^1 & \ldots & R^n \end{array} \\ \begin{bmatrix} 1 & R & \ldots & R^n \\ G & RG & & \\ \ldots & & \ldots & \\ & & & R^nG^m \end{bmatrix} \end{array}
\xrightarrow{\text{Reshape}}
\begin{array}{c} pix_1 \\ pix_2 \\ \ldots \\ pix_N \end{array}
\begin{array}{c} \begin{array}{cccccc} R^0G^0 & R^1G^0 & G^1R^0 & R^1G^1 & \ldots & R^nG^m \end{array} \\ \begin{bmatrix} 1 & 0 & 0.8 & 0 & \ldots & 0 \\ 1 & 0.9 & 0.1 & 0.09 & \ldots & 0.0081 \\ \ldots & \ldots & \ldots & \ldots & \ldots & \ldots \\ 1 & 0.1 & 0.1 & 0.01 & \ldots & 0.00001 \end{bmatrix} \end{array}
$$

Obviously the matrix to the left will be as many dimensional as color channels. Adding either new color channels or higher-order polynomial terms will result in more degrees of freedom in the function. Later we will see that models should preferably be built on unitless values rather than light intensity in different color channels.

Example: Training a contrast function for bananas.

Red and green light reflected from cucumbers, tomatoes and bananas are measured. The result becomes:

$$
\begin{array}{c} \\ Observations = \end{array}
\begin{array}{cc} R & G \\ 0 & 0.8 \\ 0.9 & 0.1 \\ 0.8 & 0.8 \\ 0.1 & 0.1 \end{array}
\begin{array}{l} \\ Cucumber \\ Tomato \\ Banana \\ Black\ background \end{array}
$$

Of course a larger training set for hundreds of banana, cucumber and tomato pixels should be used for better statistical certainty.

The correct answer[3] from the function for each observation is:

$$Provided\ answer = \begin{bmatrix} 0 \\ 0 \\ 1 \\ 0 \end{bmatrix}$$

We choose a second order polynomial contrast function of the form:

isBanana = θ_1*1+θ_2R+ θ_3G+ θ_4RG

We cannot choose a function with more polynomial terms than the number of observations. In imaging, however, we can quickly achieve thousands of pixels of each object. We now solve[2] the equation system:

$$\begin{array}{c} \\ Cucumber \\ Tomato \\ Banana \\ Background \end{array} \begin{bmatrix} 0 \\ 0 \\ 1 \\ 0 \end{bmatrix} = \begin{array}{c} \begin{array}{cccc} 1 & R & G & RG \end{array} \\ \begin{bmatrix} 1 & 0 & 0.8 & 0 \\ 1 & 0.9 & 0.1 & 0.09 \\ 1 & 0.8 & 0.8 & 0.16 \\ 1 & 0.1 & 0.1 & 0.01 \end{bmatrix} \end{array} \theta$$

Preferable the equation should be overdetermined. Function coefficients contain information from the observations, for good models or functions this information should be negligible in comparison to the information in the observations (Akaike's information criterion). Also when the quality of the function is evaluated it should not be evaluated with the training data set but rather with an evaluation data set.

The coefficients in θ become: $\theta = \begin{bmatrix} 0 \\ -1.25 \\ 0 \\ 12.5 \end{bmatrix}$

The fuzzy logic interpretation would be: "Bananas are red and green or not too red"

Note 1:

Fuzzy logic is an expansion of logic, to handle intermediate values between zero and one. Similar to Boolean algebra it has the power to convert linguistic phrases into equations. As for Boolean algebra it has only three basic functions also know from statistics:

*A and B = A*B*

*A or B = A+B-A*B*

Not A = 1-A

A, B € [0…1]

Note 2:

Solving over determined equation systems in Matlab is easily done with the backslash operator \

Note 3:

A quantifying answer can also be provided. E.g. how dry is the tomato? Answer: 70%.

4 Color data handling: Abundant color channels, Principal component analysis and physical units.

Some techniques provide abundant color channels, spectrometers provide thousands of color channels. It is not appropriate to build a contrast function on each such channel. The reason for this is that they are not independent even if they are measured independently. A substance has a spectral profile; a mixture of two non fluorescent substances has a linear combination of the spectral profiles of each substance. It is unlikely to observe thousand of substances each with a different profile. In other words, spectral channels are interconnected according to the spectral profile of present substances. An attempt to build a polynomial function on all channels will result in a singular matrix in the regression.

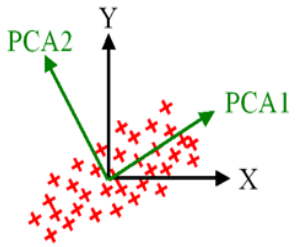

An efficient way to reduce abundant color channels is to use Principal Component Analysis (PCA). PCA is basically just a change of coordinate system, data are projected into basis functions in the order so that the basis function which best describes data becomes the first axis. Imagine the observations as a cigar-shaped cloud of points in the color space. The direction with the largest variation within the points gives the direction of the first axis in the new coordinate system, the first principal component (PC1). Now all data points are projected onto a plane orthogonal to the PC1. The new direction with biggest variance and generate PC2 etc. Finally, the same number of PC coordinates as the number of you observations is obtained.

If one categorizes people by height, weight and volume, a correlation between the observations is found. A person with big volume is likely to be heavy and tall as well. Performing a PCA would change the coordinates and interpretation of the describing coefficients. The one factor that would best describe all observation would be size of the person, this would be PC1. PC2 would be fatness of the person and even covering persons with deviates from the average by being slim or fat. Finally, PC3 would only explain very small and mostly irrelevant deviation such as do the person contain a lot of gas. We might even delete PC3.

When performing a PCA on spectral observations by the command *princomp* in Matlab the following variables shows up:

[*coeff, score, latent*] = princomp(*obs*)

obs is a matrix containing our spectral observations or color pixels. Rows represent observation or pixel number and columns represent color channels.

score is the new basis functions that the data is projected onto. Score 1 is the spectral profile that best describes all the observation, Score two is second most important etc.

coeff are the values needed to recreate the original observation from the new basis functions. These are also referred to as loadings.

latent indicates how well each score explains the whole set of observations.

By looking at the *latent* vector we estimate the number of spectral profiles in a set of observations or in a multispectral image. Even white noise will always be better described by a higher number of PC, since each new basis function contains information from the data set. Real explaining spectral profiles are revealed by a sudden drop in the explanatory grade, use *plot(log(latent),'*')*. To understand at which wavelength data differ, the basis functions in *score* can be plotted. *score(:,1)* will appear like the average spectral profile, *score(:,2)* will indicate where spectral profiles in the set differs most, etc. *score(:,end)* and basis functions in the upper end will only contain noise.

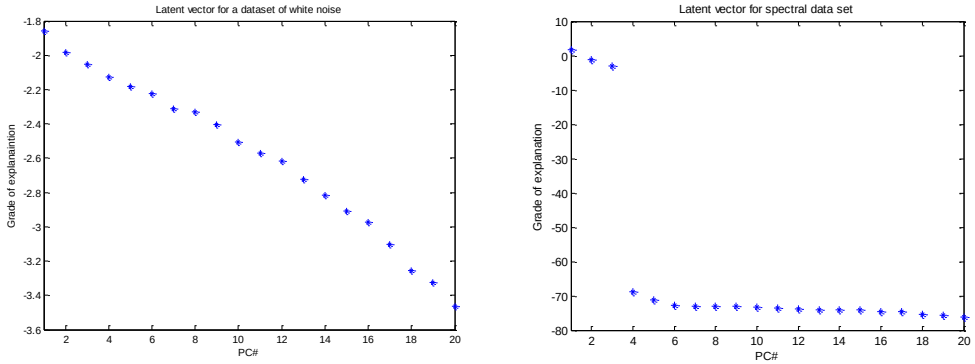

Fig.6. Left: explanatory grade of PCs for white noise. Right: explanatory grade for a spectral data set.

The original spectral data contain a physically interpretable unit, such as light intensity or absorption coefficient. When performing a PCA which is only a linear change of coordinate system the units are conserved. Since the original data can be expressed as: *obs-mean(obs)= coeff *score'* we can choose either to assign the physical units, e.g. Wm^{-2} to the coefficients or to the basis functions. This means, that the coefficients are in fact colors, and it is reasonable to think of a color space is expanded by the PCs.

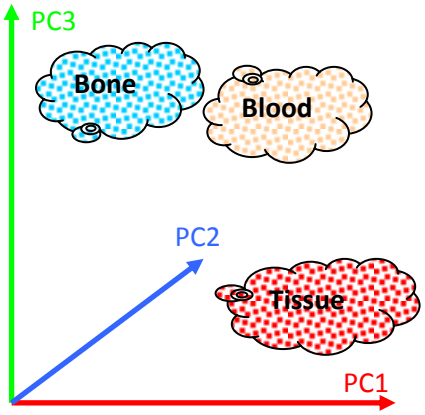

Fig.7. Color space expanded by principal components, the axis carry physical units for intensity.

Also it is reasonable to build a contrast function on the number of information-carrying PCs indicated by the *latent* vector. Everything we need is to exchange the color channels with the coefficients from the PCA. Since the basis functions are orthogonal we are certain not to have problems with singularity during the regression. One issue still remains, though: Dimensionless functions. Tomatoes illuminated by a strong light source will emit more red light than poorly illuminated tomatoes. In our perception they still have the same color and they are tomatoes regardless of how they are illuminated. This problem is overcome by introducing unitless (dimension-less) functions. Instead of feeding the regression with PC with physical units, we feed it with unitless values. These values are rather relational ratios or angles between the PCs than absolute values of light intensity for instance. Ratios suffer from division by zero and a function space from $-\infty$ to $+\infty$. Spherical coordinates cannot generate zero division errors and have a closed function space from 0 to $\pi/2$.

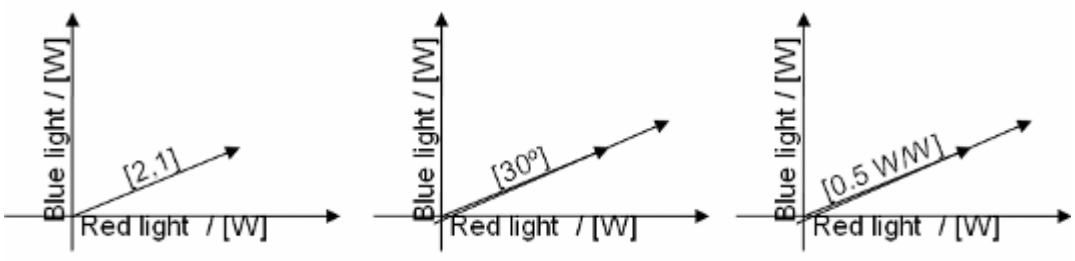

Fig: 8. Figure illustrating the same point being described in different ways. In the last two figures, vectors with the same color but different brightness are plotted

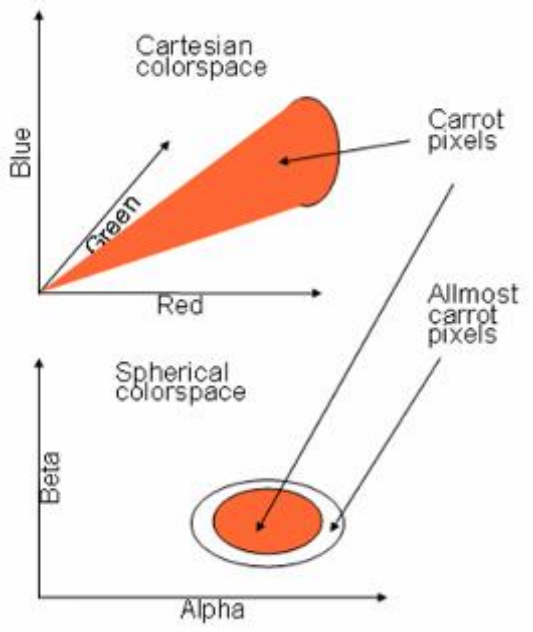

Imagine a cloud of carrot pixels in the color space with the shape of a cone. The fact that they are carrot pixels is given by the direction of the vector rather then their absolute values. The absolute values indicate how much the carrot was illuminated. By transforming an N-dim Cartesian color space into a N-dim spherical color space, we can reject the absolute value containing the physical unit, and remain with relational angles. The cone cloud becomes a circle and is now easier to identify using just a 2D color space. The rejected brightness variable still holds information about how illuminated the object was; with poor illumination the colors will have large uncertainty.

Fig: 9 Objects are often easier described in relative color space.

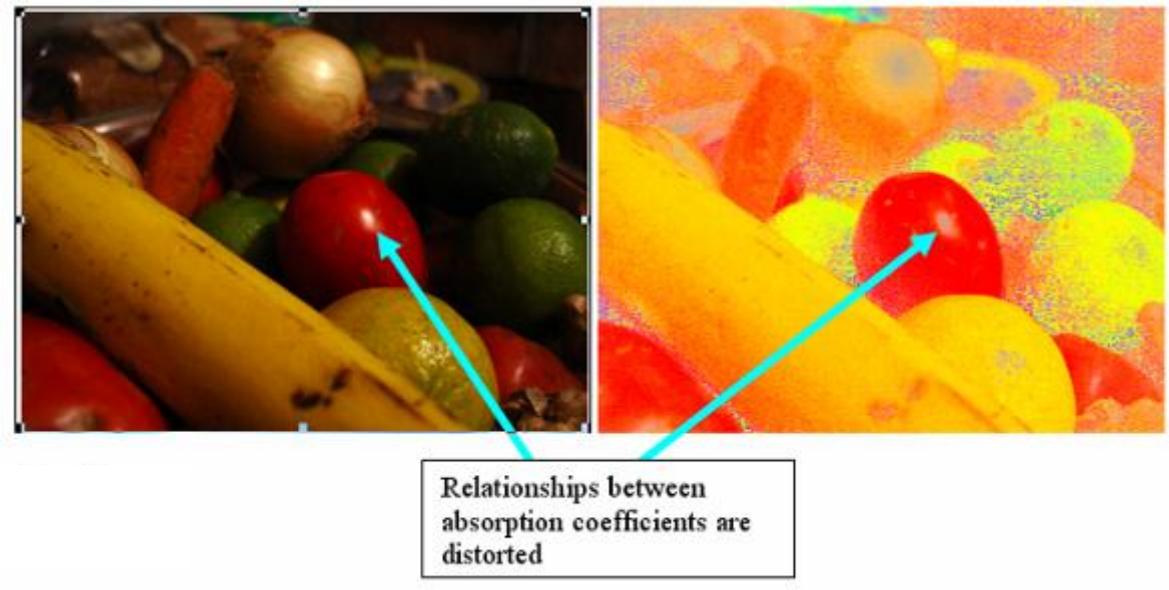

Fig: 10 Left: Normal color photo of vegetables. Right: same image with removed intensity.

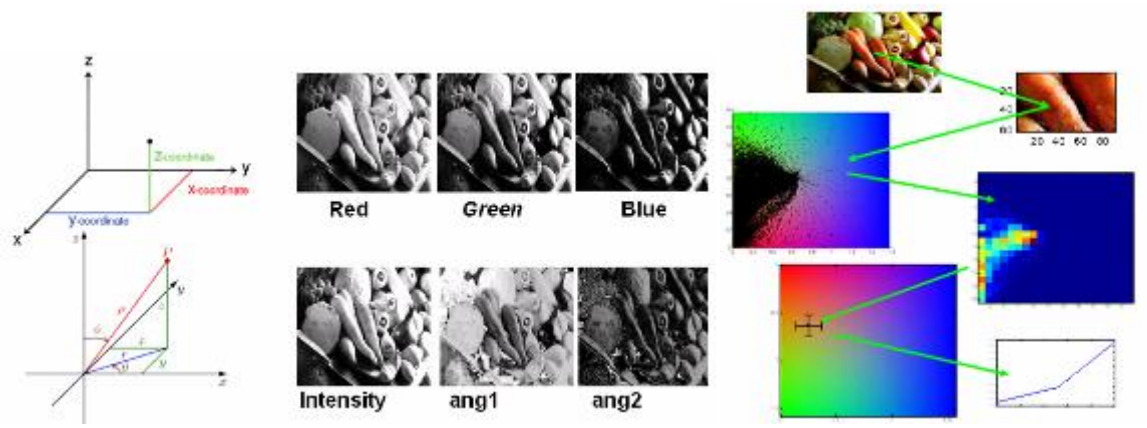

Fig: 11 Left: Ways to represent the same point. Middle: Interpretation of representing units. Right: Carrot pixels mapped out in angles in a spherical color space, histogram mean values and normalized spectral profile.

Considering light spectra, one might think of them at histograms where each mode or spectral feature represents an electronic transition and thereby represents a chemical substance. Modes and groups in color space histograms represent objects, which characteristic relation between its chemical components. However, we will have difficulty to represent much higher than 2D histograms to ourselves, and it might be difficult to comprehend a mode or cluster in a 5D color space.

5 Preparation:

- Read about color spaces. Sterling's (Swedish: starar) have four color receptors in the eye. What does their color space look like?
- Refresh transformation from Cartesian to Spherical coordinates. How will you make a 4D transformation?
- Read about projecting data onto basis functions. PCA, regression and Taylor expansion. Familiarize yourself with the Matlab functions *help, reshape, princomp, imshow, imagesc, imcrop, medfilt2, bashslash operator* \

6 Exercise:

- Take a look at the instrument and make sure you understand the operation
- Place as many different objects as possible inside the instrument enclosure. Preferably the objects should have different colors. Place also objects with similar color but different chemical composition. Place at least one wet and one dry object. Feel free to bring your own objects to the exercise.
- Turn on the power source and adjust the voltage to 10 V
- Open the application AMCAP this program captures movies and saves them to the disk. Choose file. Start preview. Set frame rate to 1 fps and time limit to 60 s. Arrange your object so that they are within the picture. Start capture. Rise the power supply voltage to 16 V and press start.
- Slowly lower the voltage to zero over a 60s time.
- Close the application, and open Matlab. Go to your working directory.
- Load the avi file with the command: *avi=importdata('mycapturefile');*
- Frames can be showed with: *imshow(avi(frameNo).cdata)*
- Determine number of frames by: *frames=length(avi)*
- Save the image resolution with: *res=size(avi(frameNo).cdata)*
- Monochromatic webcams are not easy to find, we will therefore convert to black white sequence. Also since we do spectral analysis, spatial information is irrelevant, therefore we place all pixels from a frame on one single column: *for frmNo=1:frames; M(:,frmNo)=reshape(sum(avi(frmNo).cdata,3),[prod(res(1:2)) 1]);frmNo; end*

- You now have a matrix M. Rows in the matrix are pixel numbers, or observations made at different places in the picture. Columns are different frame, thus different time, different filament temperatures and differently colored illumination.

- Perform PCA on M: *[coeff scores latent]=princomp(M);*

- Investigate spectral components: *plot(log(latent),'*')* How many do you estimate?

- Extract the most describing pictures from *score*: *PC1=reshape(score(1,:),[res(1:2)])*

- Investigate the pictures with *imagesc*, use *medfilt2* to remove noise from pictures.

- Normalize the pictures with *(PC1-min(min(PC1)))/max(max(PC1))* compose false color pictures *FCP1(:,:,1)=PC1; FCP1(:,:,2)=PC2;* etc. Present using *imshow*. Compose various false color pictures.

- Produce a unit-less false color picture.

- Choose two objects from the false color pictures and select the pixels using: *SEL1=imcrop(FCP1);* Arrange the pixels on a line as previously, transform to spherical coordinates use you own function or *cart2sph* map out the pixels from both objects in a 2D color space, use *hold on*, dots and different colors. Can the object be distinguishes in the color space?

- Make a new selection containing "everything else" than your first selection. Arrange the pixels. Construct an observation matrix with pixels from your first selection on top of the pixels of everything else. Add a zero order term to the polynomial i.e. a column of ones. Construct a correct answer vector with the correct answer of the contrast function for every row of observations. Solve the function coefficients. Apply the function to the picture. How well did the function manage?

- Increase to second order polynomial, and observe again.

6 Example of Wien shift imaging

Fig 12 Various object from the staff kitchen was placed inside the instrument.

Various objects from the department kitchen were placed into the instrument. Fifty black and white images of the scenario in Fig. 5.1.6.1 were acquired varying the power to the filaments. We now ask our selves, can these pictures be expressed as linear combination? The answer is no, because the spectral content of the illumination is different and because the objects do not have the same absorption spectra. So, how many pictures do we need to take the linear combination of in order to express each of the fifty pictures? We perform PCA on the data set and plot the explanation grade.

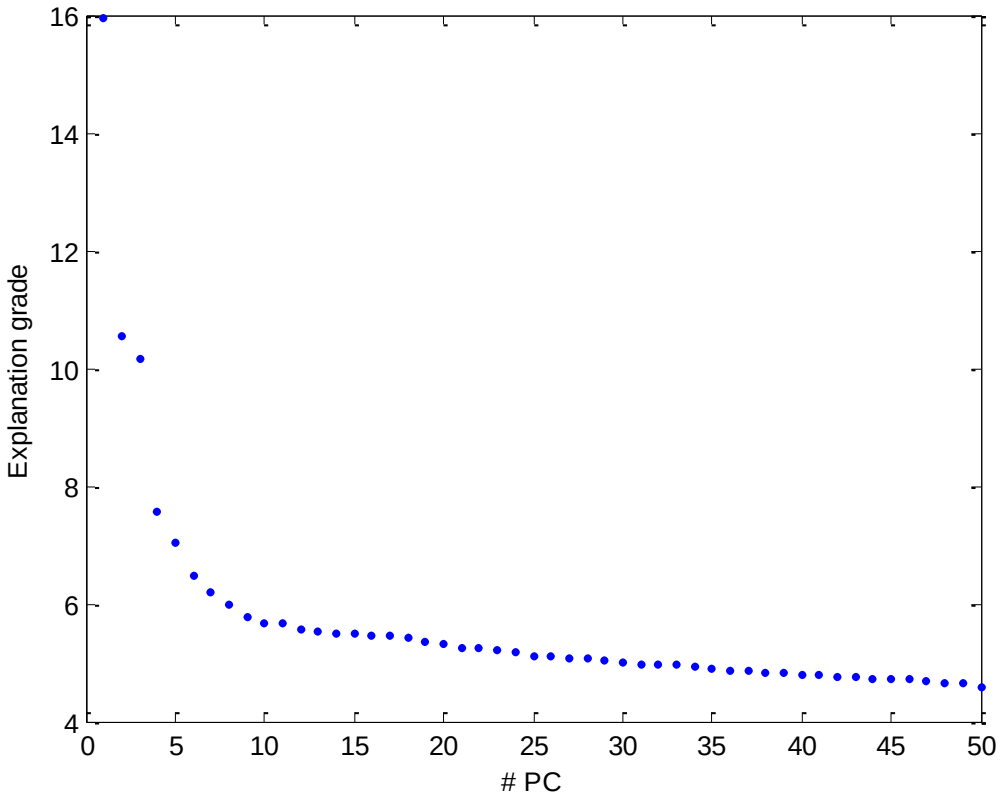

Fig 13 Latent vectors indicate linearly independent spectra detectable

The point in fig 5.1.2.2 tells us how much of the data each new PC explains. There are several information criteria and several ways to interpret such curves. We have to keep in mind that PCA is just a change of coordinates and as such is the same data from another perspective. If we include all PC we express the data completely. One approach is to identify sudden drops in the curve. Another approach is to add the information provided to the curve, in a way so that is comparable with the explanation grade. This would provide us with a minimum some where between first and last PC. A safe method is to look at de differentiated curve. By doing so we realize that by going from PC10 to PC11 nothing is gained, therefore all PCs after PC10 can be considered to be noise. If we plot the first nine PC's we see how they eventually converge towards noise.

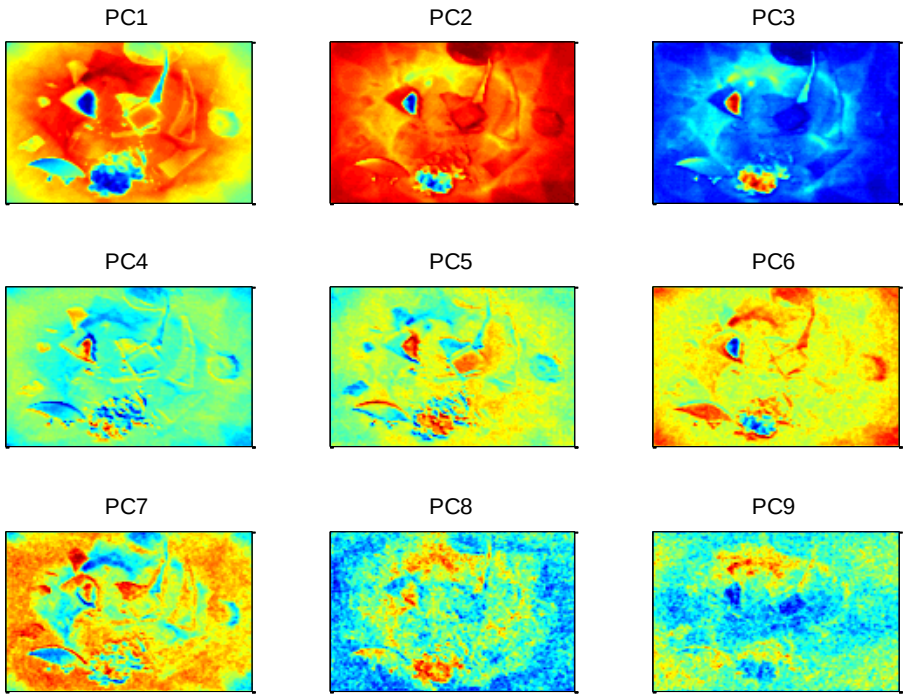

Fig. 14. PCs converge to noise

A false color photo can be generated from PC1, PC2 and PC3. Most distinctive are the object containing chlorophyll, the soil is also distinct probably because of the humidity content. The small piece of sponge reacts a lot to the changes of filament temperature. There might different reason, most likely the fact that the object is scattering, and scattering vary with the wavelengths.

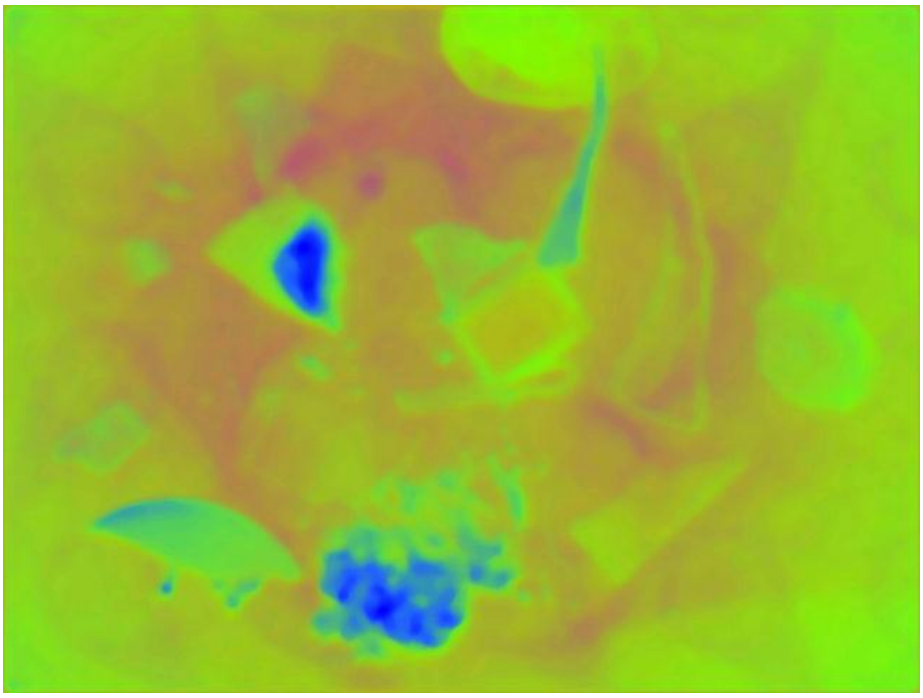

Fig 5.1.6.4 Example of false color picture

5.2 Applying estimating models to LED based fluorosensor.

Several data series was acquired during the master thesis work of Sara Ek. The data were processed in steps similar to those in chapter 5.1. The instrument provides an excitation-emission matrix of 3 x 3648 pixels. One less successful attempt was done to distinguish infant male nutmeg plants from their female counterparts. More successful model was applied to other subjects. We will concern us self with an example that distinguish papaya leafs from nutmeg leafs.

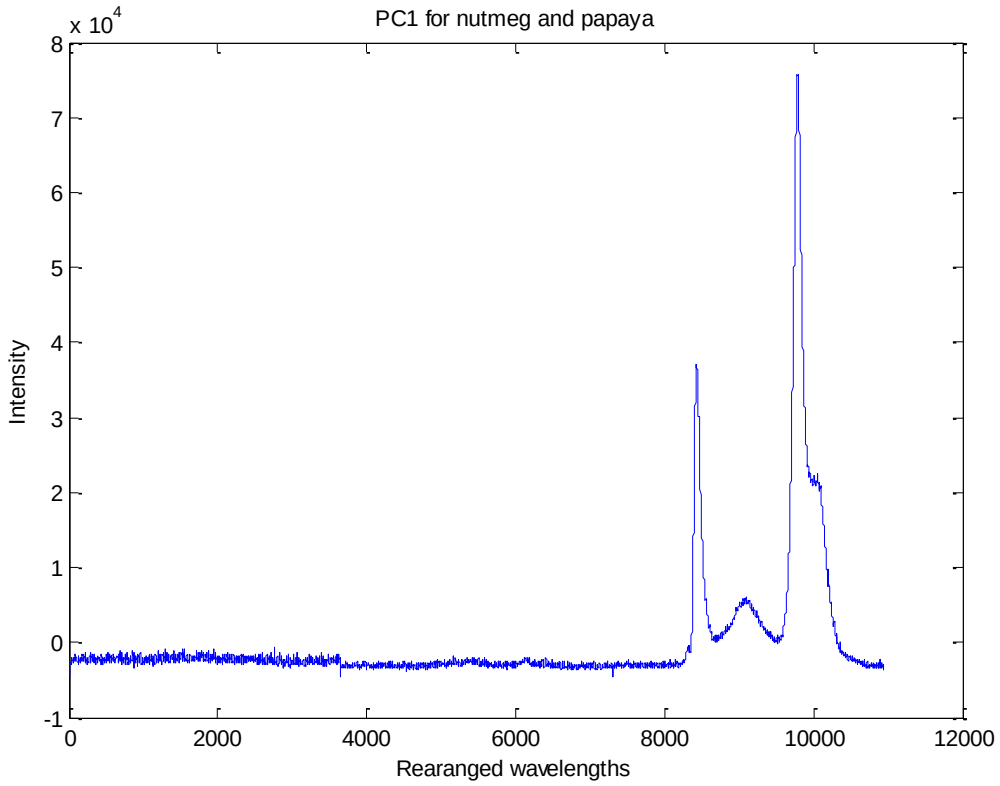

Fig 5.2.1. Rearranged spectral data

The excitation emission matrix is rearranged into a single vector. According to Sara Ek the two shortest wavelengths unfortunately were completely absorbed by a wax layer on the leafs. Noise levels for the lower two LED channels vary probably due to temperature changes and different exposure times. The variance has nothing to do with the sample, and we will have to discard the lower channels, but the analysis will continue.

The emission spectral resolution is particularly high and data was highly abundant. The modeling data were reduced with PCA. Observing the latent vector with explanation grade of each PC, we can decide to reject PC of order five and higher.

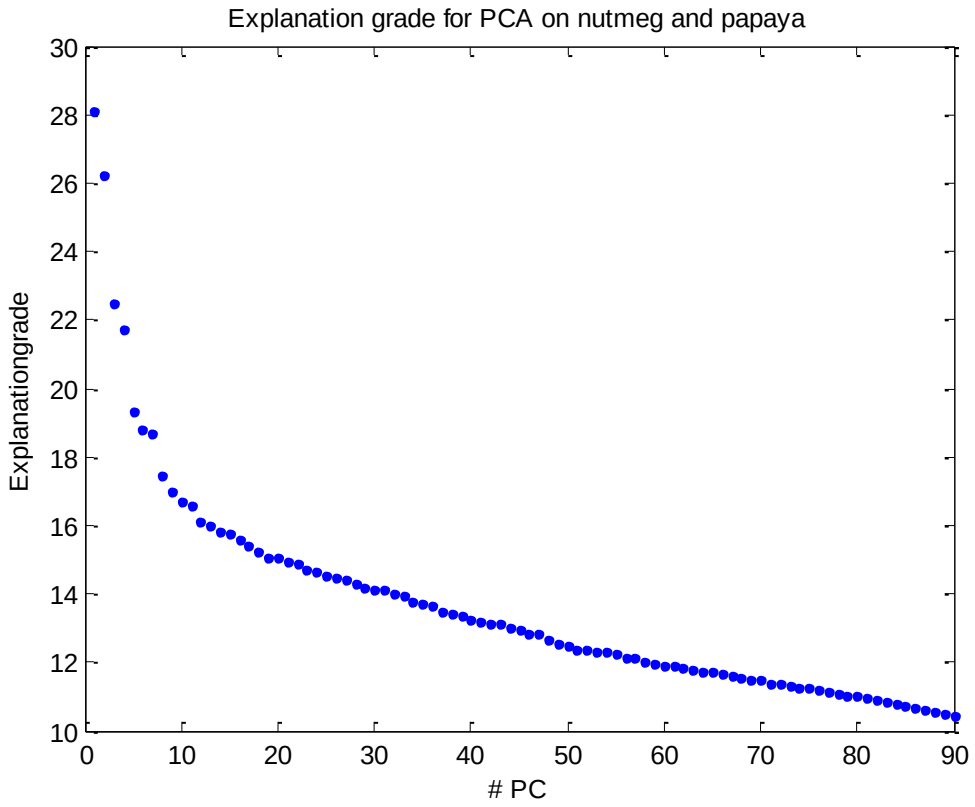

Fig 5.2.2 Explanation grade of each PC

The four first basis functions were stored for later use. Inspection of the basis functions reveals at which wavelengths spectral variance occurs. A leak of reflected light from a color filter in the instrument causes an additional spectral peak. The malfunction is irrelevant for the further data analysis.

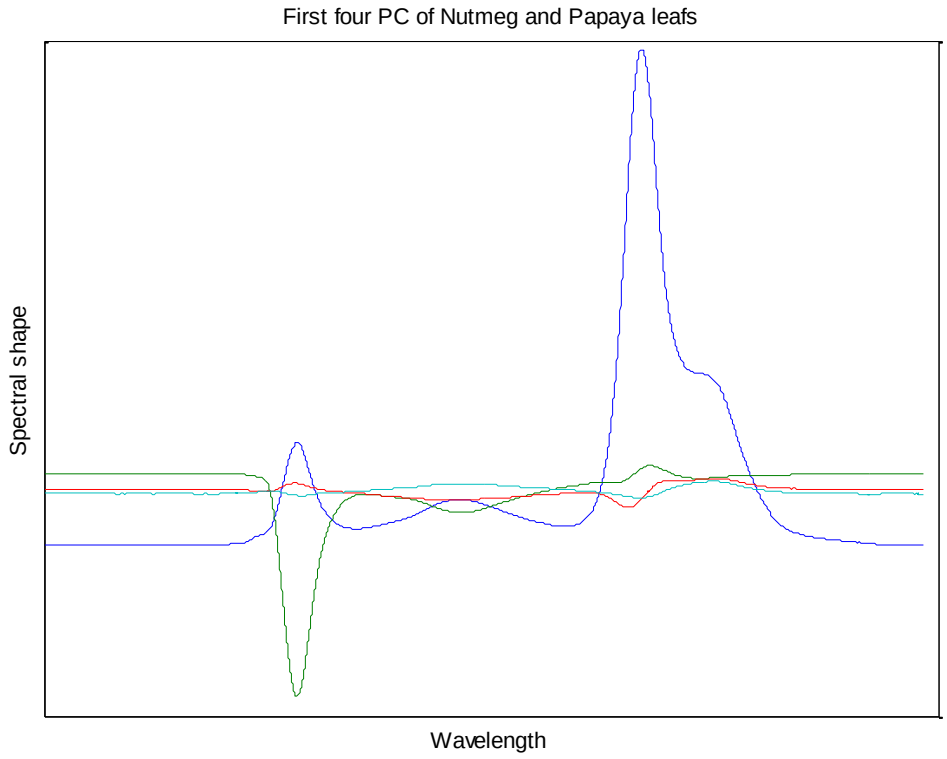

Fig 5.2.3. Shapes of principal spectral components

The four loadings describing each individual in term of the new basis functions, was normalized and transformed to generalized spherical coordinates, by the function:

```
function sph=gensph(cart)

% Generalized cartesian to spherical transformation

r=sqrt(sum(cart.^2,2));


a(:,n)=atan2(cart(:,1:end-1),cart(:,2:end));


sph=[r a];
```

The intensity information carried in ***r*** was rejected, leaving just three unit-less coordinates, representing the spectra for the individuals. When constructing the polynomial model, the degrees of freedom were limited by the length of the training data set, which were 45. A first order polynomial of the form:

$isNut = k_1+k_2*\alpha_1+k_3*\alpha_2+k_4*\alpha_3+ k_5*\alpha_1*\alpha_2 \ldots k_8*\alpha_1*\alpha_2*\alpha_3$

With a higher number of samples the model order can be increased both by higher polynomials and by combination of terms, i.e.: α_1^2 and $\alpha_1*\alpha_2$. For diagnostic purpose other observation such as: smoker/nonsmoker, diabetes, etc. can also be included at this stage. Even such terms are typically combined in medicine. E.g, Risk of stroke = Overweight * (1-Alcoholic)

This function Taylor expands M to the p'th order.

```
function P=polyth(M,p)
% P=polyth(M,p)
% Generate an N dimensional space of Taylor
% expansions to the order of p
% Where N the number of columns in M.
% Returns P with p^size(M,2) coloums

nc=size(M,2); T=[]; S=[];

for po=0:p
   T=[T M.^po];
   S=[S 1:nc];
end

C=nchoosek(1:nc*(p+1),nc);
i=find(prod(diff(sort(S(C),2),1,2),2));

L=[];
for nt=1:length(i)
    L=[L prod(T(:,C(i(nt),:)),2)];
end

P=L;
```

Model coefficients are solved by providing correct answer for each leaf:

$$\begin{bmatrix} 1 \\ 1 \\ \dots \\ 0 \end{bmatrix} = \begin{bmatrix} 1 & \alpha_1 & \dots & \alpha_1\alpha_2\alpha_3 \\ 1 & \alpha_1 & \dots & \alpha_1\alpha_2\alpha_3 \\ \dots & \dots & \dots & \dots \\ 1 & \alpha_1 & \dots & \alpha_1\alpha_2\alpha_3 \end{bmatrix} * \begin{bmatrix} k_1 \\ k_2 \\ \dots \\ k_8 \end{bmatrix}$$

The model was applied to the evaluation data set through projecting the evaluation spectra on the same basis function found by the PCA. The answer of the models are within the distributions in Fig. 5.2.4.

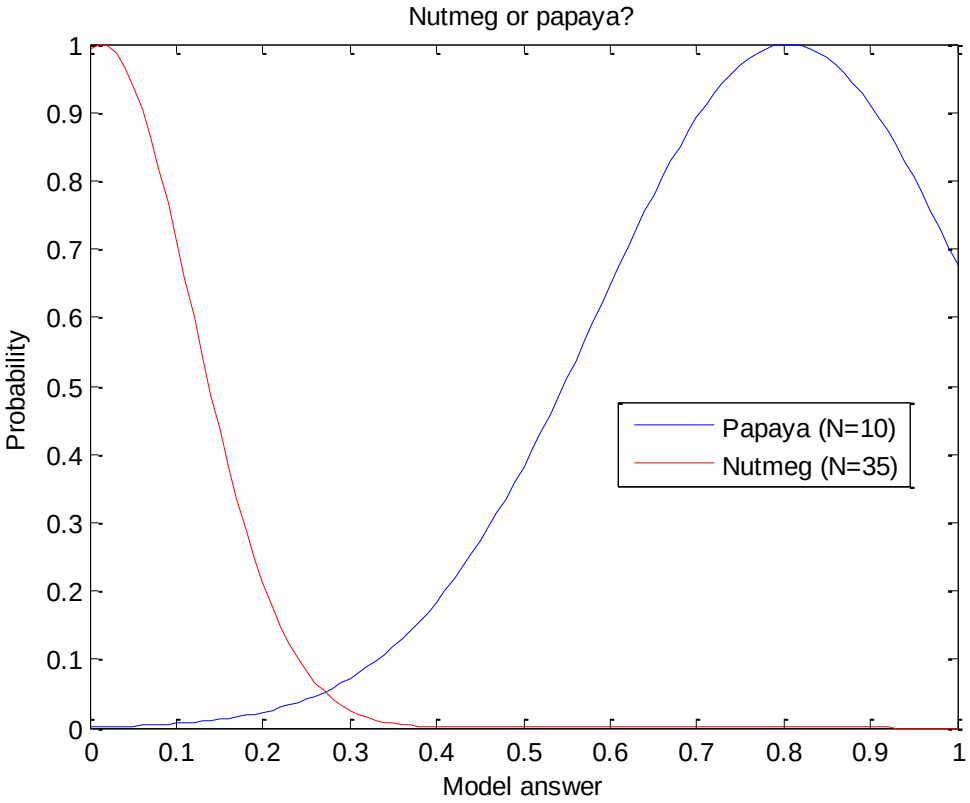

Fig 5.2.4 Number detectable differences within the group should be indicated by a sudden drop in explanatory grade.

The model output escapes the logical range from zero to one. This can be avoided by introducing a logit link function. This will not be done in this paper.

5.3 Simultaneous measurement of absorption, fluorescence and scattering

Previously we have processed spectral excitation-emission matrixes (EEM) of three different excitation wavelengths. More over the excitation light it self was filtered out. We will now see how similar approach to data processing can be applied to large EEMs and how we can reduce entire surfaces with PCA. We can even use the PCA the approximate phenomena arising from scattering and absorption.

5.3.1 Location of spectral information

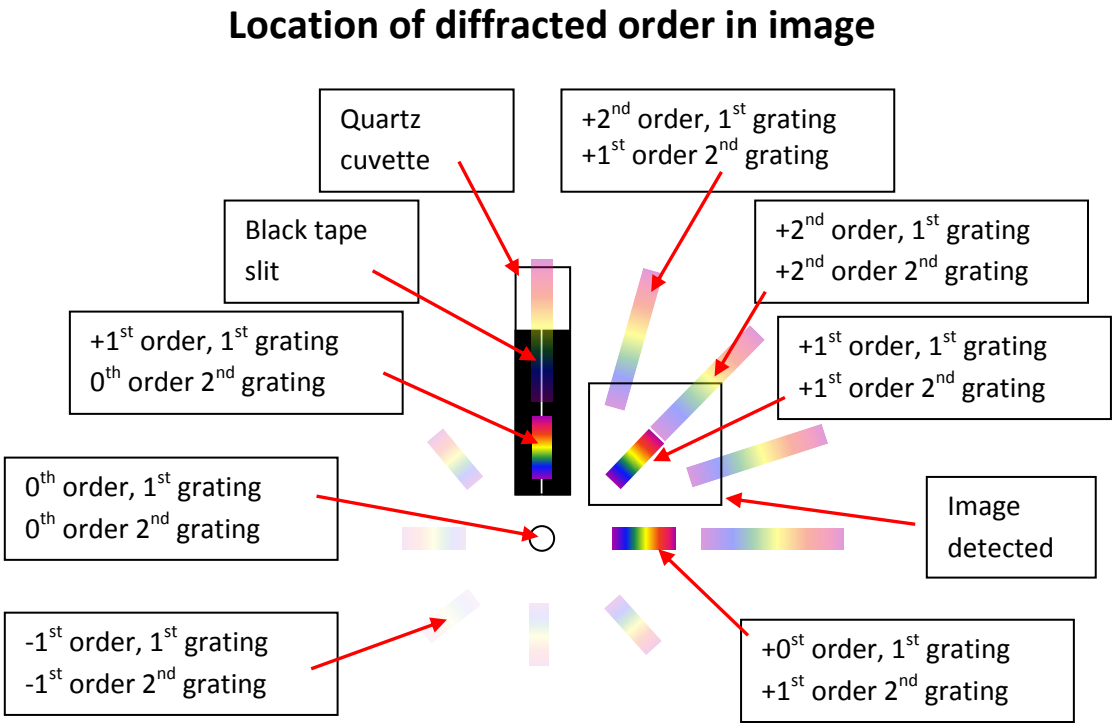

Fig 5.1.1.1 Location of different orders of diffraction in the image.

When observed with the eye or a camera, the excitation slit in the setup shown in Fig 4.1.2.4 is displaced in an infinite grid generated by the multiple orders of the two diffraction gratings. The blaze of the gratings makes the +1st orders stronger than the remaining. Overlapping orders is one issue using gratings. Several orders are imaged which makes the data slightly difficult to interpret but is no hinder for further statistical processing.

5.3.2 Throughput of system

One considerable issue of the concept was, whether any light was going to make it all the way through the setup. Light was detected and several factors will now be shown why the signal could be expected to be much greater than in this case.

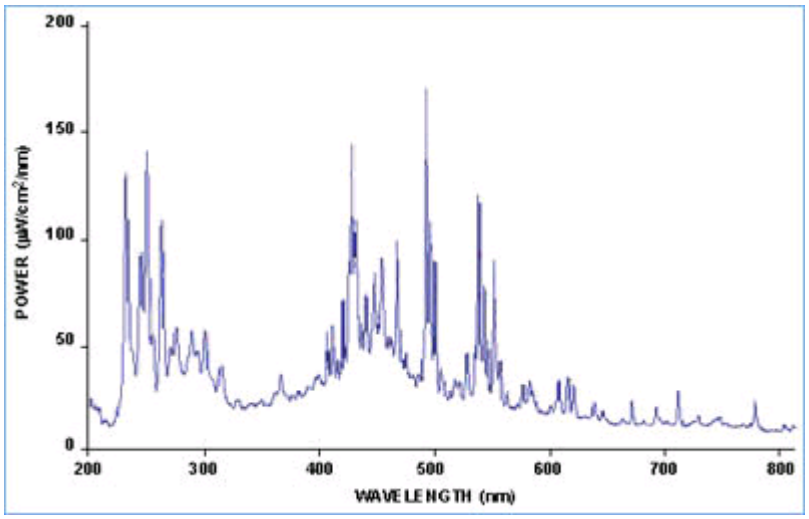

Fig. 5.1.1.1 Emission spectrum of a PX2 flash lamp

The light source used, is relatively small and weak, emitting only 50 µW/cm^{2}nm. The source is portable and can be supplied by batteries. Much stronger light sources are available. Considerable losses can be expected in the fiber coupling. The fiber is, however, not essential for the setup, and great improvement can be made by direct illumination, estimating at least a tenfold improvement. The integration time for the imager is approximately 200 ms. The flash fires with a repetition rate of 150 Hz with pulses of 200 µs. This means that the sample is only illuminated 3% of the time during the exposure time. By synchronizing the imager and flash and only expose during flash discharge one would gain a factor of 33 of signal.

The blaze angle of the gratings has not been optimized due to lack of time. Further throughput could be gained here. Gratings have considerable losses in diffractions in all other orders than the first. Prisms might replace the gratings, but involve more complexity. In present case case only a fraction of approximately 20% of the light focused on the tissue slit enters the slit. This is due to the astigmatism; a factor of five could be gained here. The inside of the slit is currently made from black tape. One issue is that black tape might not be opaque for IR, also the reflectance is high for some wavelengths, and this contributes to increased background.

The imager is rather simple, and much more sensible imagers exist. The imager has 10 bit dynamic resolution, but the application for the camera only support 8 bit files. For the data processed the signal was in order 1:150 integers. The background was in orders of 1:140 but not in the same position though. The background subtracted signal was left with only approximately 1:10 dynamic resolution. With the time constraints for the thesis no further alignment could be done.

Eventually, the whole system should be placed inside a light sealed-enclosure; this would further increase the signal-to-noise ratio. All in all, it can be estimated that the present setup efficiency to be at least a factor 10.000 or 100.000 below a professional solution. This would suggest a 20 µs exposure time with the current light source.

5.3.3 Median filtering

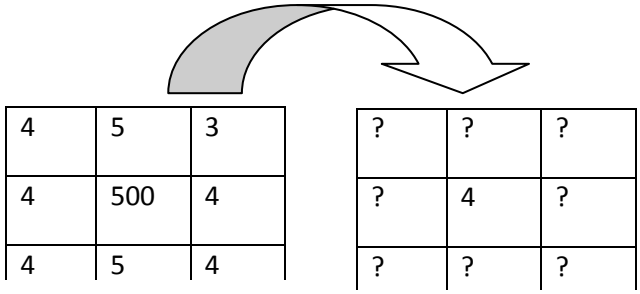

Dust on the imager and possible malfunction for single pixels on the imager result in single pixels which are not representative for the light in the image plane. Usually, such stuck pixels are either completely black or completely white. This might be a huge shift in comparison to the surrounding pixels, and principal component analysis could have difficulty to interpret the white pixels since they are not linearly dependent on the others. The pixels are consistent in time and cannot be averaged out in time. Averaging in space would still propagate the error, in a minor grade. By using a 2D median filter the pixels can be filtered out completely. The image can be resized by the filter window size afterwards, since the spectral resolution of the system limited by the tissue slit is much larger and thus the data would be redundant.

5.3.4 Spatial transformation

In case of a compact system where slight displacement of component might happen over time, one can use the spectral peaks from the xenon source as a reference and correct the image by rotating and morphing before further data analysis. This would insure consistency of the measurements. Also the perspective from where the image is taken might distort and stretch the picture, the results is that the emission axis is not perpendicular to the excitation axis. Such stretch is also easily corrected for digitally.

5.3.3 Rolling shutter issues

The fact that there is no synchronization between the flash and the rolling shutter imager, gives rise to tiny fringes along the emission axis. To avoid this a global shutter imager could be used. The signal can be filtered out by a frequency filter, or synchronization between imager and flash could ensure an even number of flashes during exposure of each pixel row.

5.3.4 Spectral resolution and reference

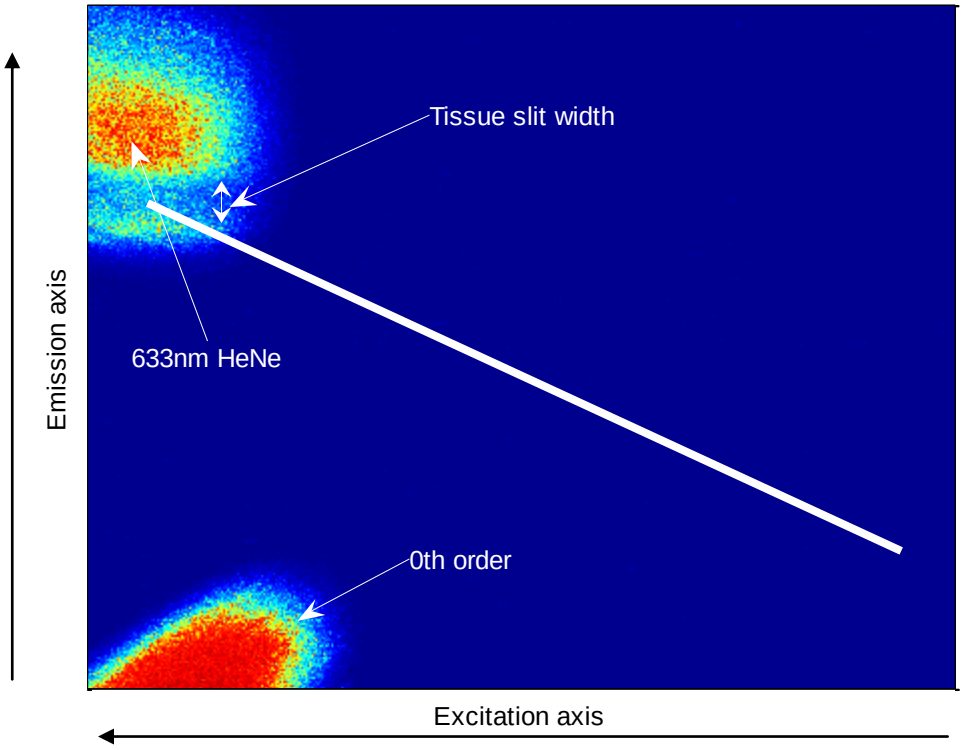

Fig. 5.1.4.1 HeNe laser reference.

A laser can be coupled to the fiber instead of the white light source. Because on the well defined emission several conclusions can be drawn. The absolute position of the 633 nm light can be determined. Since the light is completely monochromatic one single image is formed depicting the slit, as such the slit width can be determined. No smaller spectral features than the slit width can be determined and one might as well apply spatial averaging filter of the size of the slit.

The spectral resolution is relatively bad. This is mostly due to the fact that the excitation light is not completely focused.

5.3.5 Measurement on dilutions

A measurement series was done with 20 measurements. Volumes of milk powder, Coumarin 102, Rhodamin B and green household color were added gradually to a quartz cuvette. The adding was performed with an auto pipette. Each measurement provided a surface containing information of absorption, fluorescence and scattering of the content of the cuvette.

In a non scattering sample, absorption and fluorescence phenomena would contribute to a linear combination of a finite number of base surfaces relative to the present amount of substances. Thus the observations could be reduced to linear coefficients of such base surfaces. A reasonable approach to find such base surfaces is to use PCA. The number of base function would not necessarily be the same as the present substances e.g. a mixture of two fluorescent substances will not provide a linear combination of just two surfaces. Imagine for instance that one substance emits light which excites the second substance. It is understood that the observation can only be fully described by the observation for each substance alone plus the product (fuzzy *and* operator see chap. 5.1) of the two observations.

When considering a scattering sample as we do in this case, observations cannot be expected to be described by a linear combination of a finite number of surfaces. This is because the backscattered light profile from a point given by the Green's function, changes shape spatially when $\mu_{abs(\lambda)}$ and $\mu_{sca(\lambda)}$ vary. PCA is generally not a good approach to express spatially changes in a picture. However the scattered light profiles are expected to behave in a certain way and we might make a good approximation with a limited number of base surfaces. Attempts could be done to extract $\mu_{abs(\lambda)}$ and $\mu_{sca(\lambda)}$ and subtract of de-convolve the spreading profile from the observations, and then provide those side be side with the fluorescence coefficients $I_{f(\lambda ex, \lambda em)}$. The data acquired in this thesis are however far too poor for such an attempt.

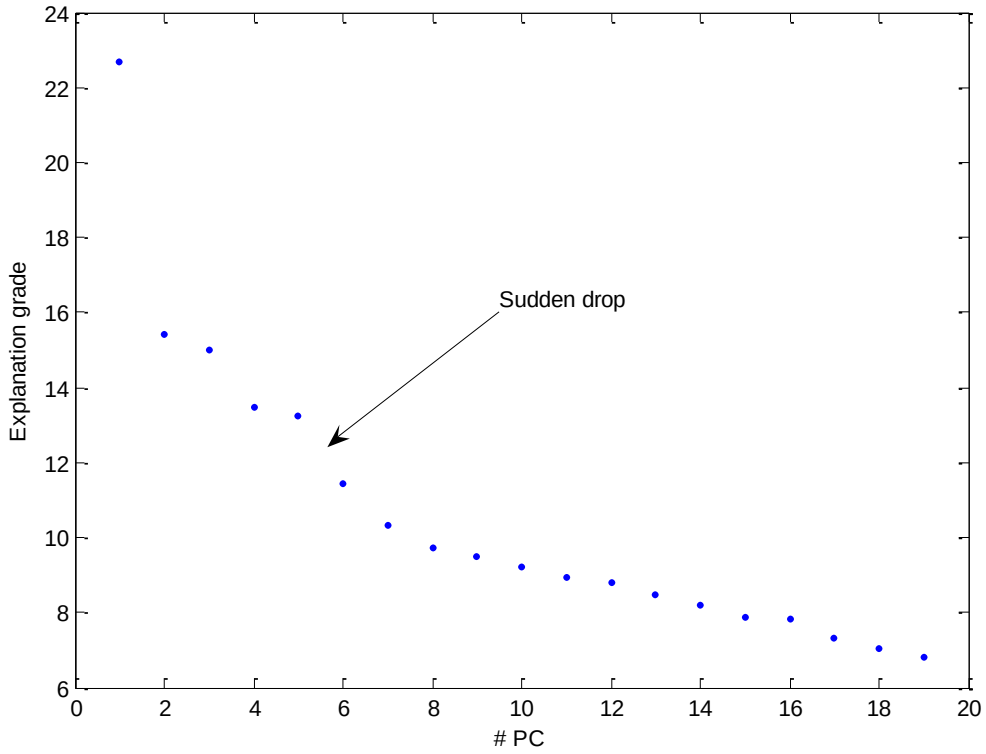

Fig. 5.1.5.1 Drop in explanation grade indicates detectable physical factors.

A decision is made to let the observations be represented by linear combinations of five base surfaces. Ten observations, now represented by five loadings, were taken to train a regression model. Spectral data are expected to correspond linearly to concentration changes, apart from the surfaces describing the spreading, but a linear approximation was chosen. No inter-combinations products in between the loading were applied, the model had 6 degrees of freedom (DOF) and the form:

$$y = \phi\theta$$

$$\begin{bmatrix} C_{milk1} & C_{cou1} & C_{Rho1} & C_{Green1} \\ C_{milk2} & C_{cou2} & C_{Rho2} & C_{Rho2} \\ \dots & \dots & \dots & \dots \\ C_{milkN} & C_{couN} & C_{RhoN} & C_{GreenN} \end{bmatrix} = \begin{bmatrix} 1 & PC1_1 & PC2_1 & \dots & PC5_1 \\ 1 & PC1_2 & PC2_2 & \dots & PC2_2 \\ \dots & \dots & \dots & \dots & \dots \\ 1 & PC1_N & PC2_N & \dots & PC5_N \end{bmatrix} \theta$$

If the models answers are supposed to be restricted to a closed or semiclosed function space a link function can be introduced. E.g., a risk for cancer must be in between 0% and 100%, in such case a logit link function is introduced of the form:

$$y = g^{-1}(\phi\theta)$$

$$g_{(x)} = \ln\left(\frac{x}{1-x}\right)$$

Link functions can also be introduced if the relation from spectral data and the parameter being estimated is expected to be logarithmic or otherwise nonlinear.

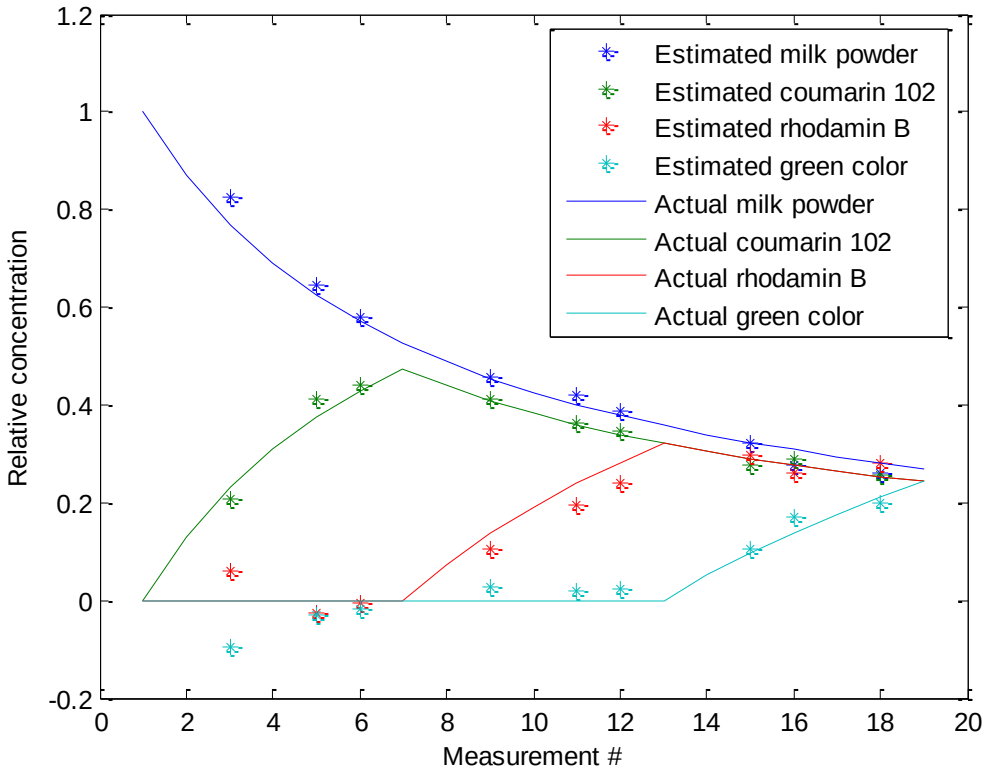

Fig. 5.1.5.2 Concentrations of different substances as additional volumes are added. The model estimates a evaluation sample group.

The model was fed with the evaluation dataset, and the estimation in Fig. 5.1.5.2. One has to keep in mind that the estimation was based on rather noisy data with a dynamic resolution of 1:10.

5.1.6 Physical interpretations

As mentioned the acquired data were of rather poor quality. The dynamic resolution is low and so is the spectral resolution. Acquisition might as well contain other artifacts.

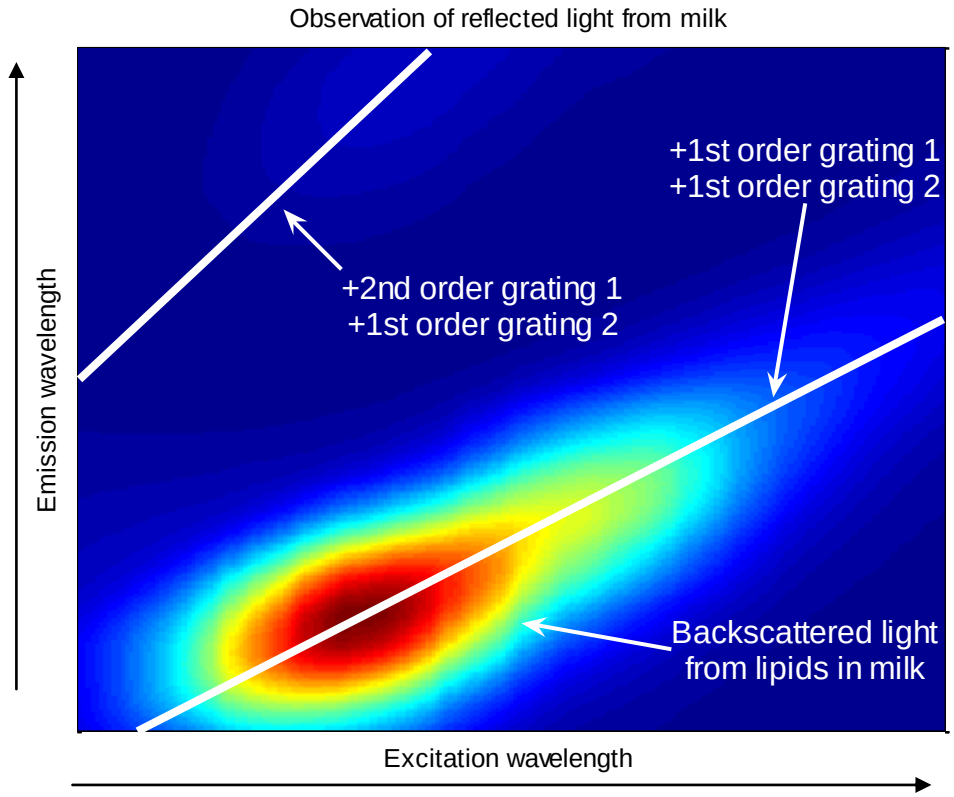

Fig. 5.1.6.1 Backscattered light

When observing the reflected light from milk, a maximum is observed at a certain wavelength. The reflected light not only represents the optical properties of the sample. The emission of the xenon flash is dominant in the UV region, and the spectrum is far from uniform. Another fact that was observed was that the acquisition is highly dependent on the quality of the slit. Small roughness in the slit results in large relative light intensities along the excitation slit.

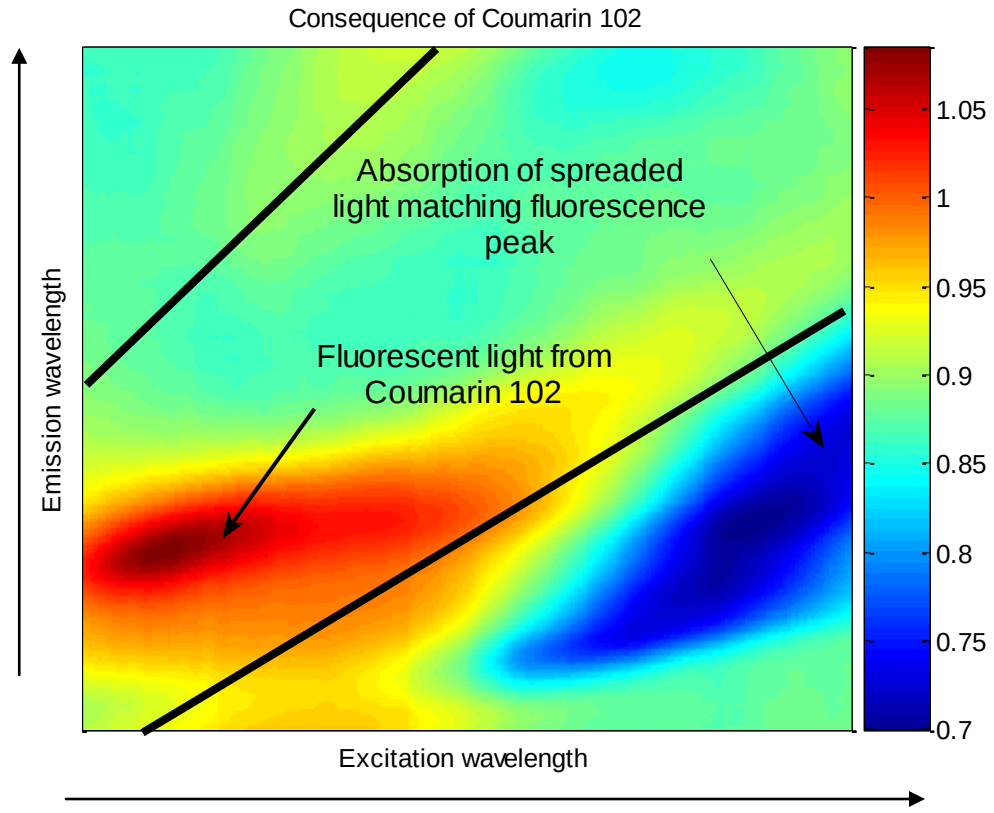

Fig. 5.1.6.2 Fluorescent light from Coumarin 102

Coumarin 102 is a fluorophore which is yellowish but emits a clear blue light when exposed to UV light. The system has poor UV sensitivity because of the transmissive glass optics. When added to the milk a fluorescent emission peak is detected. We also observe that the blue light spread in the lower triangle diminishes because of increased absorbance for that light.

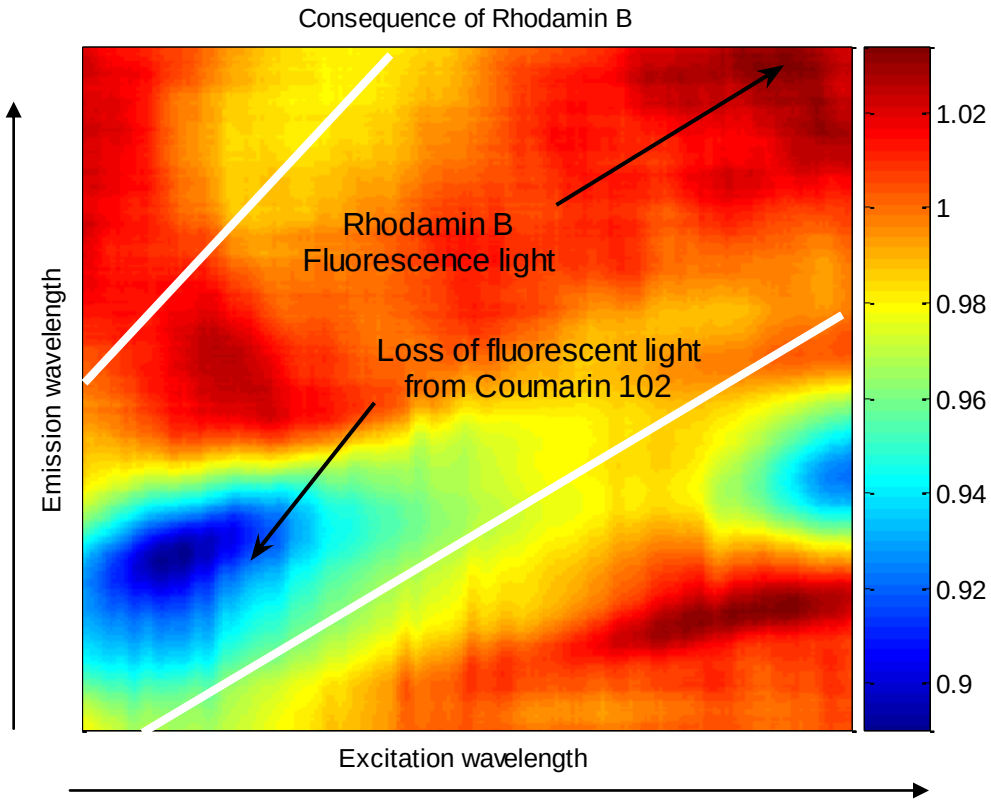

Fig. 5.1.6.3 Response to Rhodamine B

Rhodamin B is another fluorescent dye absorbing blue and green and emitting reddish light. When added it is observed how the previous fluorescent dye emission is extinguished. Emission is now instead detected in the red region.

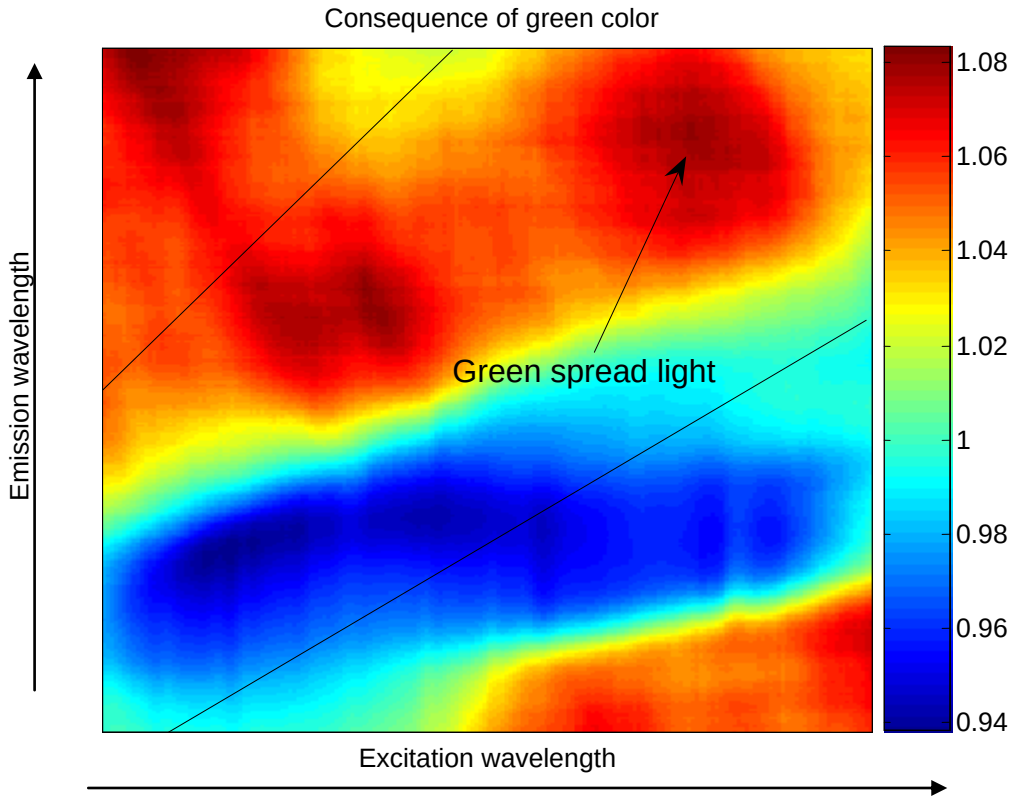

Fig. 5.1.6.4 Response to green absorbing color

The green absorbing color absorbs the blue and red light. One might wonder how light intensities are somewhere gained by adding an absorber. One has to keep in mind that all three volumes of milk, Coumarin, and Rhodamin are diluted by adding further volume. That fact might explain a gain of intensity relative the previous measurement even if the added volume is purely absorbing.

5.4 ASAP simulation

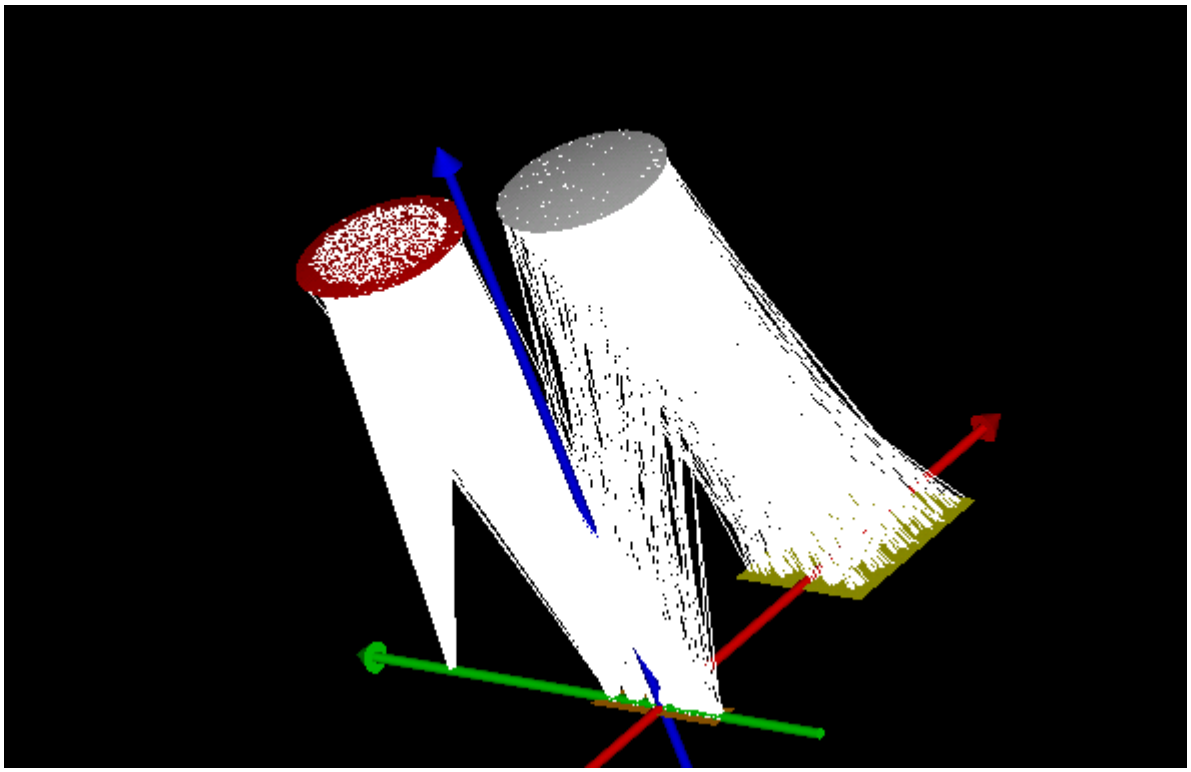

Fig: 5.4.1 Monochromatic light splitting into multiple orders diffraction in two perpendicular concave gratings.

ASAP (Advanced System Analysis Program) is an advanced software from Breault Research Organization for optical simulation. The simulation takes advantage of Monte-Carlo-based ray tracing. That is, randomized rays are generated in the light source; each ray contains the property of intensity, direction, a single wavelength and polarization. When a ray interacts with a surface the ray splits up in new rays according to the properties of the ray, properties of the surface and physical laws, e.g. Snell's law. The new rays will have modified properties in such a way, that they share the original ray intensity among them. Direction and polarization will also be changed. If direction of the new rays will lead to impact on another surface then the process is repeated. In order to insure simulation termination, a light ray will be terminated after a certain count of interaction or after certain intensity loss, determined by the user. Eventually the rays will impinge on the detection plane and properties of the ray set can be analyzed, e.g. focus, efficiency, wavelength dependence, etc.

Surfaces contain geometric information of their orientation in space. They also possess information of the refraction index on either side of the surface. Furthermore, they can have coating information with reflection and transmission spectra. Special surface effects such as diffraction gratings can also be assigned to coatings.

Volumes are contained between surfaces. Properties of the volumes can also change ray properties. Such effects are absorption, fluorescence and scattering. The tissue in this project was modeled by such a volume; a model for diffuse paper reflectance was imported.

Optical simulation provides fast and inexpensive optical experiments, and possible decision making for ordering optical components. Batch files can be made where geometrical parameters are swept to find optimal design of setups. The geometry in ASAP is best suited for a single optical axis. Changes and tuning of a true 3D geometry requires considerable time and patience, mostly because of the text based geometric construction. Also the software will only correct for the included physical phenomena and evaluating whether a result is realistic might be just as easy as creating the setup in reality.

Several setups were generated in ASAP. Overlapping spectral regions were studied for diffraction gratings. Focusing properties were studied for a prism setup. It was unrealistic to obtain any absolute estimation of the throughput efficiency of the system. Such values would have been useful for requirement for lamp emission and quantum efficiency for the detector.

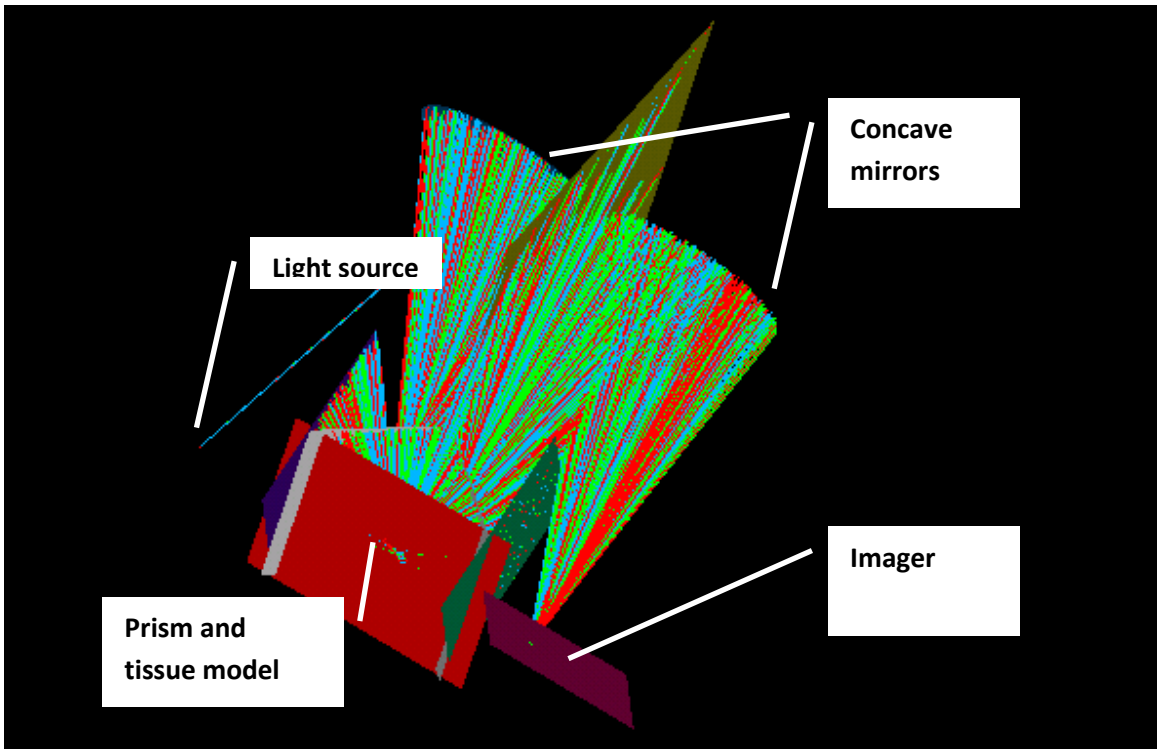

Fig: 5.4.2 Three wavelengths, focused on a prism surface by concave mirrors.

5.5 Spectral model graphical user interface

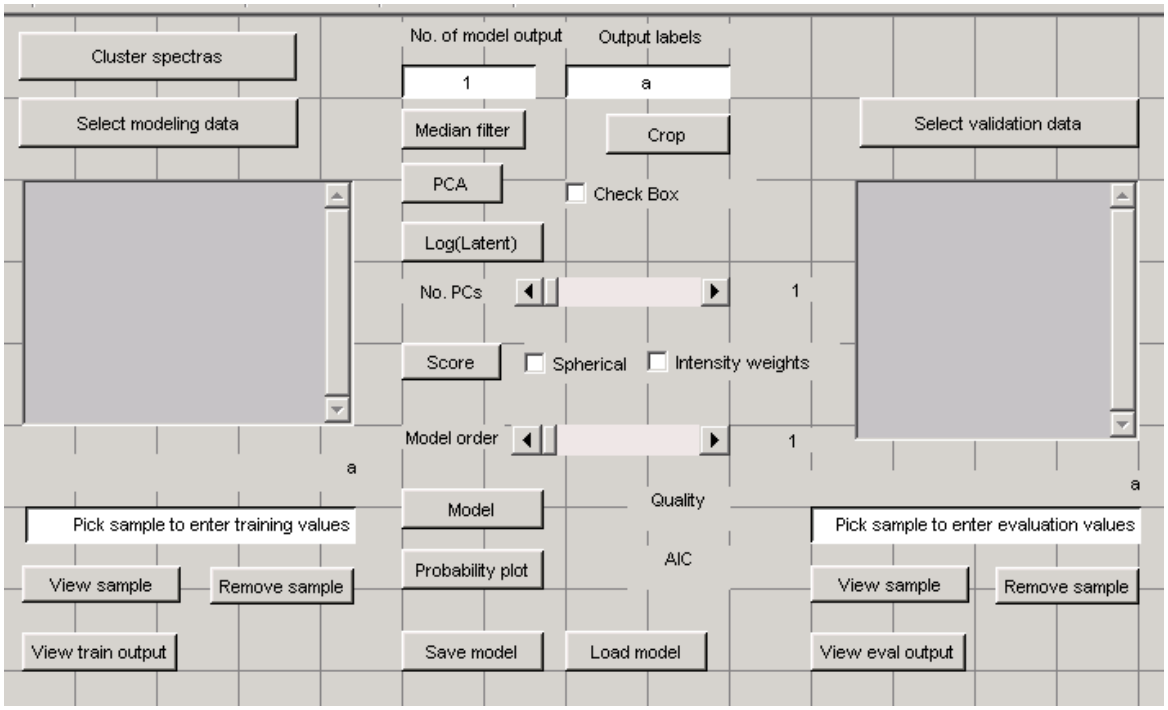

Fig. 5.5.1 Elaborated graphical user interface (GUI) for spectral modeling.

The observant reader would have under stood that the spectral data, regardless of the instrument, are processed by the same steps. The steps are:

1) Divide the set of observed spectra in one training dataset and one evaluation dataset.

2) If needed perform filtering or spatial calibration in a 2D mode.

3) The datasets are matrices, where the row represents observations and the columns variables. In all the above cases we will have a two-dimensional array of variables for each observation. One dimension is discarded and the variables are arranged in one long vector, the way they are rearranged is irrelevant as long as it is done the same way for all observations.

4) Since the data are likely to be redundant, we perform PCA on the matrix. We now observe the explanation grade of each PC. By applying a given information criterion we can decide with how many PCs we need to describe the observed data. Remaining PC are discarded as noise. The more observations, the easier it will be to determine the relevant number of PCs.

5) Each observation in the train data set can now be expressed by a few the numbers of loadings, which gives the linear combination of the PCs. If absolute intensity of the spectral data is expected to be irrelevant, then intensity information can be discarded by transforming to a spherical color space and only preserve the angular relations.

6) Now a regression model is trained by providing the correct answer related to each observation. The answers can be either deciding, e.g. *isBanana = 1*, or *wasDiagnosedWithCancer = 0*. Or the answers can be quantitative, e.g. *qualityOfBanana=40%* or *riscForCancer=10%.* When the linear equation is solved we now have a trained model in form of model coefficients.

7) The model is now fed with the evaluation data set and the quality of the performance can be evaluated.

8) The relation between spectral data and the answer might not be linear, in fact is might be given by any possible relation. Since we do not know that relation, we can increase the order of the model, eventually by doing so the model will converge toward that certain relation. Generally, models with too many degrees of freedom (DOF) in comparison to the numbers of observation they are trained on are unstable.

A graphical user interface was made to perform these steps. In this way spectral data can easily be analyzed similarly to the already existing toolbox for system identification in Matlab. Such a tool can work for educatiopnal purposes, since it might some times be difficult for a student to understand the applications and importance of spectral data. Also, this tool enables non-Matlab users and non-physicist to analyze and interpret spectral data. Eventually, it eases and fastens the evaluation of data in projects similar to those in this thesis.

The program is not completely finished since the input format is presently not defined and because of time restrictions.

6. Conclusions and future improvements

6.1 Simultaneous measurement of fluorescence, scattering and absorption

Performance of the system is still in an embryonic state, but weak results indicate that the concept is valid. A U.S. provisional has been submitted to secure possible future developments. Further development is currently unclear.

6.2 Simple inexpensive fluorosensor

A simple compact system was constructed from a Webcam and three UV diodes. Matlab and acquires data directly from the instrument. The absorption filters have been cut to fit in the instrument, but they have still not been retrieved. Evaluations of the performance still have to be done.

6.3 Wien-shift imaging

One filament based instrument has been constructed and demonstrated. An educational laboratory exercise was developed. System performance might still be increased in the following ways. The inside of instrument should preferably be covered with black absorbing paper. The polarizer should be changed to cover IR region better. Another approach would be to use a microscope with a variable ring light. The idea of using flash lights still has to be confirmed.

6.4 LED based fluorosensor

Several modifications have been done to an existing instrument. The improvements are still not verified.

7. References:

7.1 Papers and literature

Andersson-Engels, S. (2007). Prof. Dept. Physics, Lund Institute of Technology. (P. communication, Interviewer)

Capobianco, R. A. (2006). Xenon: The Full Spectrum vs. Deuterium Plus Tungsten. *Elmers, Penkin*.

Ek, S. (2006). *Master thesis, Portable Multi-wavelength Fluosensor Based on UV Light emitting Diodes.* Lund University: Lund Reports on Atomic Physics LRAP-369.

Gouzman, M. (2004). Excitation-emission fluorimeter based on linear interference filters. *Applied optics*.

Hart., S. J. (2002). Light emitting diode excitation emission matrix fluorescence spectroscopy. *The Royal Society of Chemistry*.

Herman, P. (2001). Frequency domain fluorescence microscopy with the LED as a light source. *Journal of Microscopy*.

Jobin Yvon, H. G. (2002). Linearization of the SPEX-3D(R) Spectrofluorometer.

Kumazaki, H. (2000). Tunable wavelength filter with single-mode fiber thinned by plasma etching. *Optical Society of America*.

Meingast, M. (2005). Geometric models of rolling-shutter cameras. *University of Berkeley, California*.

Schubert, E. F. (2003). *Light emitting diodes.* Cambridge University Press.

Svanberg, S. (2006). *Multispectral Imaging.* Lund Sweden: Department of Physics, Lund Institute of technology.

Svanberg, S. (3rd Edition 2001). *Atomic and Molecular Spectroscopy, Basic Aspects and Practical Applications.* Lund, Sweden: Springer-Verlag, Heidelberg.

Webinformation. (2007). *photonfocus.com*.

Yaddid-Pecht, O. (2005). *CMOS Imagers: From Phototransduction to Image Processing.* Springer-Verlag, Heidelberg.

Yavari, N. (2006). *Optical spectroscopy for tissue diagnostics and treatment control.* Bergen: Department of Physics and Technology.

7.2 Materials and expenses for setups developed.

Component	Purpose	Cost
2 Q-tec web cams	Wien Shift Imager	50€
1 Garbage bin	Wien Shift Imager	3€
10 Filament bulbs	Wien Shift Imager	3€
1 Polarization film	Wien Shift Imager	-
1 Variable power supply	Wien Shift Imager	-
1 Signal flash lamp	Excitation Emission Measurement	10€
Mightex USB CMOS imager	Excitation Emission Measurement	279€
Xenon PX2 light source	Excitation Emission Measurement	300€
Antisolarizing fiber 600um	Excitation Emission Measurement	30€
2 UV coated concave mirrors	Excitation Emission Measurement	216€
150 groove/mm grating	Excitation Emission Measurement	150€
300 groove/mm grating	Excitation Emission Measurement	150€
UV LVF Bandpass filter	Excitation Emission Measurement	500€
UV LVF Highpass filter	LED based fluorosensor	500€
LVF inline filter holder	LED based fluorosensor	100€
Circulation pump	Excitation Emission Measurement	35€